Applications of a new exact solution of the Navier-Stokes Equations to flow in pipes of varying width

by

Tracy Colgan

Thesis submitted in accordance with the requirements of the University of Liverpool for the degree of Doctor of Philosophy by Tracy Colgan

September 1987

Pooh knew what he meant,

but, being a Bear of Very Little

Brain, couldn't think of the words.

A. A. Milne

The House at Pooh Corner

ABSTRACT

Applications of a new, exact solution to the Axi-Symmetric Navier-Stokes equations have been studied. The important feature of this solution is that it is valid for all Reynolds number. All recent research in this field has needed to make a variety of assumptions regarding the physical properties of the flow. Consequently, this new solution has provoked a great deal of interest and has widespread implications in further research.

A significant feature of this new solution is the non-zero radial velocity on surfaces equidistant from the axis of the pipe, and as such, applications to tubes with impermeable boundaries requires pipes to have varying radius. The first case to be considered was that of peristaltic transport, that is the movement of fluid by travelling, sinusoidal waves of contraction along a tube. This problem is of considerable relevance in biomechanics and in the pumping of corrosive fluids. Previous research into peristalsis has tackled specific approximated cases of small and large Reynolds number and good agreement has been found between flow features of these and those of this solution.

Subsequent research has concentrated on flow through pipes of slowly varying cross-sectional area, with both porous and impermeable boundaries. Industry has expressed interest in transport of fluids along such pipes. However, the majority of the work done has been either numerical or experimental and deals only with particular flow character-

istics. The solution for the impermeable case is found as a series in the axial parameter and uses a number of computational tools, algebraic computing and numerical software packages to obtain the coefficients. The work was completed by a study of a combination of variable width and suction. Families of boundaries are obtained for the necessary streamline distributions and the corresponding mass transfer profiles are presented.

ACKNOWLEDGEMENTS

I would like to thank Dr. R.M. Terrill for his invaluable assistance and intellectual stimulation.

I thank S.E.R.C. for the financial help that they have afforded me during my period of research.

I am indebted to my colleagues David Harper and Chris Willis for generously sharing their computing skills and for proof-reading this thesis.

Finally, I wish to thank my Mother and Father for their support and tolerance throughout my education.

CONTENTS

INTRODUCTION

Recently, [1], a new exact solution of the Navier-Stokes equations has been developed. It was obtained as a solution to the problem of the steady, laminar, axi-symmetric flow of an incompressible fluid along circular pipes of constant cross-sectional area, with mass transfer at the walls. There has been a great deal of interest in flow through pipes with porous walls due to such problems as transpiration cooling, gas diffusion technology and the control of fluids in nuclear reactors. All previous research has concentrated on constant injection or suction, whereas this solution is unique in that the through flow can be varied along the length of the tube. This allows the maintenance of a fully developed velocity profile or alternatively permits the gradual transition from one prescribed velocity profile at some cross-section to another, similarly prescribed, further downstream.

The two definitive equations of viscous fluid flow are the equations of continuity and the Navier-Stokes equations. Exact solutions of this pair of equations are rare. The most notable examples are Poiseuille and Couette flows. Poiseuille flow occurs in pipes or channels with stationary walls, but with a pressure gradient and displays the characteristic parabolic velocity profile. Couette flow results from the movement of the boundary of a pipe or channel creating an axial or azimuthal shearing flow. This new solution is a combination of Poiseuille flow and a Potential flow. The laminar flow of an ideal fluid is known as Potential flow and the potential function is obtained as a solution of the axi-symmetric Laplace equation, the arbitrary constants being defined by the boundary conditions of the particular problem being considered.

The important and unique feature of this new solution is that it is valid for all Reynolds number. Reynolds number is a non-dimensional geometric constant which can be considered to be the ratio of the inertia and the viscous terms of the Navier-Stokes equations. It is considered, quantitatively to be the product of a typical velocity scale (the centre line velocity, inlet velocity, etc.) and a typical length scale (the width of a channel, radius of a pipe, etc.) divided by the kinematic viscosity of the fluid involved. Any two flows with the same initial and boundary conditions and the same Reynolds number can be considered to be dynamically similar. This is of particular relevance in 'model testing', which permits the variation of two or more of the constituent parameters, whilst maintaining the same Reynolds number, to allow the investigation of the flow in physical conditions that are more convenient than those of the unknown flow field.

Most of the previous analytical research into fluid flow has needed to make an assumption as to the size of Reynolds number. Taking this to be small (slow flow) or even zero (Stokes flow) allows the inertia terms of the Navier-Stokes equations to be neglected. Conversely, taking Reynolds number to be large (boundary layer flow) allows the viscous terms to be neglected. Both these assumptions suitably reduce the governing equations to a form in which they can be more easily solved.

This thesis investigates the applications of this new solution to a number of other problems. Even though the basic equations for each problem are the same; the assumptions, the boundary conditions and the techniques used in the solutions are different. Consequently, each sec-

tion addresses a separate problem. It is considered important to repeat the initial equations and, as such, each section can be viewed independently of the others, with its own introduction and conclusion. The work initially concentrated on the flow along pipes with impermeable boundaries. Since the solution was developed for porous pipe flow, there is a non-zero radial velocity on surfaces equidistant from the axis of the pipe. As a result, the investigation of flow through pipes with no through flow necessitates a varying cross-sectional area.

Section 1 concentrates on the first problem that was considered which was that of Peristaltic Transport. Classically, this is modelled by a pipe with a series of sinusoidal waves of small amplitude imposed upon it. This problem was tackled using a perturbation series technique, to first order when considering the classical problem, and subsequently to second order when considering a non-linear waveform as the wall profile.

Section 2 investigates the more general problem of variable width. This appeared to be a natural extension of the type of problem encountered when considering peristaltic transport. The problem of flow through pipes with slowly changing cross-sectional area has provoked both theoretical and experimental interest. This approach is totally novel in that the boundary is considered to be unknown, but that the velocity in the pipe could be described by the new solution with a suitably obtained potential function. From this supposition the wall profile is defined by the boundary conditions and this type of problem is known as a Free Boundary Problem. Some research has been made into problems of this kind, however,

other difficulties are encountered which render the problem trickier than those previous cases. This problem is also tackled using a series technique. The boundary conditions indicate that there is an infinity of zeros, or eigenvalues, of the derivative of the Bessel function of the first kind, J_1. As a result of this there is an infinity of solutions for each term in the series. As such, the effects of combining all the solutions and using all the terms in the series are investigated separately. Section 2.1 concentrates on two terms in the series but with a large number of eigenvalues. Two particular cases are presented; that of flow along a pipe with parallel walls and different radii up and downstream, and flow along a parallel pipe with a bulge or constriction. Section 2.2 considers the case of one eigenvalue and a large number of terms in the series. The first few terms are found, both analytically and using a double series method, and then an alternative perturbation parameter is used to optimise the information from the first series.

Finally, in Section 3, there is an investigation of the effects of both variable width and suction on an axi-symmetric pipe flow. Streamline distributions and their corresponding family of boundaries are obtained for a selection of different potential functions. In addition, the suction/injection profiles for each case are found.

REFERENCES

1. TERRILL, R.M., Laminar Flow in a Porous Tube, Trans. ASME, Vol. 105, 1983, pp.303

SECTION 1.

PERISTALTIC TRANSPORT

INTRODUCTION

The word peristalsis comes from the Greek word peristaltikos which means clasping and compressing. It is used to describe a progressive wave of contraction along a tube or channel whose cross-sectional area consequently varies. The wave may have an arbitary shape [1]-[5], but for simplicity it is often assumed to have a sinusoidal shape, for example, [6]-[11]. Peristalsis is regarded as having considerable relevance in biomechanics and especially as the method of transport of many of the body's fluids.

Early research in peristalsis involved the flow of urine from the kidney to the bladder [1], [7], [12], [13] and in the vascomotion of small blood vessels [7], [14], [15]. Subsequently research interest widened to include, for example, the motion of chyme in the small intestine [2], the peristaltic pumping of blood [8], [16]-[19], the transport of spermatozoa [20], the mechanical and neurological aspects of the peristaltic reflex [21], and, in plant physiology, phloem translocation by driving a sucrose solution along tubules by peristaltic contractions [32]. The application of peristaltic motion as a means of transporting fluid has aroused interest in engineering fields [10], [11], [22]. In particular, the peristaltic pumping of corrosive fluids and slurries could be useful as it is desirable to prevent their contact with the mechanical parts of the pump.

Many research workers have attempted to obtain analytical and numerical solutions for peristaltic flows. The governing equations are

non-linear so that assumptions are made about the amplitude ratio, the wave number and the Reynolds number. The amplitude ratio is the ratio of the amplitude of the wave to the average radius of the pipe and is usually taken to be small. Analytic solutions for zero Reynolds number were first considered by [6] and [23]. These flows, in which the inertia terms are neglected, are known as Stokes flows. Many analytical solutions were then developed to take account of the small non-linear effects. These solutions, as typified by [7], [16], [23], [24] and [25], assume either that the Reynolds number is small or that the product of the Reynolds number and the wave number (the ratio of the radius of the pipe to the wavelength of the wave) is small. The other limiting case of large Reynolds number has been tackled in [22] by solving the boundary layer equations.

To obtain information about flows at moderate Reynolds number it has been necessary to use numerical methods. The finite element method was used by [18], while more recently finite difference methods have been adopted by [9], [10], [11] and [26].

Recently a new solution of the Navier-Stokes equations for axisymmetric flow has appeared. This solution is valid for all Reynolds numbers and has proved to be of considerable assistance in dealing with flows through porous tubes [27], [28], [29] as well as laminar flows through circular pipes whose cross-sectional area varies slowly in the axial direction [30].

This exact solution will be used to show that for any given amplitude ratio there is a general wave shape that yields an analytical solution valid for <u>all</u> Reynolds numbers. Further this solution exhibits some

of the features that appear in the papers mentioned earlier. For example, a typical set of streamlines will appear that are consistent with those found numerically by [11] (Fig. 5(a)). It is also worth noting that the velocites shown in [11] (Fig. 8) are consistent with the solution presented in this paper.

As well as giving an insight into peristaltic flows, the solution in the present paper could be chosen as the first approximation for a numerical method for solving a wave of arbitrary shape.

There has been some confusion in the literature concerning the correct boundary conditions. Many researchers have correctly assumed that the normal and tangential velocity components of the wall and of the fluid at the wall are equal and this will be followed in Section 2. However, in some cases, for example [23], the radial velocity at the wall has been neglected although numerical solutions [18] show this to be invalid. Others [31], have replaced the radial velocity condition by a pressure difference boundary condition taken from the flexibility condition that appears in foil bearings. Again the radial boundary condition has not been satisfied and the solution is invalid.

FORMULATION OF THE PROBLEM

Consider the laminar axi-symmetric motion of the an incompressible fluid through a tube of radius R. Choose a cylindrical polar co-ordinate system (r,θ,z) where the axis Oz lies along the centre of the tube, r is the distance measured radially and θ is the azimuthal angle. Let U and V

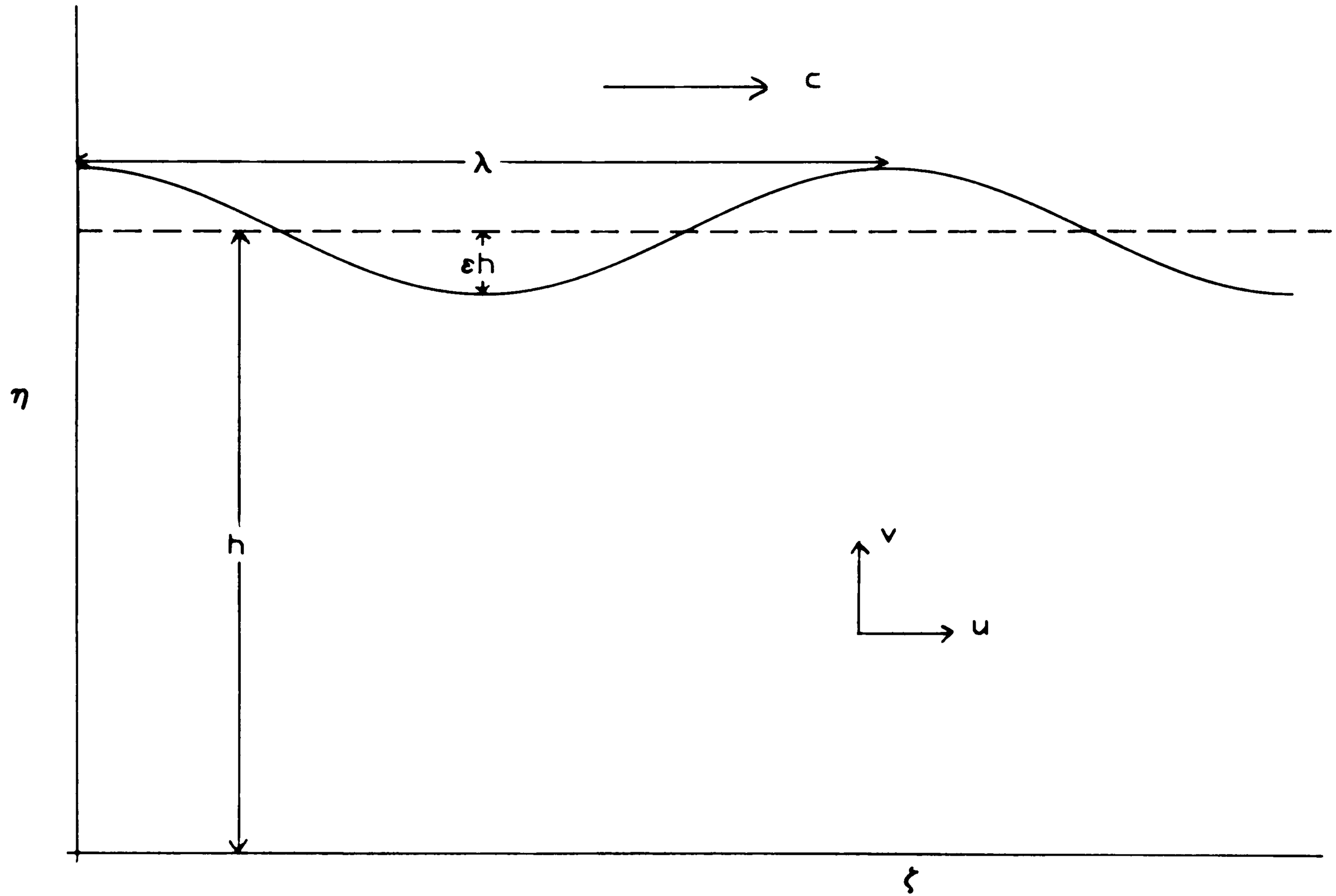

Figure 1.1

The Peristaltic geometry.

be the velocity components in the directions of z and r increasing respectively, as shown in Figure 1.1. For peristaltic flow, the equation of the wall at time t can be taken to be

$$(1.1) \qquad R(z,t) = h + \varepsilon h F\{(2\pi/\lambda)(z - ct)\} \quad , \ \varepsilon << 1 \ ,$$

where h is the average radius of the tube, εh is the amplitude of the wave, c is the velocity of the wave and λ is the wavelength. For the particular case of an infinite train of sinusoidal waves then

$$(1.2) \qquad F\{(2\pi/\lambda)(z - ct)\} \equiv \cos\{(2\pi/\lambda)(z - ct)\} \ .$$

The most popular choice of wall equation in the literature is that given by equations (1.1) and (1.2).

It will also be assumed that there is no displacement of the wall in the axial direction.

In the fixed co-ordinates (r,z) the flow in the pipe is unsteady but if moving co-ordinates (η,ζ) are chosen to travel in the positive z-direction with the same speed as the wave, then the flow can be treated as steady. The two co-ordinate frames are related by

$$(1.3) \qquad \begin{aligned} \zeta &= z - ct \ , \ \eta = r \ ; \\ u &= U - c \ , \ v = V \ ; \end{aligned}$$

where u and v are the velocity components in the directions of ζ and η respectively in the moving frame.

In the steady frame the continuity equation is

$$\frac{\partial}{\partial \eta}(\eta v) + \eta \frac{\partial u}{\partial \zeta} = 0 \ , \tag{1.4}$$

and the Navier-Stokes equations are

$$u \frac{\partial u}{\partial \zeta} + v \frac{\partial u}{\partial \eta} = -\frac{1}{\rho} \frac{\partial p}{\partial \zeta} + \nu \nabla^2 u \ ,$$

$$u \frac{\partial v}{\partial \zeta} + v \frac{\partial v}{\partial \eta} = -\frac{1}{\rho} \frac{\partial p}{\partial \eta} + \nu \left(\nabla^2 v - \frac{v}{\eta^2} \right) \ , \tag{1.5}$$

where

$$\nabla^2 \equiv \frac{\partial^2}{\partial \eta^2} + \frac{1}{\eta} \frac{\partial}{\partial \eta} + \frac{\partial^2}{\partial \zeta^2} \ , \tag{1.6}$$

and where p is the pressure, ρ the density and ν is the kinematic viscosity.

One of the boundary conditions for a flow that is axi-symmetric about the centre line is

$$v = 0 \quad \text{on } \eta = 0 \ . \tag{1.7}$$

The remaining boundary conditions are obtained by taking the velocity components of the fluid at the wall to be the same as that of the wall. For convenience, a parameter α given by

$$\alpha = 2\pi/\lambda \ , \tag{1.8}$$

is introduced. Then the velocity components at the wall

$$\eta = h + \varepsilon h F(\alpha\zeta)$$

$$\text{are} \quad u = -c \qquad \text{(from U = 0 for a fixed wall)} \tag{1.9}$$

$$\text{and} \quad v = -\alpha\varepsilon h c F'(\alpha\zeta) \ ,$$

where ' denotes differentiation with respect to $\alpha\zeta$. For the sinusoidal waves (1.2), the radial boundary condition becomes

$$v = \alpha\varepsilon h c \sin(\alpha\zeta) \quad \text{at} \quad \eta = h + \varepsilon h \cos\alpha\zeta \ . \tag{1.10}$$

THE ANALYTIC SOLUTION

The peristaltic solution will be derived from an exact solution of the Navier-Stokes equations given in [27] and will be valid for all Reynolds number. It has been shown by [27] that the equations (1.4) and (1.5) are satisfied by

$$(1.11) \qquad u = k(a^2 - \eta^2) + \frac{\partial \phi}{\partial \zeta} , \qquad v = \frac{\partial \phi}{\partial \eta} ,$$

where k and a are arbitrary constants, provided $\phi(\zeta,\eta)$ satisfies Laplace's equation

$$(1.12) \qquad \nabla^2 \phi = 0 ,$$

where ∇^2 is given in (1.6). This solution can be written

$$\underline{u} = U(\eta)\hat{\underline{z}} + \nabla\phi ,$$

where $\hat{\underline{z}}$ is a unit vector parallel to the axis of the tube. It is a combination of Poiseuille flow (the first term) and a potential flow (the second term), and consequently it is evident that the second term makes no contribution to the viscous friction. The constant k can be related to the pressure gradient in the tube. The general equation of (1.12), chosen by [27]-[29] for flows through a pipe with porous walls and by [30] for flows through a circular pipe whose cross-sectional area varies slowly in the axial direction, involved Bessel functions of the first and second kind, namely $J_0(\eta)$ and $Y_0(\eta)$, together with $\exp(\zeta)$. However, the appropriate solution of (1.12) for peristaltic flow is

$$(1.13) \qquad \phi = \sum_{n=1}^{\infty} \{A_n \cos\alpha_n\zeta + B_n \sin\alpha_n\zeta\}\{I_0(\alpha_n\eta) + D_n K_0(\alpha_n\eta)\} ,$$

where I_0 and K_0 are modified Bessel functions of the first and second kind respectively and α_n, A_n, B_n and D_n are constants to be determined. The symmetry condition (1.7) together with (1.11) and (1.13) yields

$$D_n \equiv 0 \ . \tag{1.14}$$

The values of α_n are determined by relating the general wave form $F(\alpha\zeta)$ in (1.9) to the orthogonal set of functions in (1.13). Thus, for the general waveform, the values of α_n are given by

$$\alpha_n = n\alpha \ , \tag{1.15}$$

where n is an integer. However, for the first order solution for a sinusoidal wave, the term given by n = 1 will be sufficient.

A FIRST ORDER SOLUTION

The sinusoidal wave given by (1.2) is the most popular waveform in the literature and series solutions for small Reynolds numbers can be found in, for example, [23] and [25]. A solution valid for all Reynolds numbers will now be sought by taking series expansions in ε, the ratio of the amplitude of the wave to the average radius of the tube.

For a wave of the shape (1.2), the boundary condition on ϕ can be derived from (1.9),(1.10) and (1.11) to yield that at the wall

(1.16) $$\eta_1 = h(1 + \varepsilon\cos\alpha\zeta) ,$$

the velocity components satisfy

(1.17) $$\left.\frac{\partial\phi}{\partial\eta}\right|_{\eta=\eta_1} = \alpha\varepsilon hc\sin\alpha\zeta \quad , \quad \left.\frac{\partial\phi}{\partial\zeta}\right|_{\eta=\eta_1} = -k(a^2 - \eta_1^2) - c .$$

A solution in the form

(1.18) $$\phi = \sum_{n=0}^{\infty} \varepsilon^n \phi_n(\zeta,\eta) ,$$

will now be sought, where ϕ satisfies (1.12), that is

(1.19) $$\nabla^2\phi_n = 0 \qquad n = 0, 1, 2, 3,...$$

Although the constants k, c etc. could also be written as series expansions in ε, it will be sufficient to choose

(1.20) $$a^2 = a_0^2 + \varepsilon a_1^2 + \varepsilon^2 a_2^2 + \ldots .$$

The first term $\phi_0(\zeta,\eta)$ satisfies (1.19) and, from (1.17), the boundary conditions at $\eta = \eta_1$ are

(1.21) $$\frac{\partial\phi_0}{\partial\eta} = 0 \quad \text{and} \quad \frac{\partial\phi_0}{\partial\zeta} = -k(a_0^2 - h^2) - c .$$

The appropriate solution of (1.19) satisfying (1.21) is

$$\phi_0(\zeta,\eta) \equiv 0 \ , \tag{1.22}$$

and the constant a_0 is given by

$$a_0^2 = h^2 - c/k \ . \tag{1.23}$$

The second term $\phi_1(\zeta,\eta)$ satisfies (1.19) and, from (1.17), boundary conditions of order ε, that is, at $\eta = \eta_1$

$$\begin{aligned} \frac{\partial \phi_1}{\partial \eta} &= \alpha hc \sin\alpha\zeta \ , \\ \frac{\partial \phi_1}{\partial \zeta} &= -k(a_1^2 - 2h^2\cos\alpha\zeta) \ . \end{aligned} \tag{1.24}$$

The boundary conditions (1.24) suggest that, from (1.13) and (1.14), the required solution of (1.19) is,

$$\phi_1 = (A_1\cos\alpha\zeta + B_1\sin\alpha\zeta)I_0(\alpha\eta) \ .$$

The radial velocity condition in (1.24) gives

$$A_1 \equiv 0 \ , \qquad B_1 I_0'(\alpha\eta_1) = hc \ ,$$

where ' denotes differentiation with respect to $\alpha\eta$. Now, from (1.16), to first order $\eta_1 \simeq h$ so that the solution for $\phi_1(\zeta,\eta)$ is

$$\phi_1 = hc\frac{I_0(\alpha\eta)}{I_0'(\alpha h)}\sin\alpha\zeta \ . \tag{1.25}$$

The tangential boundary condition in (1.24) will relate the pressure gradient to the velocity of propagation of the wave c. Thus

$$a_1 = 0 \ , \qquad k = \frac{B_1\alpha I_0(\alpha\eta_1)}{2h^2} \ . \tag{1.26}$$

Consequently to first order, k is given by

$$k = \frac{\alpha c I_0(\alpha h)}{2hI_0'(\alpha h)} \ . \tag{1.27}$$

Substitution from (1.21)-(1.27) into (1.11) yields the following simple expressions for the velocity components of the fluid

$$u = -c + \frac{c\alpha h I_0(\alpha h)}{2\ I_0'(\alpha h)}\left[1 - \frac{\eta^2}{h^2}\right] + \varepsilon c\alpha h\frac{I_0(\alpha\eta)}{I_0'(\alpha h)}\cos\alpha\zeta \ ,$$

$$v = \varepsilon c\alpha h\frac{I_0'(\alpha\eta)}{I_0'(\alpha h)}\sin\alpha\zeta \ . \tag{1.28}$$

Before examining solution (1.28) in detail, some preliminary observations can be made. Analytical solutions have previously been ob-

tained by taking a double series expansion in terms of the Reynolds number and a small parameter which was either the amplitude ratio or the wave number, [see [7], [16], [23] and [25]]. The choice of typical Reynolds number has alternated between $R = (ch/\nu)$ and $R_e = (ch/\nu)\alpha h$, and there has been some doubt as to which one was the more suitable. Indeed [24] examines this problem in the conclusion and decides that R_e is more appropriate. In [16], R is used throughout the analysis but finally the author writes in the conclusion:

" The results of the higher-order solutions suggest that a Reynolds number more relevant than the one introduced earlier for the problem is perhaps R_e ".

It is clear, from (1.28), that the significant parameter combination is αh, so this suggests that series expansions should have taken R_e as the parameter.

It is also evident that the velocity components of the flow and the pressure gradient are directly proportional to the velocity of the propagating wave.

To visualise the analytical solution (1.28) it will be useful to choose a suitable value of αh. Although the pipe is the most appropriate shape for physical applications, numerical work has concentrated on two dimensional flows because numerical solutions for axi-symmetric flows are more difficult due to the singularity in the governing equations when $\eta = 0$. Consequently, while αh will be chosen to have the value 0.25 to enable some comparisons to be made with numerical values obtained in two dimensional flows for moderate Reynolds number by [6], precise corre-

lation cannot be expected. The actual velocity components U and V can be obtained from (1.28) and (1.3) and their respective velocity profiles are shown in Figs. 1.2 and 1.3 for the case $\alpha h = 0.25$ and $\varepsilon = 0.1$. It should be noted that $\zeta = z - ct$, so that the velocity profiles are given at a fixed time t, t = 0 say. Fig. 1.2 illustrates the general statement that for all αh the axial velocities have a maximum value with respect to ζ when $\alpha\zeta = 2n\pi$ and a minimum value when $\alpha\zeta = (2n + 1)\pi$ where n is an integer. These values of $\alpha\zeta$ correspond to the maximum and minimum radii of the pipe. The radial velocity, as illustrated in Fig. 1.3, has the same period as the axial velocity but it is out of phase by $\pi/2$. The radial velocity increases in amplitude as η increases for all values of αh but the rate of increase depends on αh.

It is particularly interesting to observe how the velocity components change by considering the limiting cases. For $\alpha h \to 0$, (1.28) yields

$$U = c[(1 - \frac{\eta^2}{h^2}) + 2\varepsilon\cos\alpha\zeta] \ , \qquad V = \varepsilon c\alpha\eta\sin\alpha\zeta \ ,$$

which are in accord with expansions for small Reynolds numbers. The shape of U and V are only slightly different from those shown in Figs. 1.2 and 1.3. For $\alpha h \to \infty$ and using that for z large

$$I_0(z) \sim \frac{e^z}{\sqrt{(2\pi z)}} \ ,$$

then (1.28) yields that for $\eta \simeq h$

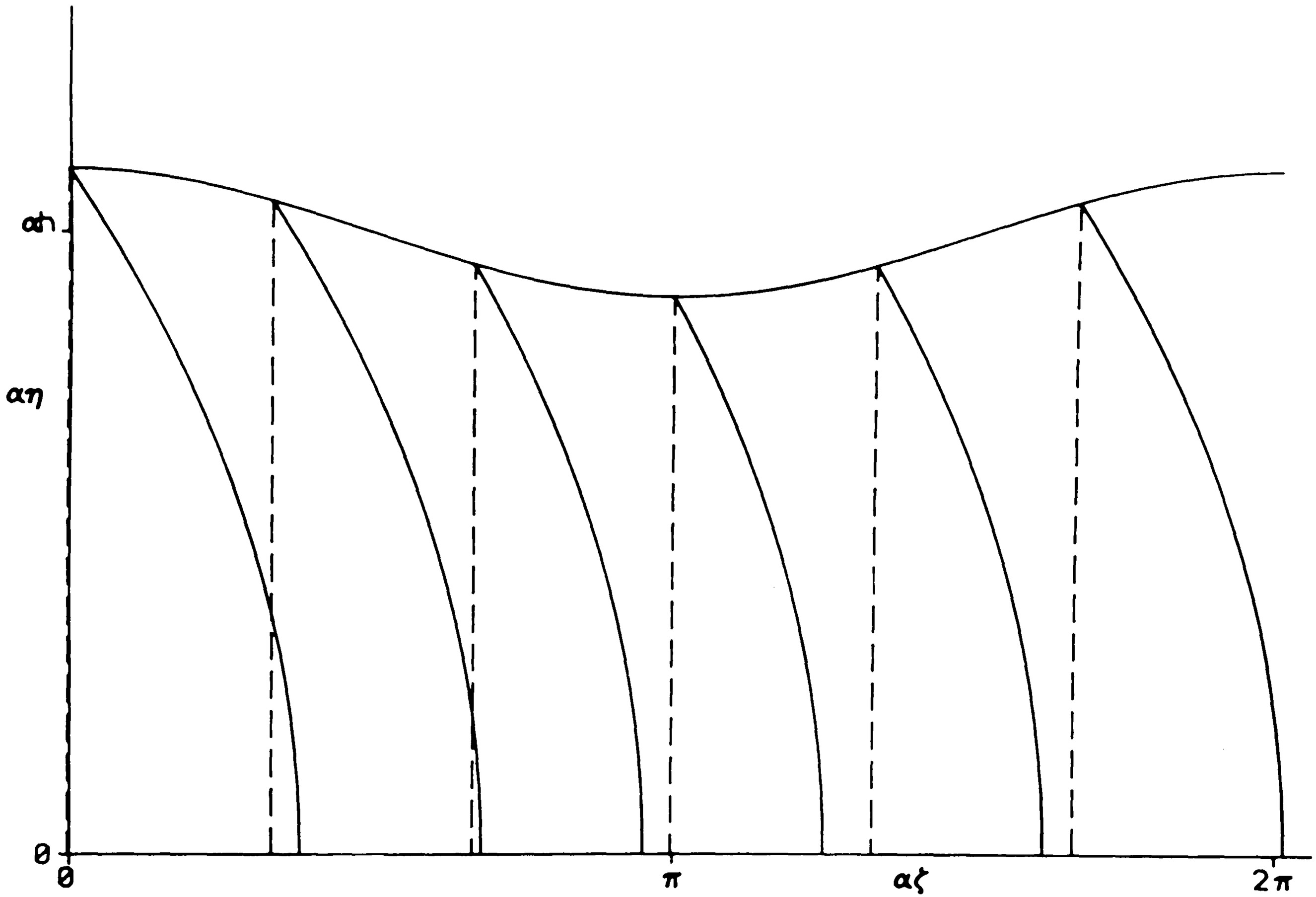

Figure 1.2

Axial velocity distribution with $\alpha h = 0.25$ and $\varepsilon = 0.1$ to $O(\varepsilon)$.

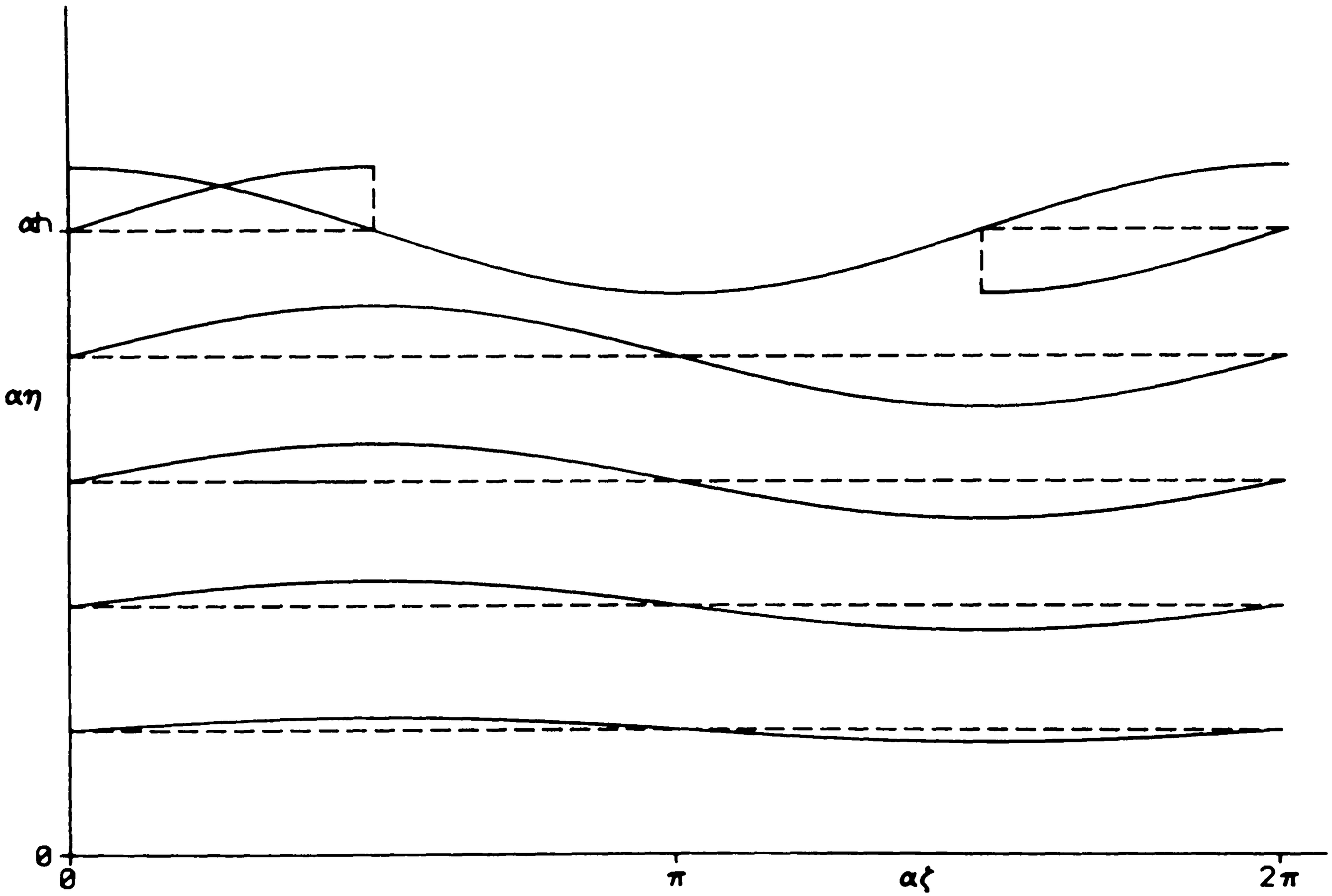

Figure 1.3

Radial velocity distribution with $\alpha h = 0.25$ and $\varepsilon = 0.1$ to $O(\varepsilon)$.

$$U \sim c\alpha h[\ \frac{1}{2}(1 - \frac{\eta^2}{h^2}) + \varepsilon\sqrt{(h/\eta)}\exp\{\alpha(\eta - h)\}\cos\alpha\zeta]\ ,$$

and

$$V \sim \varepsilon c\alpha h\sqrt{(h/\eta)}\exp\{\alpha(\eta - h)\}\sin\alpha\zeta\ ,$$

and for values of η in $0 \leq \eta < h - O(1/\alpha)$

$$U \sim \frac{c\alpha h}{2}(1 - \frac{\eta^2}{h^2})\ , \qquad V = 0\ .$$

Thus although deductions about periodicity remains unchanged, there is a dramatic change in velocity in a narrow region near the boundary of width $O(1/\alpha)$. This is precisely the behaviour that would be expected for large Reynolds numbers from boundary layer theory.

For plane two dimensional peristaltic flows, the centre line velocity of the flow has been examined by various authors, for example, [10], [11], [23] and [33]. From equations (1.3) and (1.28), the centre line velocity for a first order solution is given by:

$$\frac{U}{c}\Big|_{\eta=0} = \frac{\alpha h}{I_0'(\alpha h)}[\ \frac{I_0(\alpha h)}{2} + \varepsilon\cos\alpha\zeta]\ .$$

Again, a significant parameter in the solution is the product αh. Although the present solution is for axi-symmetric flows, it suggests that numerical solutions to the plane flow should consider values of αh rather than individual values for α and h. The numerical solutions [11] and the

series solution for small Reynolds numbers are consistent with these observations.

Since $\alpha h > 0$, $I_0(\alpha h) > 0$ and $I_0'(\alpha h) > 0$, the only quantity that may be negative is the cosine term. Clearly, as $\varepsilon > 0$ is small, $U|_{\eta=0} > 0$ for all ζ, and thus there is no reflux, reverse flow, at any point of the peristaltic cycle. This is an important requirement for industrial fluid propulsion. Details of this flow, such as the mass flow and pressure distribution will now be discussed.

STREAMLINES, PRESSURE DISTRIBUTION AND MASS FLUX

To visualise the flow the equation of the streamlines will now be found. Introducing the streamfunction ψ defined by

$$(1.29) \qquad u = \frac{1}{\eta}\frac{\partial \psi}{\partial \eta}, \qquad v = -\frac{1}{\eta}\frac{\partial \psi}{\partial \zeta},$$

then substituting for v into (1.28), integration with respect to ζ yields

$$(1.30) \qquad I_0'(\alpha h)\psi = \varepsilon \mathrm{ch}\eta I_0'(\alpha\eta)\cos\alpha\zeta + g(\eta),$$

where $g(\eta)$ is an arbitrary function of η to be determined. After substituting for ψ and u from (1.30) and (1.29) respectively into (1.28) and also noting that $I_0(\alpha\eta)$ satisfies

$$I_0''(\alpha\eta) + \frac{1}{\alpha\eta} I_0'(\alpha\eta) - I_0(\alpha\eta) = 0,$$

it can be shown that $g(\eta)$ satisfies

$$(1.31) \qquad g'(\eta) = c\eta \left[-I_0'(\alpha h) + \frac{\alpha h}{2} I_0(\alpha h)\left(1 - \frac{\eta^2}{h^2}\right)\right] .$$

Integration of (1.31) with respect to η and substitution into (1.30) gives

$$(1.32) \qquad \psi + \frac{c\eta^2}{2} = \frac{ch\eta}{I_0'(\alpha h)} \left[\frac{\alpha\eta}{4}\left(1 - \frac{\eta^2}{2h^2}\right) I_0(\alpha h) + \varepsilon I_0'(\alpha\eta)\cos\alpha\zeta \right] ,$$

where ψ is the streamfunction in the moving frame. The non-dimensional function $(\alpha^2\psi/c)$ depends only on the non-dimensional quantities αh, $\alpha\eta$, $\alpha\zeta$ and ε. Contours for constant values of $(\alpha^2\psi/c)$ have been plotted in Fig. 1.4 for $\alpha h = 0.25$ and $\varepsilon = 0.1$. The wall of the pipe is a streamline of the flow in the moving frame and the streamlines close to the wall follow the shape of the wall, as is to be expected. However, as αh increases, the width of the region in which the streamlines follows the shape of the wall narrows until it becomes a boundary layer. Indeed, it can be shown that for αh large, the streamlines away from the wall satisfy $\eta^2(2h^2 - \eta^2) = \text{constant}$.

In the fixed frame the streamfunction Ψ is given by

$$(1.33) \qquad \Psi = \psi + c\eta^2/2 ,$$

where ψ satisfies (1.32). A typical streamline pattern is illustrated in Fig. 1.5 and demonstrates a flow down the tube near the centre line. It

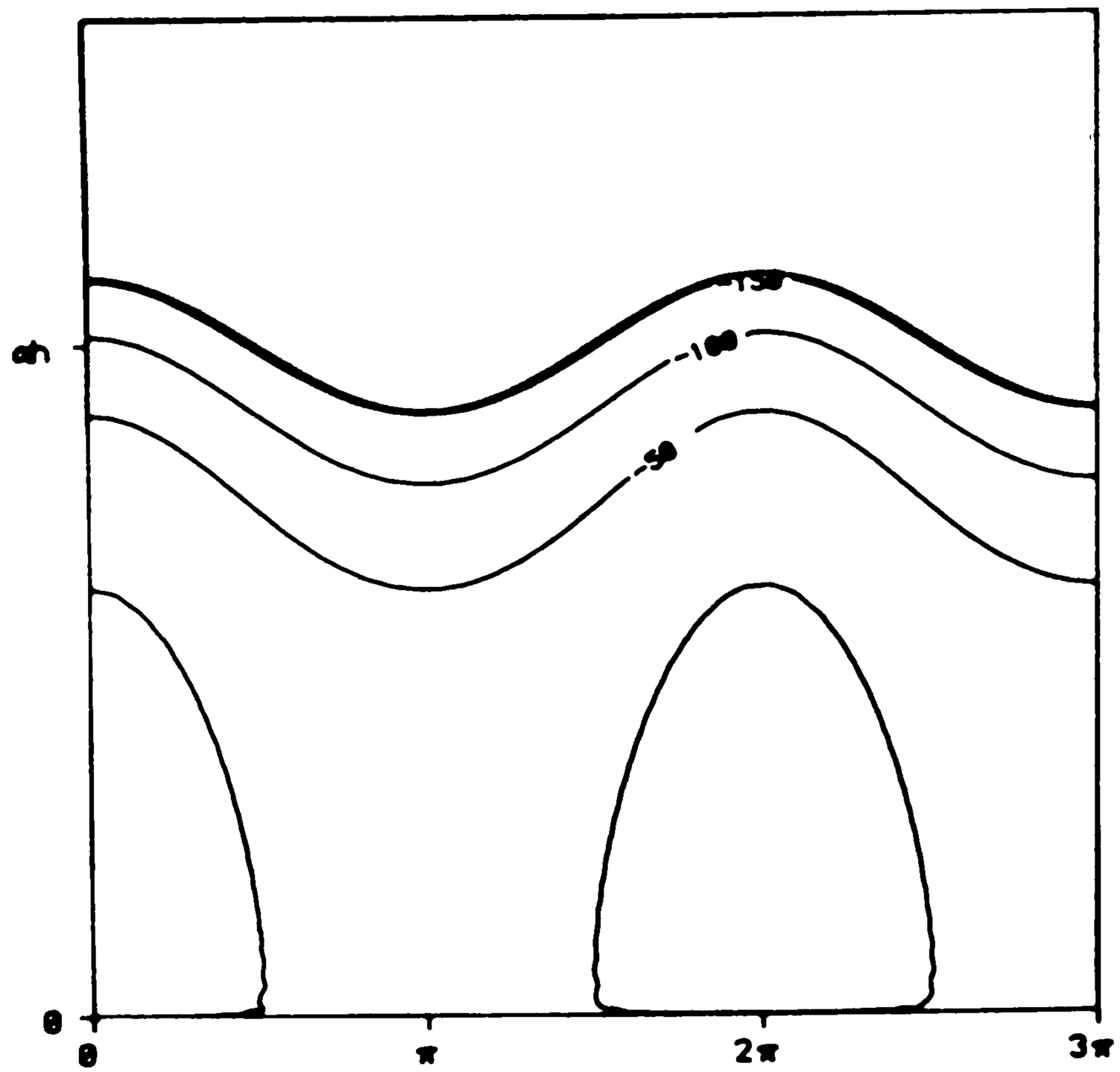

Figure 1.4

Streamlines, in the moving frame, of the peristaltic flow with $\alpha h = 0.25$ and $\varepsilon = 0.1$ to $O(\varepsilon)$.

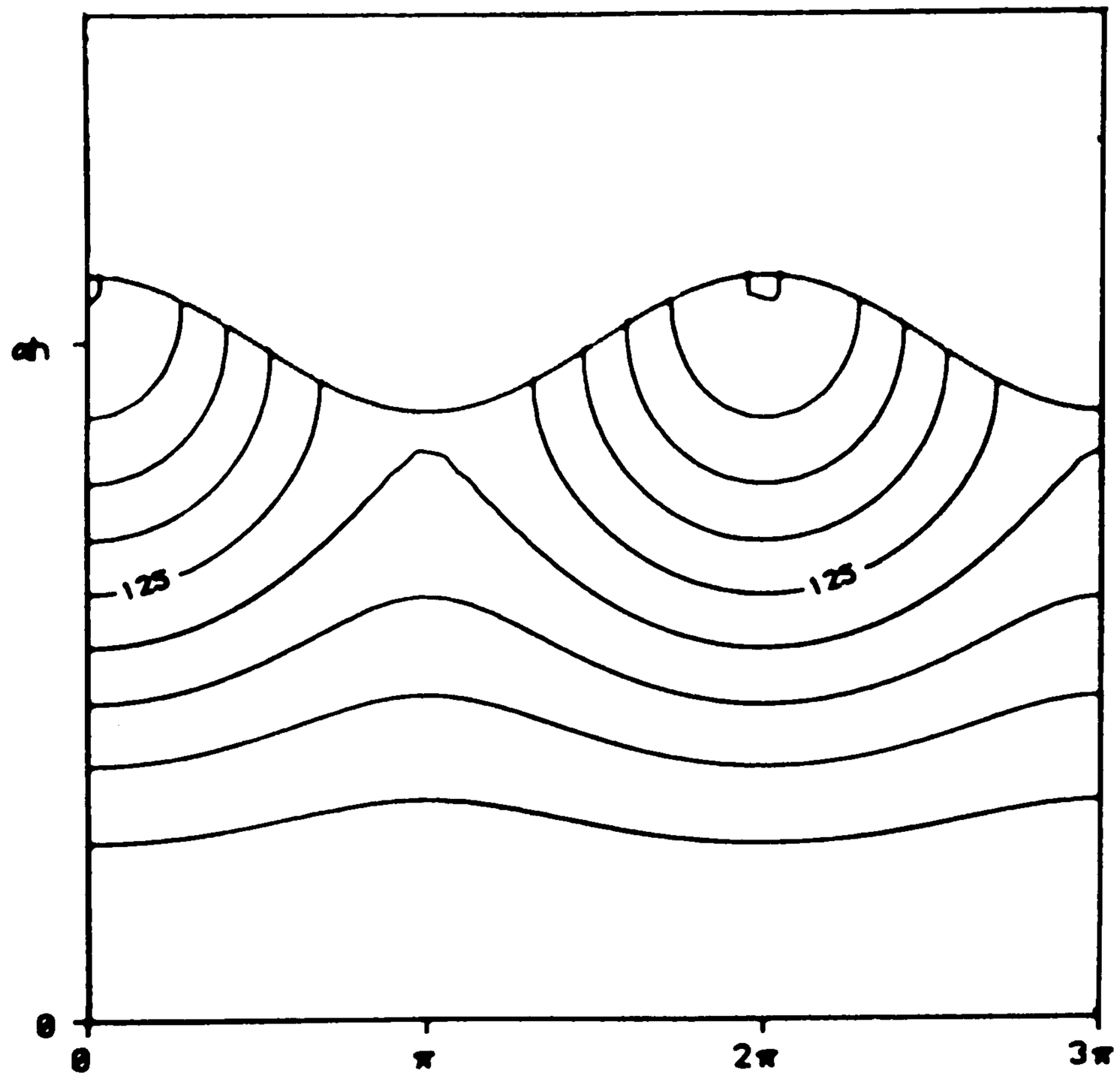

Figure 1.5

Streamlines, in the fixed frame, of the peristaltic flow with $\alpha h = 0.25$ and $\varepsilon = 0.1$ to $O(\varepsilon)$.

should be noted that in the fixed frame Ψ is a function of $(z - ct)$ and so depends on both position and time. However, choosing a fixed time, say $t = (2\pi n/\alpha c)$ where n is an integer, will give the streamline pattern shown.

The pressure distribution can be obtained by substituting for u and v from (1.11) into (1.5) and integrating each of the equations of the motion. It can be shown that the pressure, p, is given by

$$(1.34) \qquad p + \rho\{\tfrac{1}{2}(\phi_\eta^{\,2} + \phi_\zeta^{\,2}) + u_0\phi_\zeta + u_0' \int \phi_\eta d\zeta\} = p_0 - 4k\mu\zeta \ ,$$

where $u_0 = k(a^2 - \eta^2)$ and p_0 is a constant. The first-order evaluation is given by

$$(1.35) \qquad \frac{p - p_0}{\mu c\alpha} = -\frac{2I_0(\alpha h)\alpha\zeta}{\alpha h I_0'(\alpha h)} - \frac{\varepsilon R\cos\alpha\zeta}{I_0'(\alpha h)}\{\frac{I_0(\alpha h)}{\alpha h I_0'(\alpha h)}[\alpha\eta I_0'(\alpha\eta) + \frac{I_0(\alpha\eta)}{2}\alpha^2h^2[1 - \frac{\eta^2}{h^2}]] - I_0(\alpha\eta)\} \ ,$$

where $R = (hc/\nu)$ is a non-dimensional Reynolds number. Contours for $((p - p_0) / \mu c\alpha)$ are shown in Figs. 1.6 and 1.7 for $\alpha h = 0.25$ and $\varepsilon = 0.1$. For small Reynolds number the first term is dominant, showing the pressure to be independent of cross-channel position and proportional to ζ and this can clearly be seen in Fig. 1.6. For increasing Reynolds number the second term becomes more significant and the pressure exhibits an $\alpha\eta$ dependence and a more periodic nature in ζ, as illustrated in Fig. 1.7.

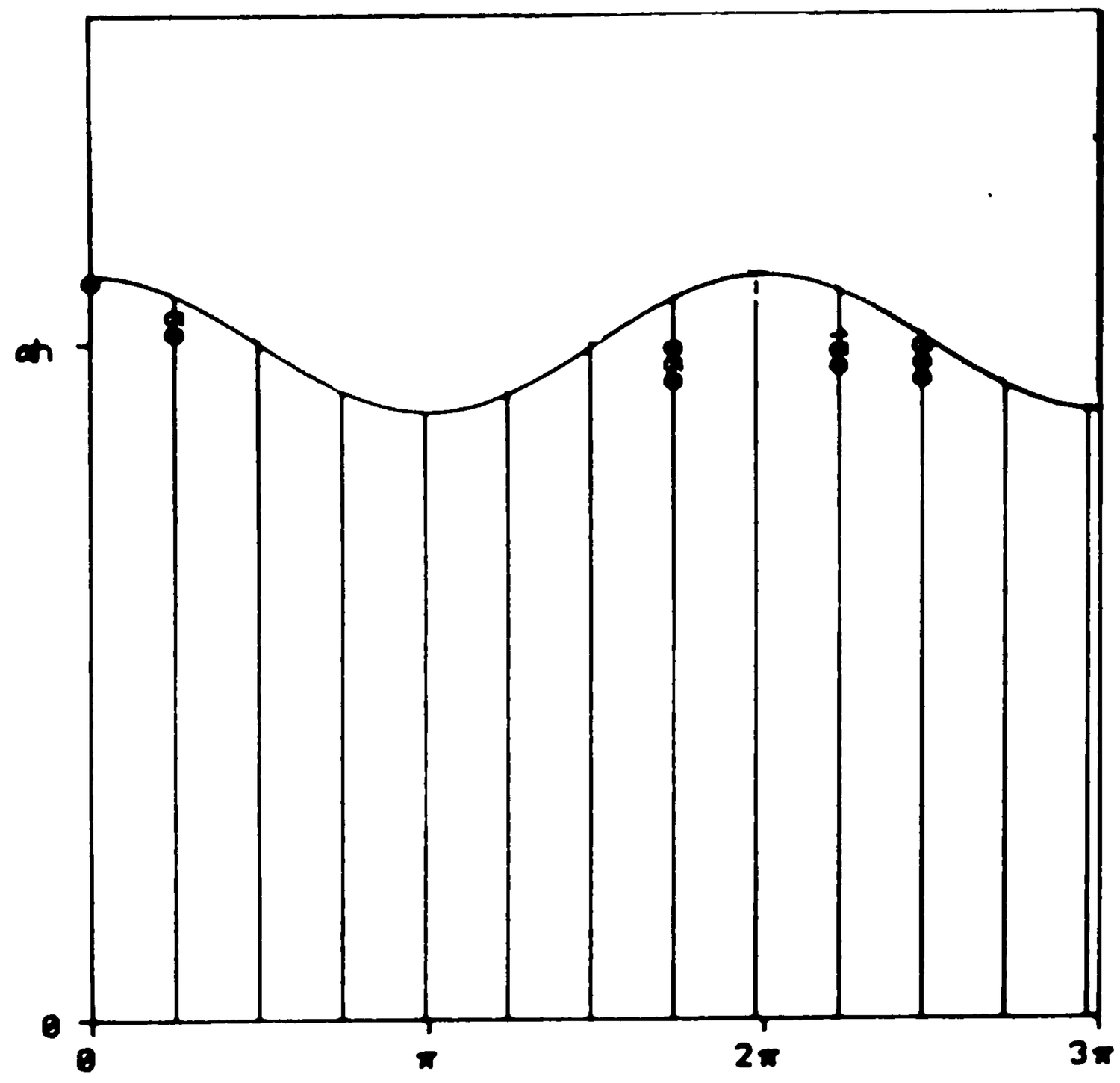

Figure 1.6

Contours for the pressure for $\alpha h = 0.25$ and $\varepsilon = 0.1$ with $R_e = 10.0$ to $O(\varepsilon)$.

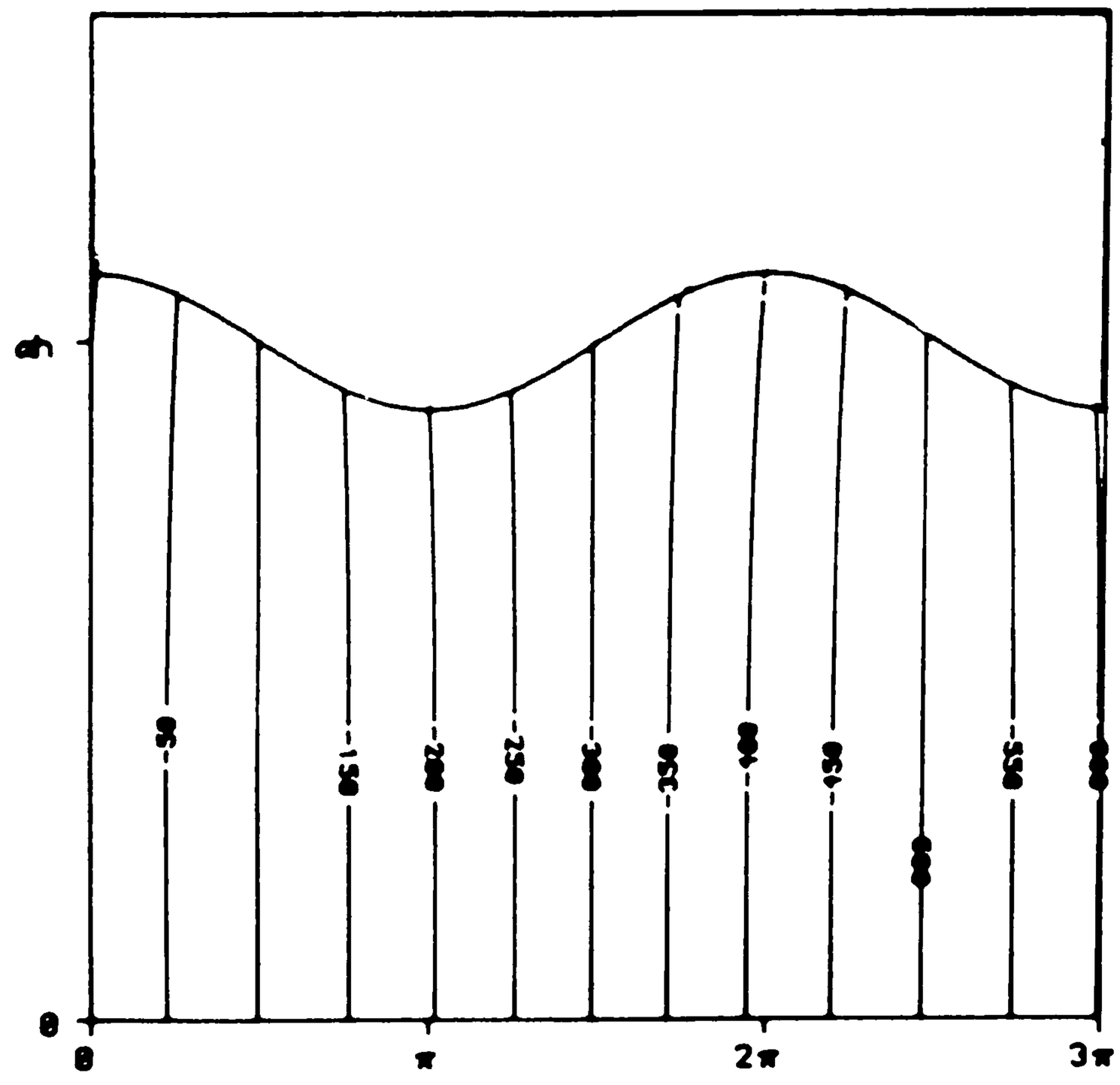

Figure 1.7

Contours for the pressure for $\alpha h = 0.25$ and $\varepsilon = 0.1$ with $R_e = 1000.0$ to $O(\varepsilon)$.

Numerical solutions and series solutions for small Reynolds numbers have usually examined the special cases of the pressure distribution on the centre line and on the boundary. For $\eta = 0$, (1.35) yields

$$(1.36) \qquad \frac{(p_{|\eta=0} - p_0)}{\mu c\alpha} = \frac{-2I_0(\alpha h)\alpha\zeta}{\alpha h I_0'(\alpha h)} - \frac{\varepsilon R}{I_0'(\alpha h)}\left\{ \frac{\alpha h I_0(\alpha h)}{2I_0'(\alpha h)} - 1 \right\}\cos\alpha\zeta \ ,$$

showing the central line pressure to be periodic of same period as the wave, but out of phase by π. On the boundary $\eta = h(1 + \varepsilon\cos\alpha\zeta)$, the pressure (1.35) to $O(\varepsilon)$is

$$(1.37) \qquad \frac{(p|_{\eta=\eta_1} - p_0)}{\mu c\alpha} = \frac{-2I_0(\alpha h)\alpha\zeta}{\alpha h I_0'(\alpha h)} \ ,$$

which shows that the pressure on the boundary decreases linearly with ζ. The relation (1.37) is the same as that obtained for small Reynolds number expansions. Consequently, increasing the Reynolds number has more influence on the centre line pressure distribution than on the boundary pressure distribution.

Due to the periodic nature of this flow, the concept of average mass flux over one wavelength will now be introduced. The actual average mass flux, at time $t = T$ is given by

$$(1.38) \qquad \frac{2\pi\rho}{\lambda}\int_0^{\lambda} \Psi|_{\eta=\eta_1}\, dz \qquad \text{at } t = T \ ,$$

where λ is the wavelength of the peristaltic wave, and Ψ is the fixed frame streamfunction. The actual mass flux is measured relative to axes in space and is different to the mass flux relative to the moving boundary. From (1.3), at a fixed time $t = T$, $dz = d\zeta$ and, after substituting (1.33) and (1.32) into (1.38) and integrating with respect to ζ, it can be shown that the average mass flux is

$$(1.39) \qquad \frac{\pi\rho c\alpha h I_0(\alpha h)h^2}{4I_0'(\alpha h)} \ .$$

It should be noted that the term of $O(\varepsilon)$ in (1.39) is identically zero. The average mass flux given by formula (1.39) is useful in calculations concerning the peristaltic pumping of fluids in a variety of engineering applications.

EXTENSION TO A SECOND-ORDER SOLUTION

It has been shown that even though the velocities and the streamfunction contain periodic terms in ε, the pressure and average mass flux are linear to first-order, and thus knowledge of the second-order solution is important for developing a deeper understanding of these quantities. For a second-order flow, the equation of the wall at time t, can be taken to be

$$R(z,t) = h + \varepsilon h F\{(2\pi/\lambda)(z - ct)\} + \varepsilon^2 h G\{(2\pi/\lambda)(z - ct)\} , \tag{1.40}$$

where h is the average radius of the tube, εh is the average amplitude of the wave and $\varepsilon^2 h$ is the amplitude of the perturbation imposed on the wave. Considering the particular case that was investigated to first-order, then

$$F\{(2\pi/\lambda)(z - ct)\} = \cos\{(2\pi/\lambda)(z - ct)\} , \tag{1.41}$$

as before and

$$G\{(2\pi/\lambda)(z - ct)\} = \gamma \cos 2\{(2\pi/\lambda)(z - ct)\} , \tag{1.42}$$

where γ is a constant to be determined by the boundary conditions.

Using the transformed co-ordinates defined by (1.3), the boundary conditions become

(1.43) $v = 0$ on $\eta = 0$,

which is identical to (1.7). By taking velocity components of the fluid at the wall to be the same as those of the wall

(1.44) $u = -c$ and $v = -\alpha\varepsilon hcF'(\alpha\zeta) - \alpha\varepsilon^2 hcG'(\alpha\zeta)$ on the wall.

In the case of an infinite train of perturbed sinusoidal waves, then (1.41) and (1.42) give:

(1.45) $v = \alpha\varepsilon hc\sin\alpha\zeta + 2\alpha\varepsilon^2 hc\gamma\sin 2\alpha\zeta$.

For a wave of this shape the boundary conditions on ϕ can be obtained from (1.11), (1.12), (1.13), (1.43) and (1.44) to yield

$$\left.\frac{\partial\phi}{\partial\eta}\right|_{\eta=\eta_2} = \alpha\varepsilon hc\sin\alpha\zeta + 2\alpha\varepsilon^2 hc\gamma\sin 2\alpha\zeta ,$$

(1.46) and

$$\left.\frac{\partial\phi}{\partial\zeta}\right|_{\eta=\eta_2} = -k(a^2 - \eta_2^2) - c ,$$

where $\eta_2 = h + \varepsilon h\cos\alpha\zeta + \varepsilon^2 h\gamma\cos 2\alpha\zeta$.

When ϕ is written as the series (1.18), the second-order boundary conditions on $\eta = \eta_2$ become

$$\left.\frac{\partial \phi_2}{\partial \eta}\right|_{\eta=h} = 2\alpha hc\gamma \sin 2\alpha\zeta - \frac{\alpha hc I_0''(\alpha h)}{2 I_0'(\alpha h)} \sin 2\alpha\zeta \ ,$$

(1.47)

$$\left.\frac{\partial \phi_2}{\partial \zeta}\right|_{\eta=h} = -k[\ a_2^2 h^2 - h^2\cos^2\alpha\zeta - 2h^2\gamma\cos 2\alpha\zeta\ ] - \alpha^2 ch^2\cos^2\alpha\zeta \ ,$$

where $'$ denotes differentiation with respect to $\alpha\eta$.

The general form, suggested by (1.13) and (1.25), of the solution is

(1.48) $$\phi_2 = B_2 I_0(2\alpha\eta)\sin 2\alpha\zeta \ .$$

Thus, imposing the radial condition (1.47) gives

(1.49) $$B_2 = \frac{ch}{I_0'(2\alpha h)}\left[\ 2\gamma - \frac{\alpha h I_0''(\alpha h)}{2 I_0'(\alpha h)}\right] \ ,$$

and hence

(1.50) $$\phi_2 = \frac{ch}{I_0'(2\alpha h)}\left[\ 2\gamma - \frac{\alpha h I_0''(\alpha h)}{2 I_0'(\alpha h)}\ \right] I_0(2\alpha\eta)\sin 2\alpha\zeta \ .$$

The constants a_2 and γ are given by the tangential condition of (1.47), that is,

(1.51) $$\frac{a_2^2}{h^2} = \frac{1}{2}\left[\ 1 - \frac{2\alpha h I_0'(\alpha h)}{I_0(\alpha h)}\ \right] \ ,$$

and

(1.52)
$$\gamma = \frac{\alpha h \left[\frac{I_0(2\alpha h) I_0''(\alpha h)}{I_0'(\alpha h) I_0'(2\alpha h)} - \frac{1}{2} \right] + \frac{I_0(\alpha h)}{4 I_0'(\alpha h)}}{\frac{4 I_0(2\alpha h)}{I_0'(2\alpha h)} - \frac{I_0(\alpha h)}{I_0'(\alpha h)}},$$

It can be shown that $\gamma > 0$ for all αh.

The substitution of (1.51) and (1.52) into (1.11) gives:

$$u = -c + \frac{c\alpha h I_0(\alpha h)}{2 I_0'(\alpha h)} \left[1 - \frac{\eta^2}{h^2} \right] + \frac{\varepsilon c\alpha h I_0(\alpha\eta)\cos\alpha\zeta}{I_0'(\alpha h)}$$

$$+ \varepsilon^2 c\alpha h \left[\frac{I_0(\alpha h)}{2 I_0'(\alpha h)} - \frac{\alpha h I_0'(\alpha h)}{I_0(\alpha h)} \right.$$

$$\left. + \frac{2}{I_0'(2\alpha h)} \left\{ 2\gamma - \frac{\alpha h I_0''(\alpha h)}{2 I_0'(\alpha h)} \right\} I_0(2\alpha\eta)\cos 2\alpha\zeta \right],$$

(1.53)
$$v = c\alpha h \left[\frac{\varepsilon I_0'(\alpha\eta)\sin\alpha\zeta}{I_0'(\alpha h)} \right.$$

$$\left. + \frac{\varepsilon^2}{I_0'(2\alpha h)} \left\{ 2\gamma - \frac{\alpha h I_0''(\alpha h)}{2 I_0'(\alpha h)} \right\} I_0'(2\alpha\eta)\sin 2\alpha\zeta \right].$$

These velocities are tabulated in Tables 1.1 and 1.2 as coefficients of ε, enabling comparison between terms of first and second order for any choice of ε. It can readily be seen from this that for $\varepsilon = 0.1$ the second order term has little effect, so the graphical profiles shown in Fig.1.8

Table 1.1

Centre-line axial velocity coefficients with $\alpha h = 0.25$

ζ	Const	$O(\varepsilon)$	$O(\varepsilon^2)$
0	4.031169	7.937824	9.133103
$\pi/4$	4.031169	5.612889	1.890584
$\pi/2$	4.031169	0.000000	-5.351934
$3\pi/4$	4.031169	5.612889	1.890584
π	4.031169	-7.937824	9.133103
$5\pi/4$	4.031169	5.612889	1.890584
$3\pi/2$	4.031169	0.000000	-5.351934
$7\pi/4$	4.031169	5.612889	1.890584
2π	4.031169	7.937824	9.133103

Table 1.2

Radial coefficients for $\zeta = \frac{1}{4}\pi$ with $\alpha h = 0.25$

η	Const	$O(\varepsilon)$	$O(\varepsilon^2)$ R
0.0	0.000000	0.000000	0.000000
0.1	0.000000	0.070167	0.090559
0.2	0.000000	0.140366	0.181289
0.3	0.000000	0.210631	0.272359
0.4	0.000000	0.280995	0.363939
0.5	0.000000	0.351491	0.456203
0.6	0.000000	0.422152	0.549322
0.7	0.000000	0.493010	0.643474
0.8	0.000000	0.564100	0.738834
0.9	0.000000	0.635454	0.835582
1.0	0.000000	0.707107	0.933902

and 1.9 are presented for the case $\alpha h = 0.25$ and $\varepsilon = 0.3$. From (1.29), the streamfunction is given by

$$(1.54)\qquad \psi + \frac{c\eta^2}{2} = ch^2 \{\frac{\alpha h I_0(\alpha h)}{4I_0'(\alpha h)}[\,1 - \frac{\eta^2}{2h^2}\,]\frac{\eta^2}{h^2} + \frac{\varepsilon\eta I_0'(\alpha\eta)\cos\alpha\zeta}{hI_0'(\alpha h)}$$

$$+ \frac{\varepsilon^2\eta}{h}\frac{1}{2I_0'(2\alpha h)}[\,2\gamma - \frac{\alpha h I_0''(\alpha h)}{2I_0'(\alpha h)}\,]\cos 2\alpha\zeta I_0'(2\alpha\eta)\}\,,$$

where γ is given by (1.52).

The second order streamfunction (1.54) can be compared with the corresponding first order approximation (1.32) given by (1.52).

The second order pressure distribution can be determined by substitution from (1.50) and (1.53) into (1.34). Hence

$$(1.55)\qquad \frac{p - p_0}{\mu c\alpha} = -\frac{2I_0(\alpha h)\alpha\zeta}{\alpha h I_0'(\alpha h)} - R\{\frac{\varepsilon\cos\alpha\zeta}{I_0'(\alpha h)}[\,\frac{I_0(\alpha h)}{2I_0'(\alpha h)}(\alpha h(1 - \frac{\eta^2}{h^2})I_0(\alpha\eta)$$

$$+ \frac{2\eta I_0'(\alpha\eta)}{h}) - I_0(\alpha\eta)\,] + \varepsilon^2[\,\frac{\alpha h}{2I_0'(\alpha h)^2}[\,\sin^2\alpha\zeta I_0'(\alpha\eta)^2$$

$$+ \cos^2\alpha\zeta I_0(\alpha\eta)^2\,] + \frac{1}{I_0'(2\alpha h)}(2\gamma - \frac{\alpha h I_0''(\alpha h)}{2I_0'(\alpha h)})[\,-2I_0(2\alpha\eta)$$

$$+ \frac{I_0(\alpha h)\alpha\eta I_0'(2\alpha\eta)}{2\alpha h I_0'(\alpha h)} + \frac{\alpha h I_0(\alpha h)I_0(2\alpha\eta)}{I_0'(\alpha h)}(1 - \frac{\eta^2}{h^2})\,]\cos 2\alpha\zeta\,]\},$$

where $R = (hc/\nu)$ is the non-dimensional Reynolds number, and γ is given by (1.52). The first order pressure distribution given by (1.35) can be compared with (1.55). In particular, it can be shown that the pressure

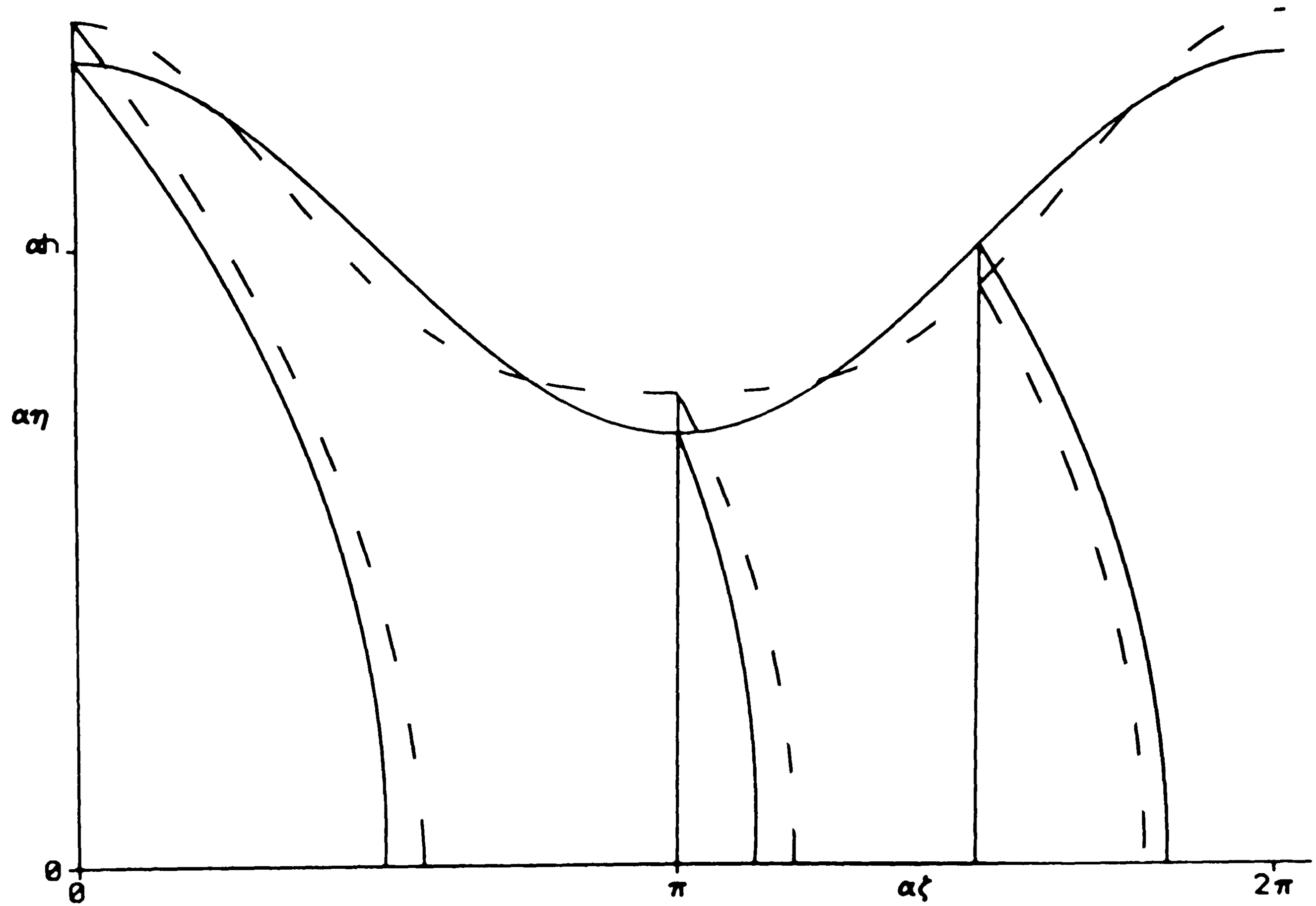

Figure 1.8

Axial velocity distribution with $\alpha h = 0.25$ and $\varepsilon = 0.3$

to ——— $O(\varepsilon)$ and — — — $O(\varepsilon^2)$.

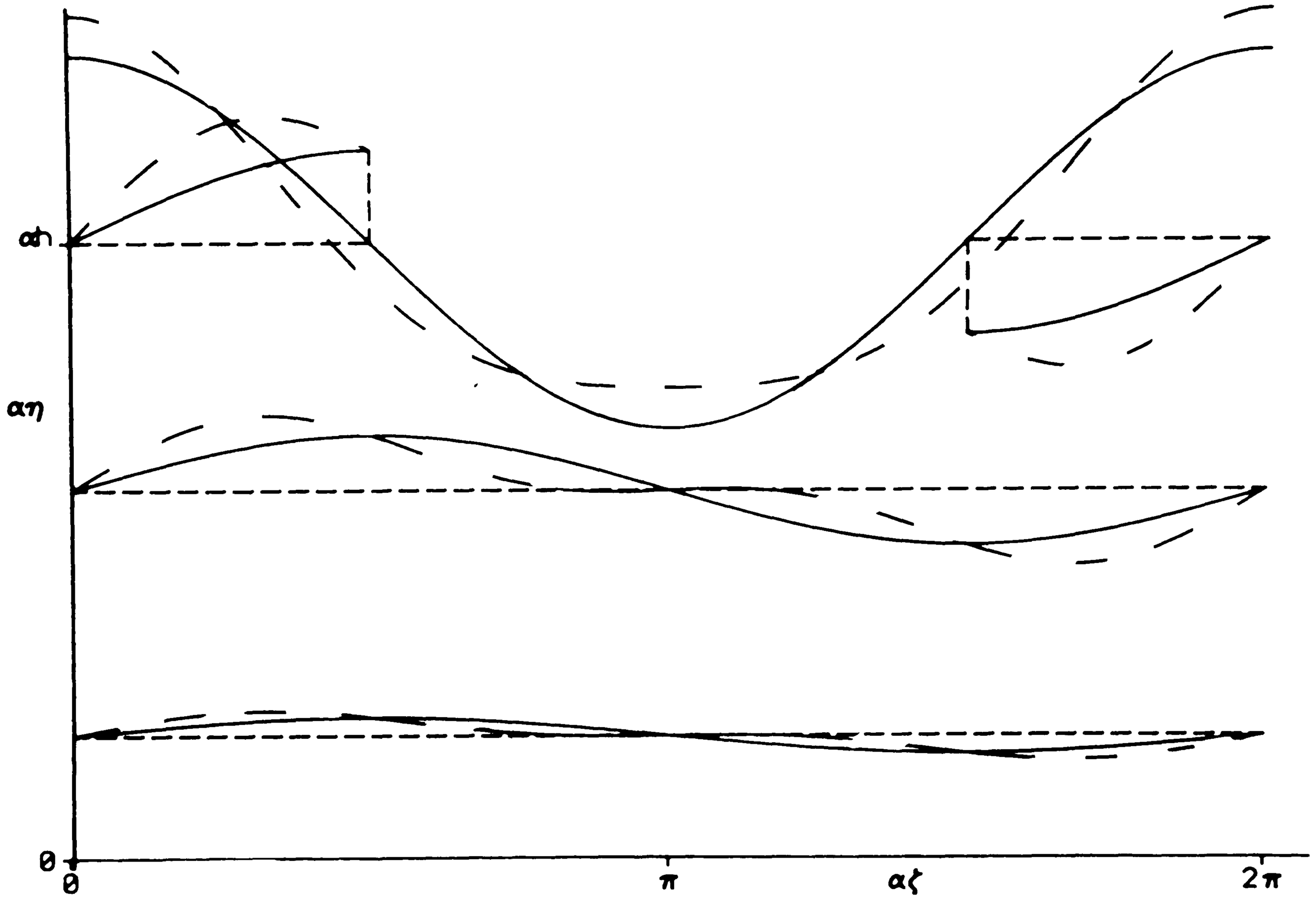

Figure 1.9

Radial velocity distribution with $\alpha h = 0.25$ and $\varepsilon = 0.3$ to ——— $O(\varepsilon)$ and — — — $O(\varepsilon^2)$.

at the boundary which, to first order, is not affected by the peristaltic wave, is modified by the second order term. The term that needs to be added to (1.37) is

$$(1.56)\qquad \frac{\varepsilon^2\alpha hR}{2}\{\sin^2\alpha\zeta+\cos^2\alpha\zeta\left(\frac{I_0(\alpha h)^2}{I_0'(\alpha h)^2}-2\right)\}$$

$$+\varepsilon^2R\left[\gamma-\frac{\alpha hI_0''(\alpha h)}{4I_0'(\alpha h)}\right]\left[\frac{I_0(\alpha h)}{I_0'(\alpha h)}-\frac{4I_0(2\alpha h)}{I_0'(2\alpha h)}\right]\cos 2\alpha\zeta\ .$$

Values of the coefficients in the series for this boundary pressure are presented in Table 1.3. The wave-average mass flux is also only changed by second-order terms, and it can be shown that the average mass flux (1.39) is increased by

$$(1.57)\qquad \frac{\varepsilon^2h^2\pi\rho c\alpha hI_0(\alpha h)}{2I_0'(\alpha h)}$$

Consequently to this order there is a net transport over a wavelength.

CONCLUSION

The axi-symmetric peristaltic problem has been studied using the new exact solution of the Navier-Stokes equations (1.11), which allows a solution to be found that is valid for all Reynolds numbers. For this solution ϕ is described by an asymptotic series in the dimensionless quantity $\varepsilon << 1$, where to first order εh is the amplitude of the

Table 1.3

Coefficients of $\frac{P - P_0}{\mu c \alpha}$ for $\eta = 1.0$ with $\alpha h = 0.25$

ζ	Const	$O(\varepsilon)$	$O(\varepsilon^2)$
0	0.000000	0.000000	3.937581
$\pi/4$	-50.657163	0.000000	4.000081
$\pi/2$	-101.314326	0.000000	4.062581
$3\pi/4$	-151.971489	0.000000	4.000081
π	-202.628651	0.000000	3.937581
$5\pi/4$	-253.285814	0.000000	4.000081
$3\pi/2$	-303.942977	0.000000	4.062581
$7\pi/4$	-354.600140	0.000000	4.000081
2π	-405.257303	0.000000	3.937581

peristaltic wave. The solution and flow characteristics have been found to $O(\varepsilon^2)$.

A good correlation, typified by the streamline patterns, has been found between the flow features of this solution and those obtained using large or small Reynolds number approximations. In addition some interesting observations have been made by considering the limiting cases $\alpha h \to 0$ and $\alpha h \to \infty$ of the velocity components. The former case shows good agreement with solutions for small Reynolds number and the latter demonstrates a boundary layer-like effect.

The higher-order solution has been studied to clarify the effects of the peristaltic wave on the average mass flux and boundary pressure, which are not altered to first-order but which do have correction terms to $O(\varepsilon^2)$.

Throughout this work a Reynolds number of $(ch/\nu)\alpha h$ has been used. The work clearly demonstrates that the important parameter combination is αh and consequently that in obtaining numerical solutions or series expansions, the appropriate Reynolds number is $(ch/\nu)\alpha h$ rather than (ch/ν).

REFERENCES

1. LYKOUDIS, P.S. and ROOS, R. , The fluid mechanics of the ureter from the lubrication theory point of view, J. Fluid Mech., Vol. 43, 1970, pp 661-674.

2. LEW, H.S., FUNG, Y.C. and LOWENSTEIN, C.B. , Peristaltic carrying and mixing of chyme in small intestine, J. Biomechanics, Vol. 4, 1971, pp 297-315.

3. MANTON, M.J. , Long wavelength peristaltic pumping at low Reynolds numbers, J. Fluid Mech., Vol 68, 1975, pp 467-476.

4. LIRON, N. , On peristaltic flow and its efficiency, Bull. Math. Biol, Vol. 38, 1976, pp 573-596.

5. MAHRENHOLTZ, O.H. and ZIMMERMAN, P.U. , The influence of the wall form on peristaltic transport, Biorheology, Vol. 15, 1978, pp 501-511.

6. BURNS, J.C. and PARKS, T. , Peristaltic motion, J. Fluid Mech., Vol. 29, 1967, pp 731-743.

7. FUNG, Y.C. , and YIH, C.S. , Peristaltic Transport, J. Appl. Mech., Vol. 35, 1968, pp 669-675.

8. JAFFRIN, M.Y. and SHAPIRO, A.H. , Peristaltic pumping, A. Rev. Fluid Mech., Vol. 3, 1971, pp 13-36.

9. BROWN, T.D. and HUNG, T.K. , Computational and experimental investigation of two-dimensional non-linear peristaltic flows, J Fluid Mech., Vol 83, 1977, pp 249-272.

10. AYUKAWA, K. ,KAWA, T. and KIMURA, M. , Streamlines and pathlines in peristaltic flows at high Reynolds numbers, Bull. Japan Soc. Mech. Engrs., Vol. 24, 1981, pp 948-955.

11. TAKABATAKE, S. and AYUKAWA, K. ,Numerical study of two-dimensional peristaltic flows, J.Fluid Mech., Vol. 122, 1982, pp 439-465.

12. BERGMAN, H. , The Ureter, Harpers and Row, New York, 1967.

13. LYKOUDIS, P.S. , The ureter as a peristaltic pump, Urodynamics, Academic Press, New York, 1971.

14. BUGLIARELLO, G. and SEVILLA, J. ,Velocity distribution and other characteristics of steady and pulsatile blood flow in fine glass tubes, Biorheology, Vol. 7, 1970, pp 85-107.

15. GOLDSMITH, H.L. and SKALAK, R. , Hemodynamics, Annual Rev. of Fluid Mech., 1975, p213.

16. ZIEN, T.F. and OSTRACH, S. , A long wave approximation to peristaltic motion, J. Biomechanics, Vol. 3, 1970, pp 63-75.

17. WEINBERG, S.L. ,ECKSTEIN, E.C. and SHAPIRO, A.H. , An experimental study of peristaltic pumping, J Fluid Mech. ,Vol. 49, 1971, pp 461-479.

18. TONG, P. and VAWTER, D. , An analysis of peristaltic pumping, J. Appl. Mech., Vol. 39, 1972, pp 857-862.

19. GUPTA, B.B. and SHESHADRI, V. , Peristaltic pumping in non-uniform tubes, J. Biomechanics, Vol. 9,1976, pp 105-109.

20. GUHA, S.K. , KAUR, H. and AHMED, A.H. , Mechanisms of spermatic fluid transport in the vas deferens, Med. Biol. Engng., Vol. 13, 1975, pp 518-522.

21. BERTUZZI, A. MANCINELLI, R. ,PESCATORI, M. and SALINARI, S. ,An analysis of the peristaltic reflex, Bul. Cybernetics, Vol. 35, 1979, pp 205-212.

22. HANIN, M. , The flow through a channel due to transversely oscillating walls, Israel J. Tech., Vol. 6, 1968, pp 67-71.

23. SHAPIRO, A.H., JAFRIN, M.Y. and WEINBERG, S.L. , Peristaltic pumping with long wavelengths at low Reynolds numbers, J. Fluid Mech., Vol. 37, 1969, pp 799-825.

24. YIN, F. and FUNG, Y.C. Peristaltic waves in circular cylindrical tubes, J. Appl. Mech., Vol. 36, 1969, pp 579-587.

25. CHOW, T.S. Peristaltic transport in a circular cylindrical pipe, J. Appl. Mech., Vol. 37, pp 901-905.

26. HUNG, T.K. and BROWN, T.D. , Solid particle motion in two dimensional peristaltic flows, J. Fluid Mech., Vol. 73, 1976, pp 77-97.

27. TERRILL, R.M. , Laminar Flow in a porous tube, Trans. ASME, Vol. 105, 1983, pp 303-307.

28. TERRILL, R.M. , A note on laminar flow through a porous pipe with slip, IMA Journ. of Appl. Maths, Vol. 33, 1984, pp 169-174.

29. TERRILL, R.M. , Fluid flow in a region bounded by a porous cylindrical pipe, Phy. of Fluids, Vol. 29, 1986, pp 625-627.

30. TERRILL, R.M. , Laminar flows in circular pipes whose cross-sectional area varies slowly in the axial direction, Phy. of Fluids, to be published.

31. MITTRA, T.K. and PRASAD, S.N. , On the influence of wall properties and Poiseuille flow in peristalsis, J. Biomechanics, Vol. 6, 1973, pp 681-693.

32. AIKMAN, D.P. and ANDERSON, W.P. , A quantitative investigation of a peristaltic model for phloem translocation, Ann. of Botany, Vol. 35, 1971, pp 761-772.

33. JAFFRIN, M.Y. , Inertia and streamline curvature effects on peristaltic pumping, Int. J. Engng. Sci., Vol. 11, 1973, pp 681-699.

SECTION 2.

VARIABLE WIDTH

INTRODUCTION

This section considers in detail the problem of the steady, laminar, axi-symmetric flow of an incompressible fluid along circular cylindrical pipes of slowly varying cross-sectional area. An application of the new solution presented in [1] was briefly sketched by Terrill [2], however, it is important to develop some of these ideas and results further. The method used in [2] considers the radius R and the potential function ϕ to be series expansions in a non-dimensional axial variable. This method, if in a slightly amended form, will be employed in this section. It soon becomes apparent that there is an infinite number of solutions, or eigenvalues, for each term in the series for ϕ. To investigate the effect of using all possible solutions for each term, as opposed to the effect of higher order terms, it is necessary initially to consider the two problems independently.

Section 2.1 investigates the effect of using all the possible solutions, by considering the first order solution to give some understanding of boundary shapes and their corresponding velocity profiles. The solution is illustrated by considering two special cases; that of flow along a parallel pipe with different upstream and downstream radii, and flow along a parallel pipe with a small bulge or constriction. Since this is the first order solution, the extent of the variation of the wall shape needs to be small.

The effect of higher order terms is presented in Section 2.2. For simplicity, this is investigated initially by using only one particular

eigenvalue for each term in the series. As well as throwing light on the series, this case demonstrates the power of analytic programming and introduces an improved approach to the convergence of series which could have widespread applications. The section is concluded with a brief presentation of the complicated general solution which is obtained by combining both cases. This includes 'cross' terms, which occur as a result of the presence of more than one eigenvalue.

FORMULATION OF THE PROBLEM

Consider the steady, laminar, axi-symmetric motion of an incompressible fluid through a tube of radius R(z). Choose a cylindrical polar co-ordinate system (r,θ,z) where the axis Oz lies along the centre of the tube, r is the distance measured radially and θ is the azimuthal angle. Let u and v be the velocity components in the directions of z and r increasing respectively. Then for axi-symmetric flow, the Navier-Stokes equations are

$$u\frac{\partial u}{\partial z} + v\frac{\partial u}{\partial r} = -\frac{1}{\rho}\frac{\partial p}{\partial z} + \nu\nabla^2 u \ ,$$

$$u\frac{\partial v}{\partial z} + v\frac{\partial v}{\partial r} = -\frac{1}{\rho}\frac{\partial p}{\partial r} + \nu\left(\nabla^2 v - \frac{v}{r^2}\right) \ , \tag{2.1}$$

with the equation of continuity

$$\frac{\partial}{\partial r}(rv) + r\frac{\partial u}{\partial z} = 0 \quad , \tag{2.2}$$

where

$$\nabla^2 \equiv \frac{\partial^2}{\partial r^2} + \frac{1}{r}\frac{\partial}{\partial r} + \frac{\partial^2}{\partial z^2} \quad , \tag{2.3}$$

and where p is the pressure, ρ the density and ν is the kinematic viscosity.

The boundary conditions for this axi-symmetric flow are

$$v = 0 \qquad \text{on } r = 0 \qquad \text{(symmetry)}, \tag{2.4}$$

and

$$\begin{aligned} u &= 0 \quad , \\ & \qquad \text{on } r = R(z) \\ v &= 0 \quad , \end{aligned} \tag{2.5}$$

where R(z) is the pipe boundary.

It has been shown by [1] that the equations (2.1) and (2.2) are satisfied by

$$u = \lambda(a^2 - r^2) + \frac{\partial \phi}{\partial z} \quad , \qquad v = \frac{\partial \phi}{\partial r} \quad , \tag{2.6}$$

where λ and a are arbitrary constants, provided $\phi(\zeta,\eta)$ satisfies Laplace's equation

$$\nabla^2\phi = 0 \quad . \tag{2.7}$$

However, the profile of the tube, R(z), is not known and it is convenient to select co-ordinates (η,ζ) so that the boundary becomes the surface $\eta = 1$, that is

$$\zeta = z \quad , \qquad \eta = \frac{r}{R(z)} \quad . \tag{2.8}$$

In this new frame the solution, (2.7), is

$$\begin{aligned} u &= \lambda[a^2 - \eta^2 R(\zeta)^2] + \frac{\partial\phi}{\partial\zeta} - \eta\frac{R'(\zeta)}{R(\zeta)}\frac{\partial\phi}{\partial\eta} \quad , \\ v &= \frac{1}{R(\zeta)}\frac{\partial\phi}{\partial\eta} \quad , \end{aligned} \tag{2.9}$$

where ' denotes differentiation with respect to ζ, provided that

$$\nabla^2\phi = 0 \quad , \tag{2.10}$$

where

$$\nabla^2 \equiv \frac{\partial^2}{\partial\eta^2} + \frac{1}{\eta}\frac{\partial}{\partial\eta} + R(\zeta)^2\frac{\partial^2}{\partial\eta^2} + R'(\zeta)^2\eta^2\frac{\partial^2}{\partial\eta^2}$$

(2.11)

$$+ [2R'(\zeta)^2 - R(\zeta)R''(\zeta)]\eta\frac{\partial}{\partial\eta} - 2R(\zeta)R'(\zeta)\eta\frac{\partial^2}{\partial\eta\partial\zeta} .$$

On substituting for u and v from (2.9) into the boundary conditions (2.4) and (2.5) the relations

$$\frac{\partial\phi}{\partial\eta} = 0 \qquad \text{on } \eta = 0 \text{ and } \eta = 1 ,$$

(2.12)

$$\frac{\partial\phi}{\partial\zeta} = -\lambda[a^2 - R(\zeta)^2] \qquad \text{on } \eta = 1 ,$$

are obtained. These form the boundary conditions from which, first the potential function and then the wall profile, can be found.

2.1 THE FIRST ORDER SOLUTION

The first order solution will now be derived from (2.10) and (2.11) using boundary conditions (2.12). The shape of the wall R(z), has now to be determined, and it should be stressed that there are only particular wall shapes which will yield solutions vaild for all Reynolds numbers. However, these flows, of which Poiseuille is a special case, are physically extremely interesting. Writing the wall and the potential function as series in a small parameter ε, then

$$R = R_0(1 + \varepsilon R_1) \quad , \tag{2.13}$$

and

$$\phi = \lambda \varepsilon \phi_1(\eta, z) \quad . \tag{2.14}$$

From (2.12) R_0, the first approximation to the pipe radius, is equal to a. Substituting (2.13) and (2.14) into (2.10)-(2.12) yield to first order

$$\frac{\partial^2 \phi_1}{\partial \eta^2} + \frac{1}{\eta}\frac{\partial \phi_1}{\partial \eta} + R_0^2 \frac{\partial^2 \phi_1}{\partial z^2} = 0 \quad , \tag{2.15}$$

subject to the boundary conditions

$$\frac{\partial \phi_1}{\partial \eta} = 0 \quad \text{on } \eta = 0,\ 1, \tag{2.16}$$

and

$$(2.17) \qquad \frac{\partial \phi_1}{\partial z} = 2R_0^2 R_1 \quad \text{on } \eta = 1.$$

Solving produces

$$\phi_1 = \{A\exp(\alpha z/R_0) + B\exp(-\alpha z/R_0)\}\{J_0(\alpha\eta) + CY_0(\alpha\eta)\} ,$$

where A, B, C and α are arbitrary constants to be determined and J_0 and Y_0 are Bessel functions of the first and second kind respectively. As $Y_0(\alpha\eta)$ is infinite at $\eta = 0$, then $C \equiv 0$ and the boundary condition on ϕ_1 at $\eta = 0$ is automatically satisfied. Applying condition (2.16) demands that $J_1(\alpha) = 0$; hence $\alpha = \alpha_n$ are the zeros of J_1, namely 3.8317, 7.0156 etc. Thus, the general solution of (2.15) can be written

$$(2.18) \qquad \phi_1 = \sum_{n=1}^{\infty} [A_n\exp(\alpha_n z/R_0) + B_n\exp(-\alpha_n z/R_0)]J_0(\alpha_n\eta).$$

From (2.17) it can readily be seen that

$$(2.19) \qquad R_1 = \frac{1}{2R_0^3}\sum_{n=1}^{\infty} [A_n\exp(\alpha_n z/R_0) - B_n\exp(-\alpha_n z/R_0)]\alpha_n J_0(\alpha_n).$$

Substituting for (2.18) and (2.19) into (2.6) yields, to first order,

$$(2.20)\qquad \frac{u}{\lambda R_0^{\,2}} = (1-\eta^2) - \frac{\varepsilon}{R_0^{\,3}}\sum_{n=1}^{\infty}\alpha_n J_0(\alpha_n)\left[A_n\exp(\alpha_n z/R_0) - B_n\exp(-\alpha_n z/R_0)\right]\left[\eta^2 - \frac{J_0(\alpha_n\eta)}{J_0(\alpha_n)}\right],$$

and

$$(2.21)\qquad \frac{v}{\lambda R_0^{\,2}} = -\frac{\varepsilon}{R_0^{\,3}}\sum_{n=1}^{\infty}\alpha_n\left[A_n\exp(\alpha_n z/R_0) + B_n\exp(-\alpha_n z/R_0)\right]J_1(\alpha_n\eta),$$

Clearly $\varepsilon = 0$ is a cylindrical pipe of constant cross-section and the solution reduces to Poiseuille flow.

To understand the first order solution, some simple examples will now be considered.

CASE 1.

A Semi-Infinite Pipe, the radius of which changes from R_0 for large positive z to $R_0 + \varepsilon^*$ at $z = 0$.

Consider a semi-infinite pipe ($0 \le z \le \infty$) of radius $R(z)$ such that $R(z) \to R_0$, and $R = R_0 + \varepsilon^*$ at $z = 0$, where ε^* is small. It can readily be seen from (2.19) that the condition $R_1 \to 0$ as $z \to \infty$ demands that $A_n \equiv 0$ for all n. Thus, to first order, the wall is given by

$$(2.22)\qquad R = R_0\left[1 - \varepsilon\sum_{n=1}^{\infty}x_n\exp(-\alpha_n z/R_0)\right],$$

where $x_n = \dfrac{\alpha_n B_n J_0(\alpha_n)}{2R_0^3}$ and the axial velocity is given by

$$\frac{u}{\lambda R_0^2} = (1 - \eta^2) + 2\varepsilon \sum_{n=1}^{\infty} \left[\eta^2 - \frac{J_0(\alpha_n \eta)}{J_0(\alpha_n)}\right] x_n \exp(-\alpha_n z/R_0) \quad . \tag{2.23}$$

The unknown constants x_n depend on the constraints on the wall shape that are imposed. Suppose that in the neighbourhood of $z = 0$, $R(z)$ is parallel to the axis of the pipe. To achieve this, $R'(z)$ and higher order derivatives can be chosen to be zero at $z = 0$. The number of conditions N, defines the number of constraints x_n that can be uniquely determined. Thus at $z = 0$,

$$R = R_0 + \varepsilon^*$$

and

$$R' = R'' = \ldots = R^{(N-1)} = 0. \tag{2.24}$$

Taking $x_j \equiv 0$ for $j \geq N + 1$, then (2.24) implies that the x_n are solutions of

$$\sum_{n=1}^{N} x_n = -\frac{\varepsilon^*}{\varepsilon R_0} \quad , \quad \sum_{n=1}^{N} \alpha_n{}^k x_n = 0 \qquad k = 1, 2, \ldots, N-1.$$

For N small, the exact solution can be easily obtained for $N = 2$,

$$x_1 = \frac{\alpha_2 \varepsilon^*}{\varepsilon R_0(\alpha_1 - \alpha_2)} \quad , \quad x_2 = \frac{-\alpha_1 \varepsilon^*}{\varepsilon R_0(\alpha_1 - \alpha_2)} \quad , \quad x_j = 0 \qquad j \leq 3.$$

However, for larger values of N, the system of differential equations is solved by using a numerical matrix inversion routine from the NAg library. This is a software development covering the full range of possible numerical requirements. This allows the user an algorithm of guaranteed efficiency and stability, giving good results economically. Values of x_n are given in Table 2.1 for N = 1,4,6,10 with $\varepsilon = 0.005$ and $\varepsilon^*/R_0 = 0.005$. Figure 2.1 illustrates the wall profiles for these values of N, and shows that as N increases, the wall is parallel to the axis near z = 0, for a larger range of z. Substituting the obtained values of x_n into (2.23) gives the axial velocities for each case. Figures 2.2-2.5 show these velocity profiles when N = 6 and 10, $\varepsilon = 0.005$ and $|\varepsilon^*/R_0| = 0.005$ for both converging (Figs. 2.3 and 2.5), and diverging (Figs. 2.2 and 2.4) boundaries, (clearly taking ε^* negative gives a narrowing pipe). In these figures $u/\lambda R_0^2$ is plotted against η for specific values of z/R_0, λ negative gives Poiseuille flow into a contracting or expanding pipe. It can be seen that deviation from the parabolic profile occurs earlier, that is, at larger values of z, for larger values of N. This is expected since using more terms in the series accelerates the departure from the limit $R = R_0$. The most marked effect of the change of radius on the flow is the change in velocity on the axis of the pipe. For $\varepsilon^* > 0$, reflux occurs if $N \geq 4$; when N = 6 the back flow begins near $z = 0.13R_0$ and when N = 10 near $z = 0.33R_0$.

Table 2.1

Values for the coefficients x_n, when $\varepsilon = 0.005$ and $\varepsilon^*/R_0 = 0.005$.

	N = 1	N = 4	N = 6	N = 10
x_2	-	1.63781, 1	4.44159, 1	1.48450, 2
x_3	-	-1.13544, 1	-6.16956, 1	-4.13399, 2
x_4	-	2.89973	4.73137, 1	7.40684, 2
x_5	-	-	-1.91924, 1	-9.02066, 2
x_6	-	-	3.22964	7.59395, 2
x_7	-	-	-	-4.37165, 2
x_8	-	-	-	1.64864, 2
x_9	-	-	-	-3.67993, 1
x_{10}	-	-	-	3.69313

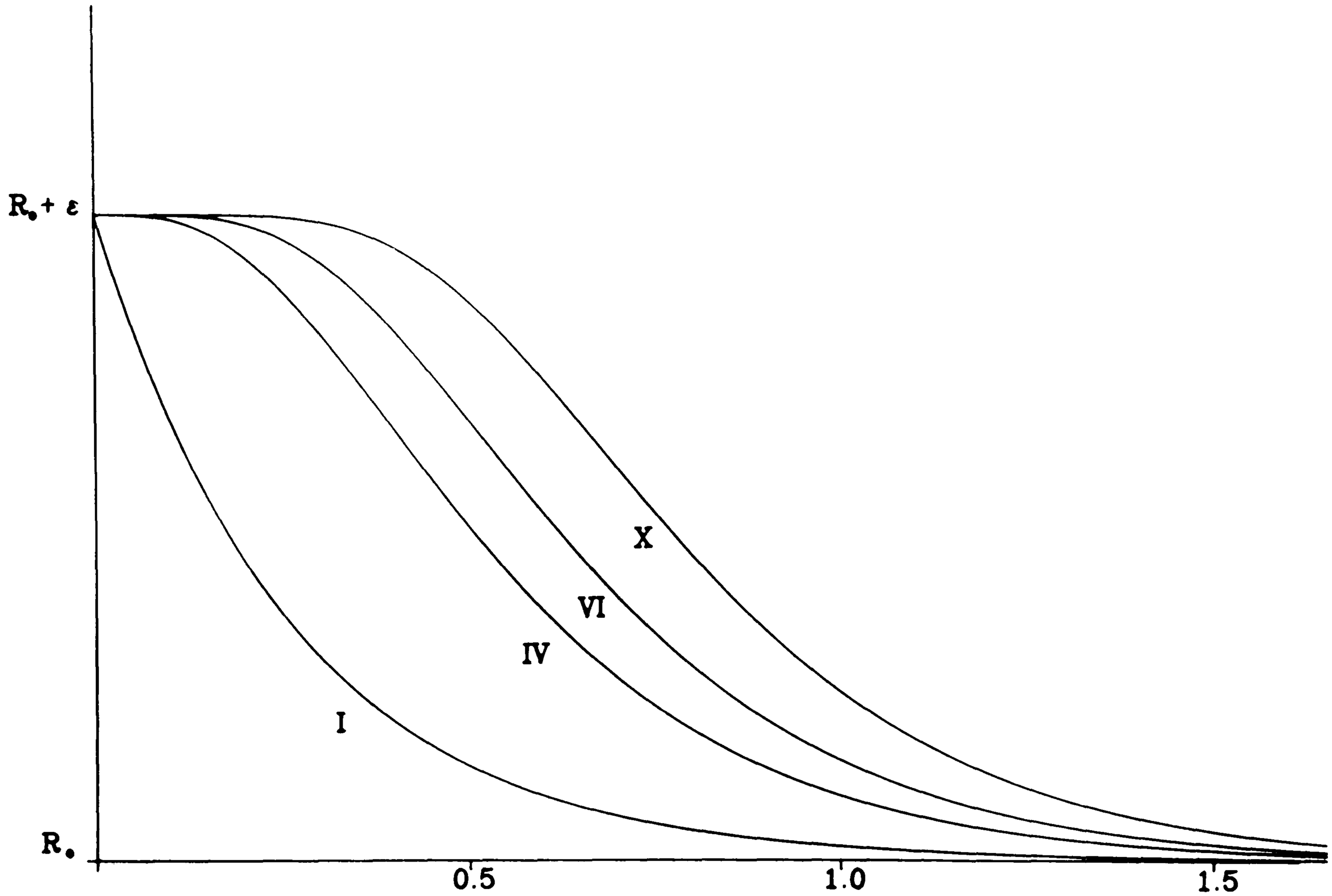

Figure 2.1

Wall profiles for N = 1,4,6,10 with $\varepsilon = 0.005$ and $\varepsilon^*/R_0 = 0.005$.

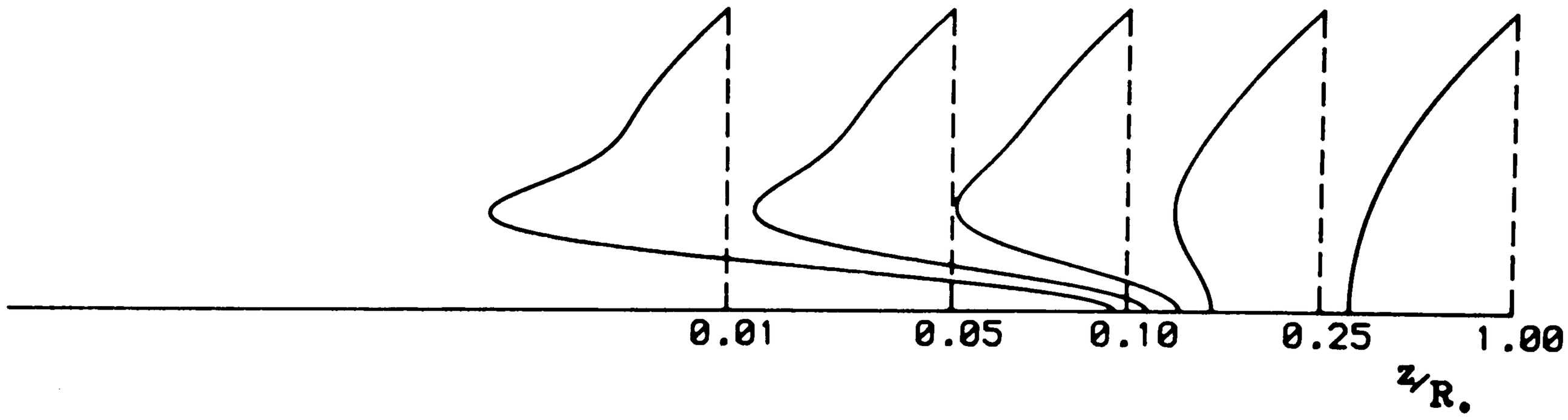

Figure 2.2

Axial velocity profiles for N = 6 with $\varepsilon = 0.005$ and $\varepsilon^*/R_0 = 0.005$.

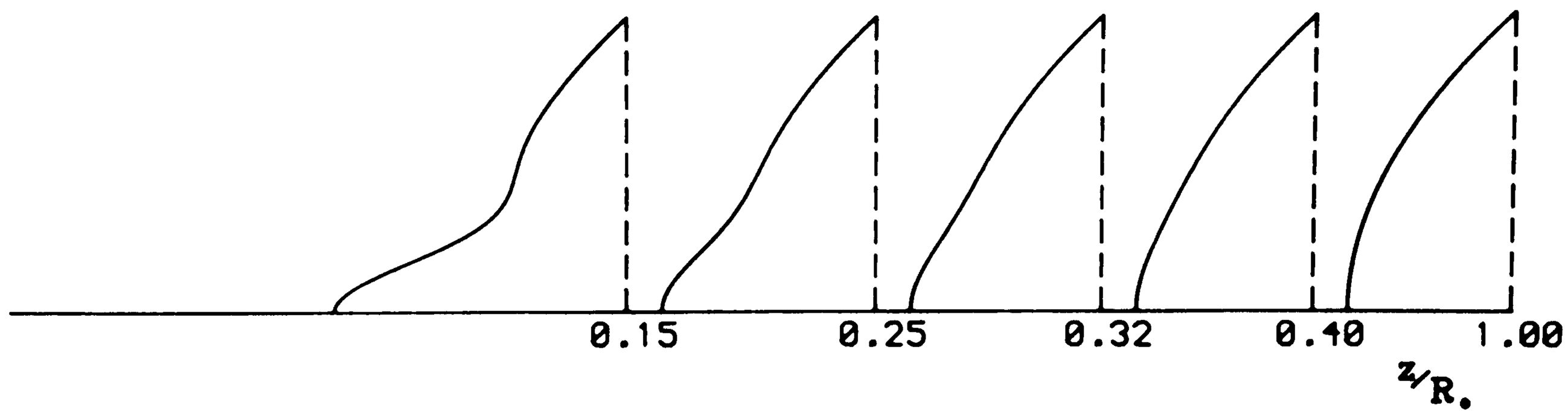

Figure 2.3

Axial velocity profiles for N = 6 with $\varepsilon = 0.005$ and $\varepsilon^*/R_0 = -0.005$.

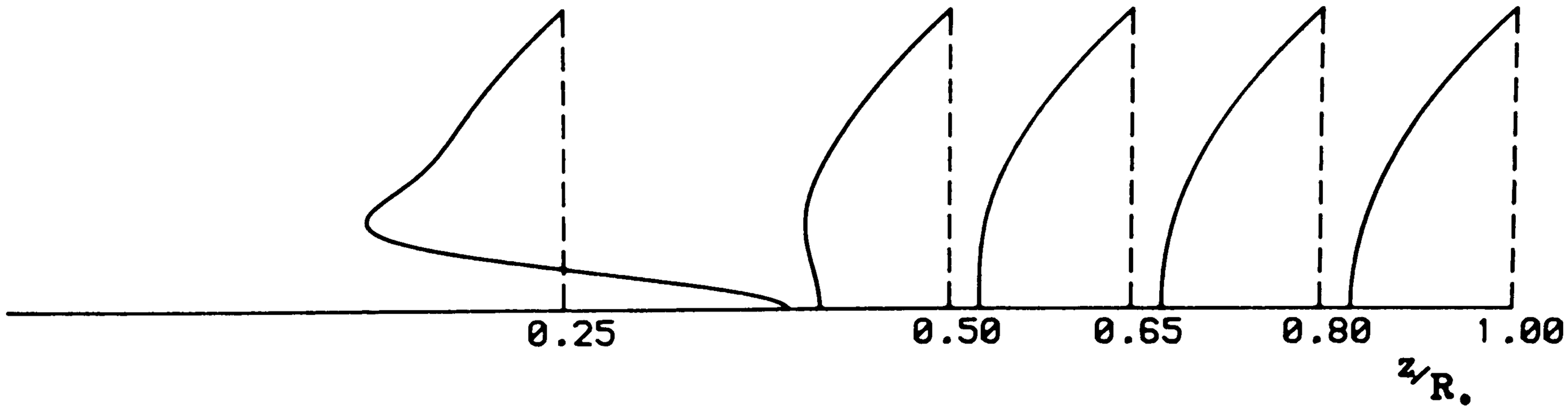

Figure 2.4

Axial velocity profiles for N = 10 with $\varepsilon = 0.005$ and $\varepsilon^*/R_0 = 0.005$.

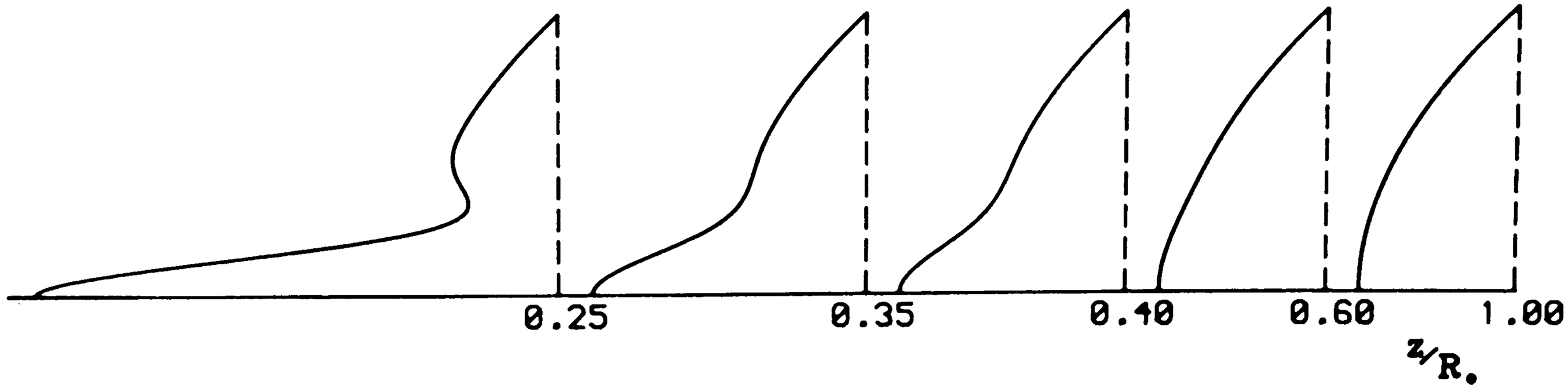

Figure 2.5

Axial velocity profiles for N = 10 with $\varepsilon = 0.005$ and $\varepsilon^*/R_0 = -0.005$.

CASE 2.

A Semi-Infinite Pipe with radius $R = R_0$ at both $z = 0$ and $z = \infty$.

Consider a semi-infinite pipe ($0 \leq z \leq \infty$) with $R = R_0$ at $z = 0$ and $R \to R_0$ as $z \to \infty$, and let $R(z) - R_0$ be small, but non-zero, for some intermediate values of z. Clearly, the constants x_n in (2.22) can be chosen such that R(z) and some of its derivatives are specified at certain values of z in $0 \leq z < \infty$. The most interesting case is for the pipe to have the same radius in a large neighbourhood of $z = 0$ as it has $z \to \infty$, and to require that the pipe passes through a specified point. This is achieved by choosing

$$
\begin{aligned}
& R \to R_0 && \text{at } z \to \infty \ , \\
& R = R_0 && \text{at } z = 0 \ , \\
(2.25) \qquad & R = R_0 + \varepsilon^* && \text{at } {}^{z}/_{R_0} = z^* \ , \\
& R' = \ldots = R^{(N-1)} && \text{at } z = 0 \ ,
\end{aligned}
$$

where N is an integer, ε^* is small and the boundary passes through $(z^*, R_0 + \varepsilon^*)$. The system of simultaneous equations generated by (2.25) and (2.22) are

$$
\sum_{n=1}^{N} x_n = 0 \ , \quad \sum_{n=1}^{N} x_n \exp(-\alpha_n z^*) = - \frac{\varepsilon^*}{\varepsilon R_0} \ ,
$$

and

$$
\sum_{n=1}^{N} \alpha_n{}^k x_n = 0 \qquad k = 1, \ \ldots, \ N-2 \ .
$$

Table 2.2 lists the values obtained for x_n together with the position of the peak when $\varepsilon = 0.001$, ${}^{\varepsilon^*}/_{R_0} = 0.001$, $z^* = 0.5$ and N is chosen to be

4,8,12 and 15. Figure 2.6 shows the boundaries for these values, and illustrates the increase in magnitude of the maximum displacement and its migration in the direction of z increasing with increasing N. The larger the value of N that is chosen, the further the peak, or trough, in the the pipe is from $z = 0$. This is caused by increasing the flatness at $z = 0$ by making more derivatives vanish there. The axial velocity is given by the substitution of the values obtained for x_n into (2.23). Taking $\lambda < 0$ and plotting $u/\lambda R_0^2$ against η for specific values of z/R_0 for N = 4,8,12 and 15 demonstrates the deformation of the parabolic flow from infinity caused by the change in pipe radius.

Again, the addition of more terms to the series causes the radius to grow (for $\varepsilon^* > 0$) or contract (for $\varepsilon^* < 0$) from $R = R_0$, and for the radius to reach its maximum or minimum value earlier, that is, for larger z. For $\varepsilon^* > 0$, Figures 2.7-2.10 illustrate this trend and as N increases, the reflux begins at an earlier cross-section. Near the axis of the pipe and, to a lesser extent, the outer wall, the axial velocity decreases with decreasing z; however, for $0.4 < \eta < 0.6$ there is a marked increase. For $\varepsilon^* < 0$, this behaviour is reversed, and this is illustrated in Figures 2.11-2.14.

The wall profiles and their solutions that have been presented in this section will prove useful in the understanding of higher order solutions presented in Section 2.2.

Table 2.2

Values for the coefficients x_n, when $\varepsilon = 0.001$, $\varepsilon^*/R_0 = 0.001$, with the boundary passing through (0.5,1.001).

	N = 1	N = 4	N = 6	N = 10
x_1	4.04628, 1	1.01734, 2	2.56573, 2	5.14026, 2
x_2	-1.22272, 2	-7.23208, 2	-2.88070, 3	-7.36612, 3
x_3	1.22923, 2	2.18805, 3	1.45541, 4	4.84335, 4
x_4	-4.11133, 1	-3.66525, 3	-4.39291, 4	-1.95031, 5
x_5	-	3.67749, 3	8.82081, 4	5.38663, 5
x_6	-	-2.21170, 3	-1.23837, 5	-1.08060, 6
x_7	-	7.38525, 2	1.24093, 5	1.62454, 6
x_8	-	-1.05646, 2	-8.87788, 4	-1.85983, 6
x_9	-	-	4.44455, 4	1.62958, 6
x_{10}	-	-	-1.48304, 4	-1.08759, 6
x_{11}	-	-	2.96859, 3	5.44295, 5
x_{12}	-	-	-2.70065, 2	-1.98079, 5
x_{13}	-	-	-	4.95524, 4
x_{14}	-	-	-	-7.62779, 3
x_{15}	-	-	-	5.45113, 2
z/R_0	0.39344	0.60491	0.73082	0.80057
Peak R	1.00217	1.00219	1.00330	1.00500

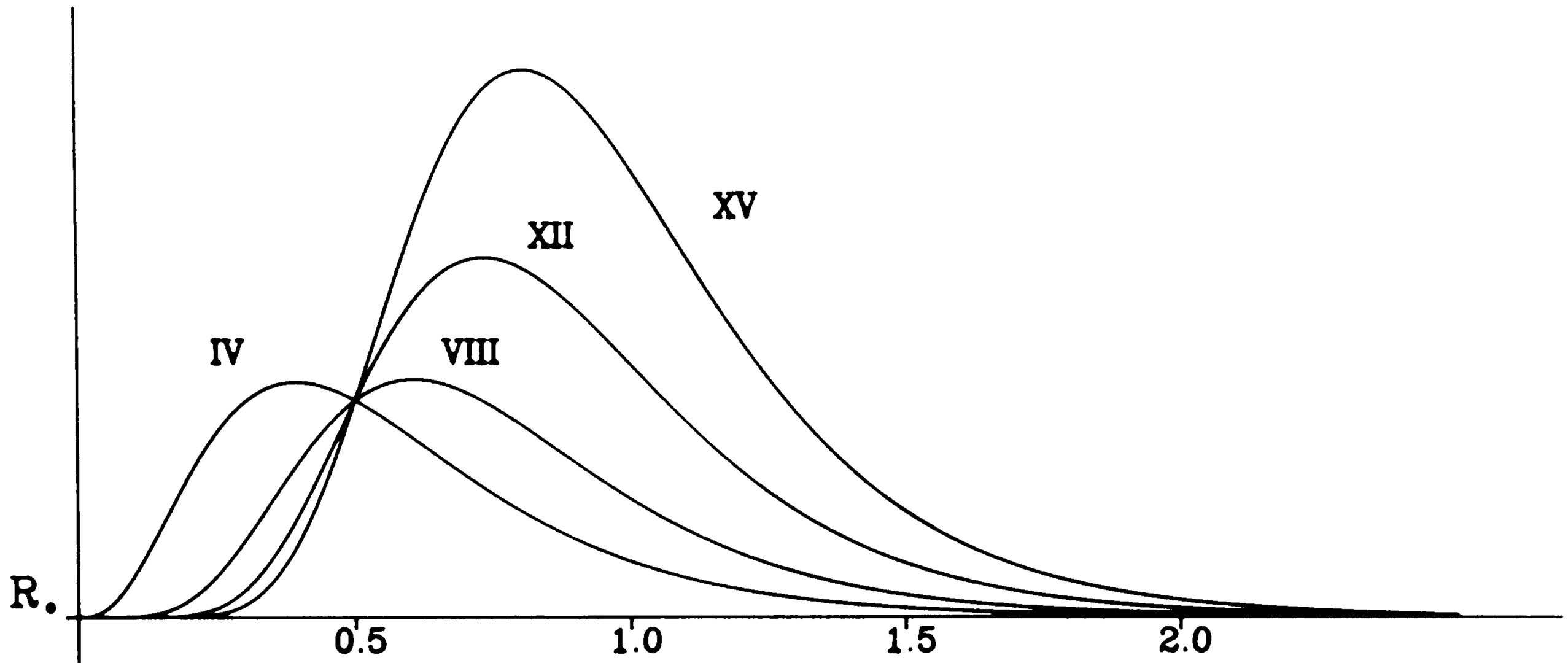

Figure 2.6

Wall profiles for N = 4,8,12,15 with $\varepsilon = 0.001$, $\varepsilon^*/R_0 = 0.001$ with the boundary passing through (0.5,1.001).

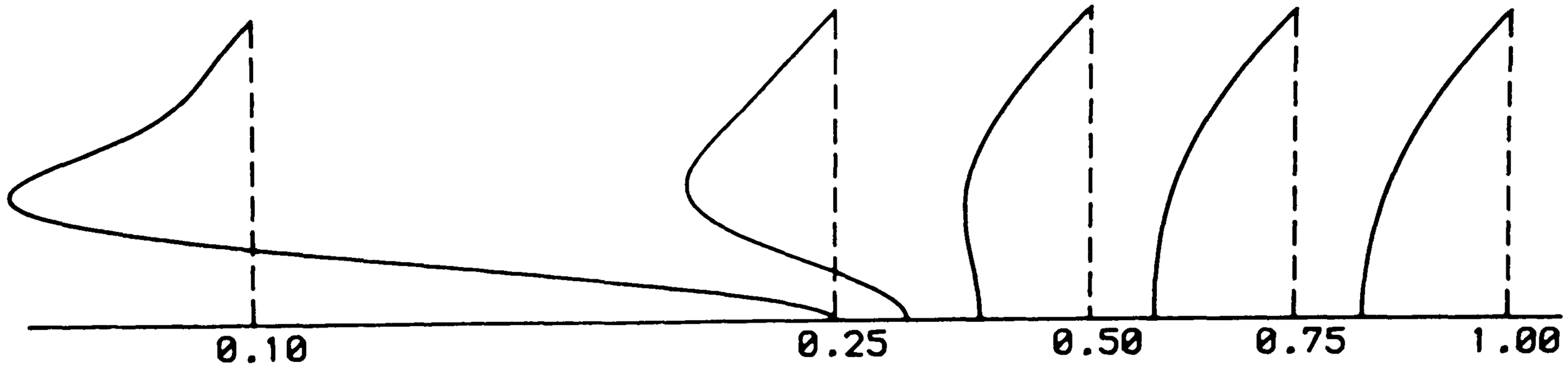

Figure 2.7

Axial velocity profiles for N = 4 with $\varepsilon = 0.001$, $\varepsilon^*/R_0 = 0.001$ and passing through (0.5,1.001).

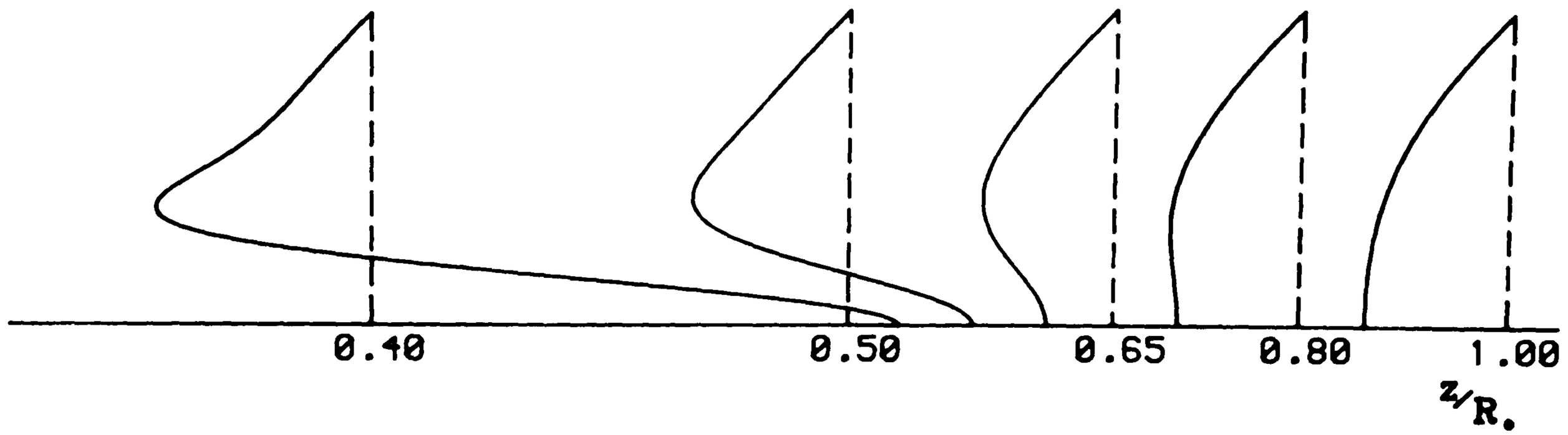

Figure 2.8

Axial velocity profiles for N = 8 with $\varepsilon = 0.001$, $\varepsilon^*/R_0 = 0.001$ and passing through (0.5,1.001).

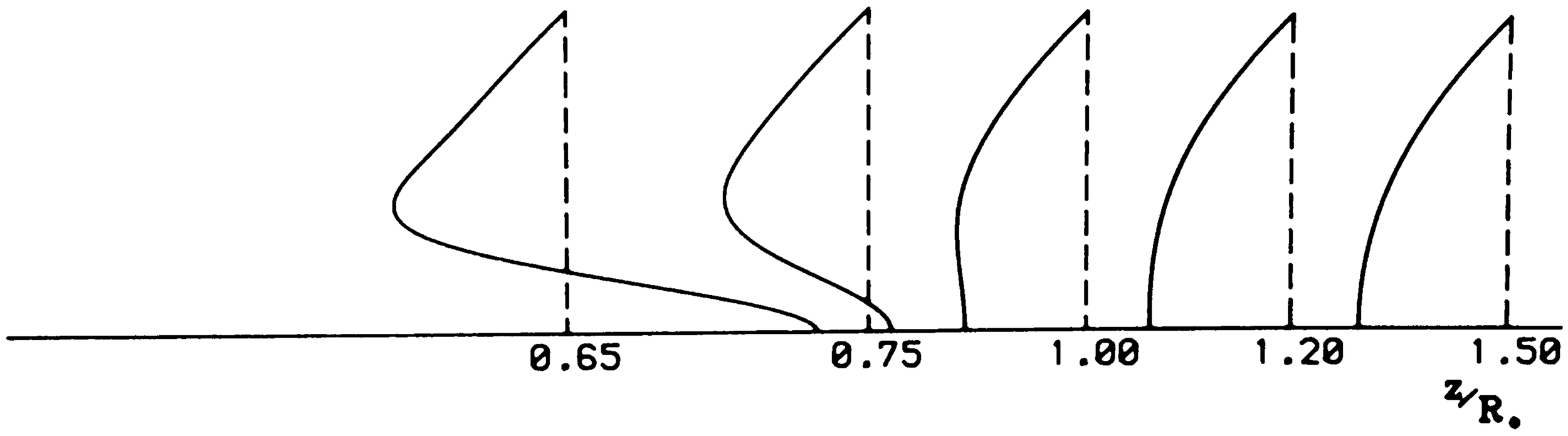

Figure 2.9

Axial velocity profiles for N = 12 with $\varepsilon = 0.001$, $\varepsilon^*/R_0 = 0.001$ and passing through (0.5,1.001).

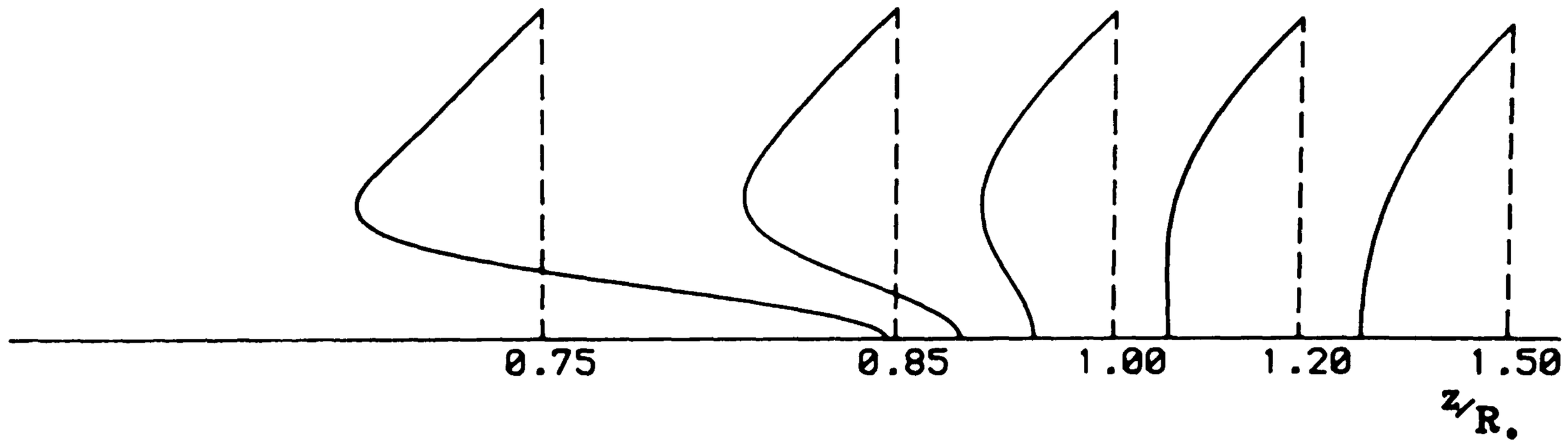

Figure 2.10

Axial velocity profiles for N = 15 with $\varepsilon = 0.001$, $\varepsilon^*/R_0 = 0.001$ and passing through (0.5,1.001).

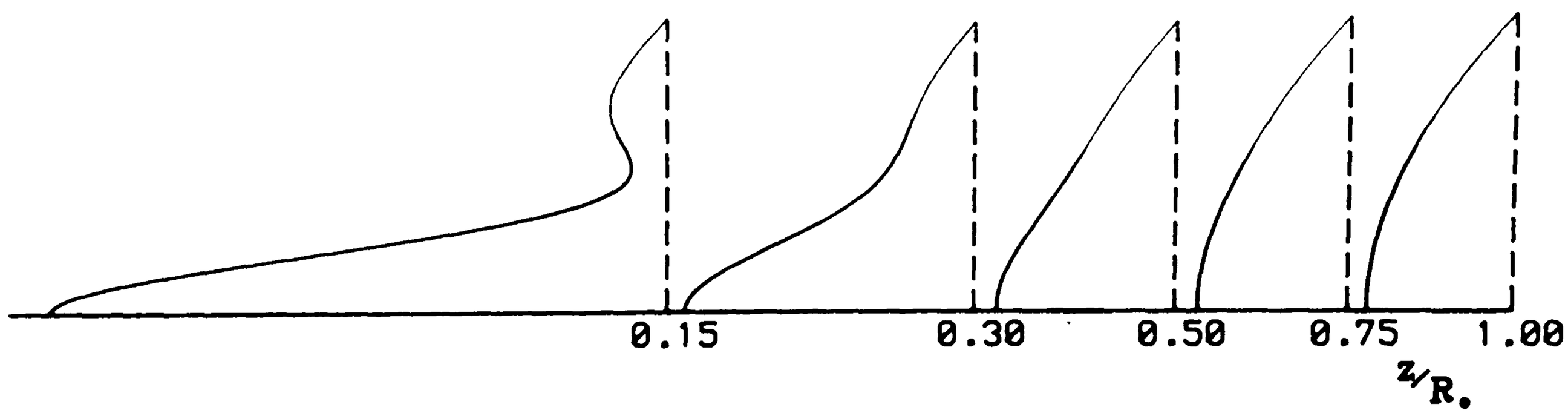

Figure 2.11

Axial velocity profiles for N = 4 with $\varepsilon = 0.001$, $\varepsilon^*/R_0 = 0.001$ and passing through (0.5,0.999).

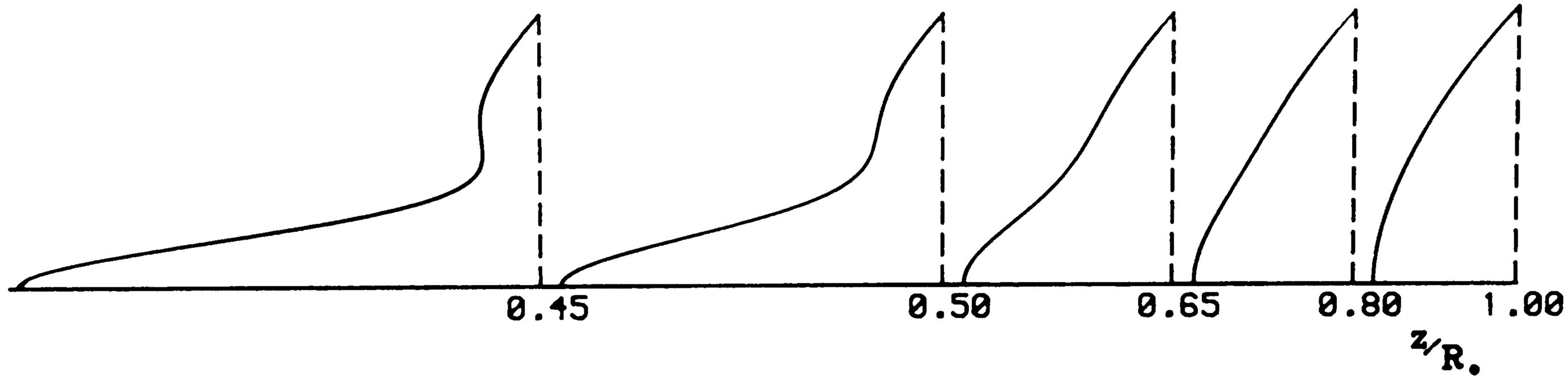

Figure 2.12

Axial velocity profiles for N = 8 with $\varepsilon = 0.001$, $\varepsilon^*/R_0 = 0.001$ and passing through (0.5,0.999).

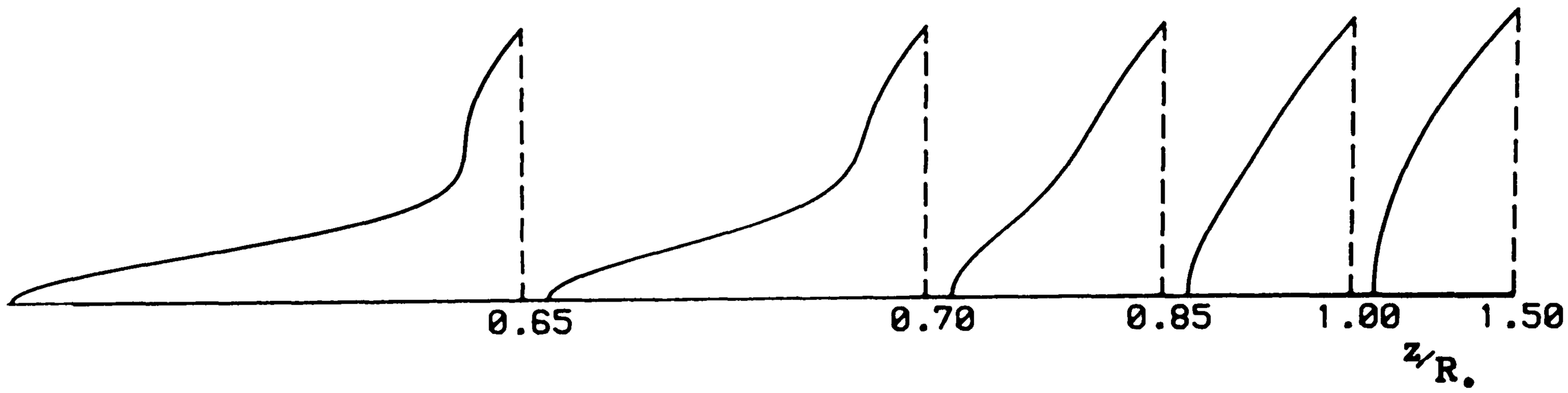

Figure 2.13

Axial velocity profiles for N = 12 with $\varepsilon = 0.001$, $\varepsilon^*/R_0 = 0.001$ and passing through (0.5,0.999).

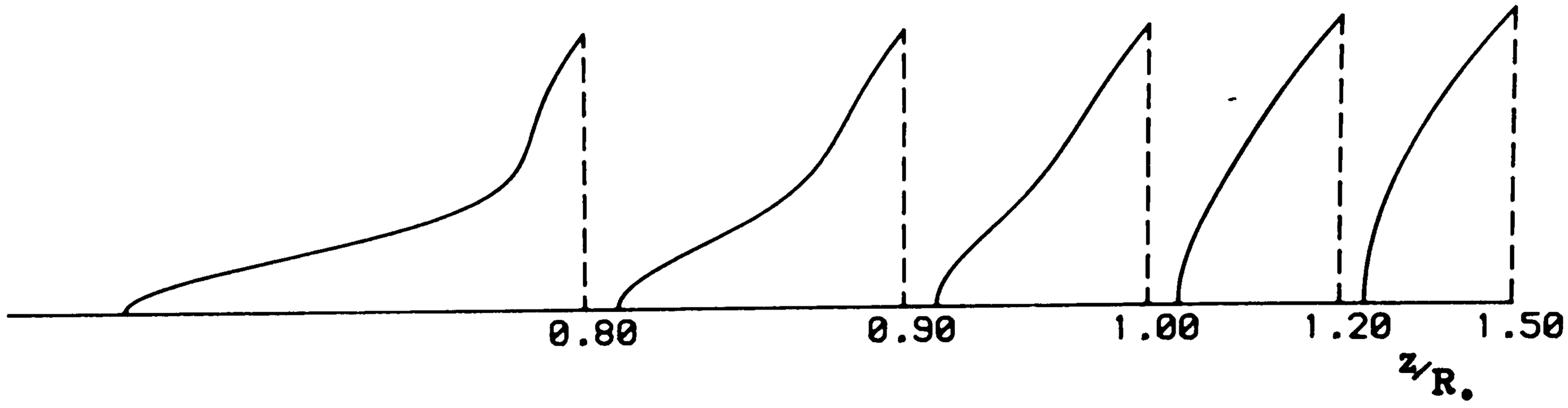

Figure 2.14

Axial velocity profiles for N = 15 with $\varepsilon = 0.001$, $\varepsilon^*/R_0 = 0.001$ and passing through (0.5,0.999).

2.2 THE HIGHER ORDER SOLUTION

THE ANALYTIC SOLUTION

The solution will be derived from (2.10) and (2.11) using boundary conditions (2.12). However, neither $R(\zeta)$ nor $\phi(\eta,\zeta)$ is known. The obvious technique is to write both ϕ and R as series expansions in ζ, with constant coefficients in the series for R, and coefficients that are functions of η in the ϕ series. The method suggests assuming either a polynomial or an exponential series in ζ. The exponential series is chosen because it allows a system of differential equations to be obtained which in conjunction with the boundary conditions, can be solved sequentially. This is the result of only one new variable being introduced in each successive equation. Consequently, the forms of R and ϕ are chosen to be

$$(2.26) \qquad \phi = \sum_{k=0}^{\infty} \phi_k e^{-k\alpha\zeta} \qquad R = \sum_{k=0}^{\infty} R_k e^{-k\alpha\zeta} \quad ,$$

where R_k is a constant, $\phi_k = \phi_k(\eta)$ and α is a constant to be determined. On substitution for R and ϕ from (2.26) into (2.10) and (2.11) the general equation for the nth term is given by

$$\phi_n'' + \frac{1}{\eta}\phi_n' + \alpha^2 R_0^2 n^2 \phi_n = -\alpha \sum_{\substack{k=1 \\ k+l \le n}}^{n-1} \sum_{l=0}^{n-1} [(n - k - 1)l\eta^2 \phi_k''$$

(2.27)

$$+ (2nl - 4kl - 3l^2)\eta\phi_k' + k^2\phi_k] R_{n-k-l} R_l \qquad n \geq 2 \ ,$$

with

$$\phi_0'' + (1/\eta)\phi_0' = 0 \ , \tag{2.28}$$

and

$$\phi_1'' + (1/\eta)\phi_1' + \alpha^2\phi_1 = 0 \ , \tag{2.29}$$

where ' denotes differentiation with respect to η. The boundary conditions are given by

$$\frac{\partial \phi_k}{\partial \eta} = 0 \qquad \text{on } \eta = 0 \text{ and } \eta = 1 \tag{2.30}$$

and

$$-n\alpha\phi_n = \lambda \sum_{j=0}^{n} R_j R_{n-j} \qquad \text{on } \eta = 1 \qquad n \geq 1 \ , \tag{2.31}$$

with $\lambda(R_0^2 - a^2) = 0$ from the zero term. From this it can readily be seen that $R_0^2 = a^2$, where R_0 is the radius of the pipe for large ζ, and without loss of generality, can be taken to be unity. Hence

$$R_0^2 = a^2 = 1 \ . \tag{2.32}$$

The first term in the expansion for ϕ given by integrating (2.28) and applying condition (2.30) yields ϕ_0 is a constant, which can be taken to be zero. For the second term in ϕ, it can easily be seen that the general solution of (2.29) is of the form

$$\phi_1 = AJ_0(\alpha\eta) + BY_0(\alpha\eta) \quad , \tag{2.33}$$

where J_0 and Y_0 are Bessel functions of the first and second kinds respectively and α, A and B are constants to be determined [3]. Now ϕ_1 is finite at $\eta = 0$ and so $B \equiv 0$. Applying conditions (2.30) yields

$$-\alpha AJ_1(\alpha\eta) = 0 \qquad \text{on } \eta = 0 \text{ and } \eta = 1 \ .$$

The condition at $\eta = 0$ is automatically satisfied, while the condition at $\eta = 1$ implies that α_n is a zero of J_1, namely 3.8317, 7.0156, 10.1735 etc. The full solution would be the sum over all the eigenvalues as illustrated in Section 2.1. However, to investigate the higher order terms it will be sufficient to select only one arbitrary eigenvalue, and this case will be considered here. The boundary condition (2.31) demands

$$\alpha\phi_1|_{\eta=1} = 2\lambda R_0 R_1 \quad ,$$

which relates the initial coefficients in the two series by

$$A = \frac{-2\lambda R_1}{\alpha J_0(\alpha)} \quad . \tag{2.34}$$

Since λ is an arbitrary parameter of the problem, and R_1 can be included as part of the independent variable of the equations, new series are chosen to facilitate as general a solution as possible, namely,

$$\Phi_k = \frac{\phi_k}{\lambda R_1{}^k} \quad \text{and} \quad \mathcal{R}_k = \frac{R_k}{R_1{}^k} \quad , \tag{2.35}$$

where $\Phi_0 = 0$, $\Phi_1 = {}^{-2}/_{[\alpha J_0(\alpha)]}\, J_0(\alpha\eta)$ and $\mathcal{R}_1 = 1$. Then (2.27) becomes

$$\Phi_n'' + \frac{1}{\eta}\Phi_n' + \alpha^2 n^2 \Phi_n = -\alpha \sum_{k=1}^{n-1} \sum_{\substack{l=0 \\ k+l \le n}}^{n-1} [(n - k - 1)l\eta^2 \Phi_k'' \tag{2.36}$$

$$+ (2nl - 4kl - 3l^2)\eta\Phi_k' + k^2\Phi_k]\, \mathcal{R}_{n-k-l}\mathcal{R}_l \qquad n \ge 2 \quad ,$$

where ' denotes differentiation with respect to η. The boundary conditions are

$$\frac{\partial \Phi_k}{\partial \eta} = 0 \qquad \text{on } \eta = 0 \text{ and } \eta = 1 \quad , \tag{2.37}$$

$$-\alpha n \Phi_n \big|_{\eta=1} = \sum_{k=0}^{n} \mathcal{R}_k \mathcal{R}_{n-k} \qquad \text{on } \eta = 1 \quad . \tag{2.38}$$

THE SOLUTION FOR SUCCESSIVE N

For n = 1

From (2.23)

$$\Phi_1 = A_1 J_0(\alpha\eta) \quad , \qquad A_1 = -\frac{2}{\alpha J_0(\alpha)} \quad ,$$

while

$$\Re_1 = 1 \quad .$$

For n = 2

Equation (2.36) reduces to

$$\frac{\partial^2 \Phi_2}{\partial \eta^2} + \frac{1}{\eta}\frac{\partial \Phi_2}{\partial \eta} + 4\alpha^2 \Phi_2 = -\alpha^2 A_1 [2J_0(\alpha\eta) - 3\alpha\eta J_0'(\alpha\eta)] \quad ,$$

where ' denotes differentiation with respect to the argument. On integration this yields

$$\Phi_2 = A_2 J_0(2\alpha\eta) - A_1 \alpha\eta J_1(\alpha\eta) \quad ,$$

where A_2 is an arbitrary constant of the integration to be determined and A_1 is given above. Application of (2.37) gives

$$A_2 = \frac{-\alpha A_1 J_0(\alpha)}{2J_1(2\alpha)} ,$$

and (2.38) determines

$$\Re_2 = -\alpha A_2 J_0(2\alpha) - \tfrac{1}{2} \quad .$$

For n = 3

In this case (2.36) becomes

$$\frac{\partial^2 \Phi_3}{\partial \eta^2} + \frac{1}{\eta}\frac{\partial \Phi_3}{\partial \eta} + 9\alpha^2 \Phi_3 = A_2\alpha^2[5\alpha\eta J_0'(2\alpha\eta) - 8J_0(2\alpha\eta)]$$

$$+ A_1\Re_2\alpha^2[8\alpha\eta J_0'(\alpha\eta) - 2J_0(\alpha\eta)] - \tfrac{1}{2}A_1\alpha^2[8\alpha^2\eta^2 J_0(\alpha\eta)$$

$$+ 12\alpha\eta J_0'(\alpha\eta) + 2J_0(\alpha\eta)] \quad ,$$

where ' denotes differentiation with respect to the argument. Integration yields

$$\Phi_3 = A_3 J_0(3\alpha\eta) - 2A_2\alpha\eta J_1(2\alpha\eta) - A_1\Re_2\alpha\eta J_1(\alpha\eta)$$
$$-\tfrac{1}{2}A_1\alpha^2\eta^2 J_0(\alpha\eta) + \tfrac{1}{2}A_1\alpha\eta J_1(\alpha\eta) \quad ,$$

where A_3 is a constant of integration to be determined. The boundary condition (2.37) gives

$$A_3 = \frac{1}{3J_1(3\alpha)}[-4\alpha A_2 J_0(2\alpha) + 2\,\mathcal{R}_2 + 1] \quad ,$$

and from (2.38)

$$\mathcal{R}_3 = -\frac{3\alpha}{2}[A_3 J_0(3\alpha) - 2\alpha A_2 J_1(2\alpha) + \alpha] - \mathcal{R}_2$$

For n = 4

Now (2.36) yields

$$\frac{\partial^2 \Phi_4}{\partial \eta^2} + \frac{1}{\eta}\frac{\partial \Phi_4}{\partial \eta} + 16\alpha^2 \Phi_4 = A_1 \mathcal{R}_3 \alpha^2 [15\alpha\eta J_0'(\alpha\eta) - 2J_0(\alpha\eta)]$$

$$+A_2 \mathcal{R}_2 \alpha^2 [12\alpha\eta J_0'(2\alpha\eta) - 8J_0(2\alpha\eta)] + A_3 \alpha^2 [7\alpha\eta J_0'(3\alpha\eta)$$

$$- 18J_0(3\alpha\eta)] - A_2 \alpha^2 [24\alpha^2\eta^2 J_0(2\alpha\eta) + 14\alpha\eta J_0'(2\alpha\eta)$$

$$+ 4J_0(2\alpha\eta)] - A_1 \mathcal{R}_2 \alpha^2 [15\alpha^2\eta^2 J_0(\alpha\eta) + 19\alpha\eta J_0'(\alpha\eta)$$

$$+ 2J_0(\alpha\eta)] - \tfrac{1}{2} A_1 \alpha^3 \eta [5\alpha^2\eta^2 J_0'(\alpha\eta) - 7\alpha\eta J_0(\alpha\eta)$$

$$- 10J_0'(\alpha\eta)] \quad ,$$

where ' denotes differentiation with respect to the argument. Integration yields the solution

$$\Phi_4 = A_4 J_0(4\alpha\eta) - 3A_3\alpha\eta J_1(3\alpha\eta) - 2A_2\mathcal{R}_2\alpha\eta J_1(2\alpha\eta) - A_1\mathcal{R}_3\alpha\eta J_1(\alpha\eta)$$

$$- 2A_2\alpha^2\eta^2 J_0(\alpha\eta) + A_2\alpha\eta J_1(2\alpha\eta) - A_1\mathcal{R}_2\alpha^2\eta^2 J_0(\alpha\eta)$$

$$+ A_1\mathcal{R}_2\alpha\eta J_1(\alpha\eta) + (1/6)A_1\alpha^3\eta^3 J_1(\alpha\eta) + (1/6)A_1\alpha^2\eta^2 J_0(\alpha\eta)$$

$$- (1/3)A_1\alpha\eta J_1(\alpha\eta) ,$$

where A_4 is given by (2.37) as

$$A_4 = \frac{1}{4J_1(4\alpha)} [- 9\alpha A_3 J_0(3\alpha) - 4\alpha A_2\mathcal{R}_2 J_0(2\alpha) - 2\alpha A_2 J_0(2\alpha)$$

$$+ 4\alpha^2 A_2 J_1(2\alpha) + 2\mathcal{R}_3 + 2\,\mathcal{R}_2 - (1/3)\alpha^2] ,$$

and (2.38) gives

$$\mathcal{R}_4 = -2\alpha[A_4 J_0(4\alpha) - 3\alpha A_3 J_1(3\alpha) - 2\alpha A_2\mathcal{R}_2 J_1(2\alpha) - 2\alpha^2 A_2 J_0(2\alpha)$$

$$+ \alpha A_2 J_1(2\alpha) - \alpha^2 A_1\mathcal{R}_2 J_0(\alpha) - (1/3)\alpha] - \mathcal{R}_3 - \tfrac{1}{2}\,\mathcal{R}_2^{\,2} .$$

For n = 5

For this case (2.36) becomes

$$\frac{\partial^2\Phi_5}{\partial\eta^2} + \frac{1}{\eta}\frac{\partial\Phi_5}{\partial\eta} + 25\alpha^2\Phi_5 = A_1\mathcal{R}_4\alpha^2[24\alpha\eta J_0'(\alpha\eta) - 2J_0(\alpha\eta)]$$

$$+ A_2\mathcal{R}_3\alpha^2[21\alpha\eta J_0'(2\alpha\eta) - 8J_0(2\alpha\eta)] + A_3\mathcal{R}_2\alpha^2[16\alpha\eta J_0'(3\alpha\eta)$$

$$- 18J_0(3\alpha\eta)] + A_4\alpha^2[9\alpha\eta J_0'(4\alpha\eta) - 32J_0(4\alpha\eta)]$$

$$- A_1\mathcal{R}_3\alpha^2[24\alpha^2\eta^2 J_0(\alpha\eta) + 28\alpha\eta J_0'(\alpha\eta) + 2J_0(\alpha\eta)]$$

$$- A_3\alpha^2[72\alpha^2\eta^2 J_0(3\alpha\eta) + 26\alpha\eta J_0'(3\alpha\eta) + 9J_0'(3\alpha\eta)]$$

$$- A_1\mathcal{R}_2{}^2\alpha^2[12\alpha^2\eta^2 J_0(\alpha\eta) + 14\alpha\eta J_0'(\alpha\eta) + J_0(\alpha\eta)]$$

$$- A_2\mathcal{R}_2\alpha^2[84\alpha^2\eta^2 J_0(2\alpha\eta) + 37\alpha\eta J_0'(2\alpha\eta) + 8J_0(2\alpha\eta)]$$

$$- A_2\alpha^2[14\alpha^3\eta^3 J_0'(2\alpha\eta) - 30\alpha^2\eta^2 J_0(2\alpha\eta) - 7\alpha\eta J_0'(2\alpha\eta)]$$

$$- A_1\mathcal{R}_2\alpha^2[12\alpha^3\eta^3 J_0'(\alpha\eta) - 15\alpha^2\eta^2 J_0(\alpha\eta) - 24\alpha\eta J_0'(\alpha\eta)]$$

$$+ (1/6)A_1\alpha^2[6\alpha^4\eta^4 J_0(\alpha\eta) + 14\alpha^3\eta^3 J_0'(\alpha\eta) - 17\alpha^2\eta^2 J_0(\alpha\eta)$$

$$- 37\alpha\eta J_0'(\alpha\eta)] ,$$

where ' denotes differentiation with respect to the argument. On integration this yields

$$\Phi_5 = A_5 J_0(5\alpha\eta) - 4A_4\alpha\eta J_1(4\alpha\eta) - 3A_3\mathcal{R}_2\alpha\eta J_1(3\alpha\eta)$$

$$- 2A_2\mathcal{R}_3\alpha\eta J_1(2\alpha\eta) - A_1\mathcal{R}_4\alpha\eta J_1(\alpha\eta) - A_1\mathcal{R}_3[\alpha^2\eta^2 J_0(\alpha\eta)$$

$$- \alpha\eta J_1(\alpha\eta)] - \tfrac{1}{2}A_3[9\alpha^2\eta^2 J_0(3\alpha\eta) - 3\alpha\eta J_1(3\alpha\eta)]$$

$$- \tfrac{1}{2}A_1\mathcal{R}_2{}^2[\alpha^2\eta^2 J_0(\alpha\eta) - \alpha\eta J_1(\alpha\eta)] - A_2\mathcal{R}_2[4\alpha^2\eta^2 J_0(2\alpha\eta)$$

$$- 2\alpha\eta J_1(2\alpha\eta)] + (1/3)A_2[4\alpha^3\eta^3 J_1(2\alpha\eta) + 2\alpha^2\eta^2 J_0(2\alpha\eta)$$

$$- 2\alpha\eta J_1(2\alpha\eta)] + \tfrac{1}{2}A_1\mathcal{R}[\alpha^3\eta^3 J_1(\alpha\eta) + \alpha^2\eta^2 J_0(\alpha\eta)$$

$$- 2\alpha\eta J_1(\alpha\eta)] + (1/24)A_1[\alpha^4\eta^4 J_0(\alpha\eta) - 2\alpha^3\eta^3 J_1(\alpha\eta)$$

$$- 3\alpha^2\eta^2 J_0(\alpha\eta) + 6\alpha\eta J_1(\alpha\eta)] \ ,$$

where (2.37) gives

$$A_5 = \frac{1}{5J_1(5\alpha)}\{-16\alpha A_4 J_0(4\alpha) - 9\alpha A_3\mathcal{R}_2 J_0(3\alpha) - 4\alpha A_2\mathcal{R}_3 J_0(2\alpha)$$

$$+ (9/2)\alpha A_3[3\alpha J_1(3\alpha) - J_0(3\alpha)] + 4\alpha A_3\mathcal{R}_2[2\alpha J_1(2\alpha) - J_0(2\alpha)]$$

$$+ 2\,\mathcal{R}_4 + \mathcal{R}_3 + \mathcal{R}_2{}^2 + (4/3)\alpha^2 A_2[2\alpha J_0(2\alpha) + J_1(2\alpha)]$$

$$- (1/6)\alpha^2 - \alpha^2 \mathcal{R}_2\} ,$$

and from (2.38)

$$\mathcal{R}_5 = -(5/2)\alpha\{A_5 J_0(5\alpha) - 4\alpha A_4 J_1(4\alpha) - 3\alpha A_3 \mathcal{R}_2 J_1(3\alpha)$$

$$- 2\alpha A_2 \mathcal{R}_3 J_1(2\alpha) + 2\alpha \mathcal{R}_3 - (3/2)\alpha A_3[3\alpha J_0(3\alpha) - J_1(3\alpha)]$$

$$+ \alpha \mathcal{R}_2^2 - 2\alpha A_2 \mathcal{R}_2[2\alpha J_0(2\alpha) - J_1(2\alpha)]$$

$$+ (2/3)\alpha A_2[2\alpha^2 J_1(2\alpha) + \alpha J_0(2\alpha) - J_1(2\alpha)] - \alpha \mathcal{R}_2$$

$$- (1/12)\alpha[\alpha^2 - 3]\} - \mathcal{R}_4 - \mathcal{R}_3 \mathcal{R}_2 .$$

The numerical value of the coefficients A_n, $\mathcal{R}_n$ and the value of the potential function evaluated on the wall for n = 1, ..., 5, evaluated using the exact solutions with $\alpha = 3.83171$ are presented in Table 2.3.

The ease with which these solutions were obtained using the Computer Algebraic Manipulation System REDUCE [4] demonstrates the power of algebraic computation. This is a computer package for carrying out algebraic operations accurately, no matter how complicated the expressions become. It can manipulate polynomials, both expanding and factorizing them, extracting various parts as required. It can also perform differentiation and integration and allows the definition of differential operators. Using this facility to define the relations between the Bessel Functions

Table 2.3

The values for A_n and $\mathcal{R}_n$ evaluated from the exact solution with $\alpha = 3.83171$.

n	A_n	$\mathcal{R}_n$	$\Phi_n\|_{\eta=1}$
1	1.29596	1.00000	-0.52196
2	5.76515	-5.82488	1.38969
3	4.66803,1	4.62982,1	-7.04183
4	4.83666,2	-4.16886,2	4.61443,1
5	5.74607,3	3.98671,3	-3.44509,2

and their derivatives, and to specify differential operators to act upon these functions, allows these higher order solutions to be determined and differentiated exactly, without the need for extensive, demanding algebra. It should now be feasible to use the computer to obtain long and complicated analytical solutions to problems which previously were tackled by a mixture of analytic and numerical methods.

AN ALTERNATIVE APPROACH

This exact technique could easily be used for n larger than 5, but, the complexity and length of the solution for Φ_n and $\Re_n$ suggest investigating alternative approaches to produce further values. A completely numerical solution encounters many difficulties. It is necessary to solve the axi-symmetric Laplace equation with a singularity on the axis, in a region whose boundary R(z) is unknown and has to be determined from the boundary conditions. The natural development would be to take the velocity profile obtained analytically as a boundary condition for a solution on a region downstream. However, two major difficulties still remain. The centre line singularity can be dealt with by mapping it to infinity, and there has been some research into Free-Boundary problems, but the combination of the two appears to be unique and a suitable numerical method of tackling the problem has not yet been devised. Consequently, it was decided to use the exponential series method employed in the analytic solution and to numerically solve the system of equations produced. How-

ever, this does not remove the problem at $r = 0$. Previously, [5], the difficulty of the singularity was overcome by writing the solution as a series in η, for η small, to provide a starting value for a numerical technique. The series method will now be used all the way across the pipe, and enough terms are retained to ensure convergence of ϕ and $\partial\phi/\partial\eta$ on the outer wall.

THE SERIES METHOD

Returning to (2.36), it is known that

$$\Phi_n'' + \frac{1}{\eta}\Phi_n' + \alpha^2 n^2 \Phi_n = -\alpha \sum_{\substack{k=0 \\ k+l \le n}}^{n-1} \sum_{l=0}^{n-1} [(n - k - 1)l\eta^2 \Phi_k'' + (2nl - 4kl - 3l^2)\eta\Phi_k' + k^2\Phi_k] \mathcal{R}_{n-k-l}\mathcal{R}_l \qquad n \ge 2 \ ,$$

with $\Phi_1 = {}^{-2}/_{[\alpha J_0(\alpha)]} J_0(\alpha\eta)$, and boundary equations (2.37) and (2.38) giving

$$\frac{\partial \Phi_k}{\partial \eta} = 0 \quad \text{on } \eta = 0, 1 \qquad \text{and} \qquad -\alpha n \Phi_n \big|_{\eta=1} = \sum_{k=0}^{n} \mathcal{R}_k \mathcal{R}_{n-k} \ .$$

The power series form for Φ_k is chosen to be

$$\Phi_k = A_k \sum_{j=0}^{\infty} c_{k,j} (\alpha\eta)^{2j} \ , \tag{2.39}$$

where $c_{k,0} = 1$. Using the notation adopted for the analytic solution the value of Φ_k on the centre line is written as A_k. The symmetry about $\eta = 0$ means that only the even powers of η need to be considered.

On substitution of (2.39) into (2.36) and equating powers of $(\alpha\eta)$, the general recurrence relation for $c_{k,j}$ is determined to be

$$c_{n,j-1} = -\frac{1}{4(j+1)^2}\Big[nc_{n,j} + \sum_{\substack{k=1 \\ k+l\le n}}^{n-1}\sum_{l=0}^{n-1} 2jl(n-k-1)(2j-1) + 2j(2nl-4kl-3l^2)+k^2\Big]\frac{A_k}{A_n}\, c_{k,j}\mathcal{R}_{n-k-1}\mathcal{R}_l \qquad n \ge 2 \tag{2.40}$$

with

$$A_1 = -\frac{2}{\alpha J_0(\alpha)} \quad \text{and} \quad c_{1,j+1} = -\frac{c_{1,j}}{4(j+1)^2}\,, \tag{2.41}$$

and boundary condition

$$\sum_{j=0}^{\infty} jc_{n,j}\alpha^{2j} = 0\,. \tag{2.42}$$

The condition on $\eta = 0$ is automatically satisfied.

From (2.40) it can be seen that the values of $c_{k,j}$ depend on A_k, and in order to determine them it is necessary to obtain a value for A_k. It would be possible to improve the initial approximation by using (2.42) as a basis for an iterative scheme. However, $c_{k,j}$ will be determined using an algorithm developed from the analytic solution. It can be shown that

$$(2.43) \qquad \left.\frac{\partial \Phi_n}{\partial \eta}\right|_{\eta=1} = -n\alpha A_n J_1(n\alpha) + Fn(\ldots) \quad ,$$

where Fn is a combination of previously determined constants. Let $A_n^{(I)}$ and $A_n^{(E)}$ be the initial approximation and the exact value respectively. Then, from the boundary conditions

$$-n\alpha A_n^{(E)} J_1(n\alpha) + Fn(\ldots) = 0 \quad ,$$

and hence

$$A_n^{(E)} = \frac{Fn(\ldots)}{n\alpha J_1(n\alpha)} \quad .$$

Substituting from (2.43) for Fn(...) gives

$$A_n^{(E)} = A_n^{(I)} + \frac{1}{n\alpha J_1(n\alpha)} \left.\frac{\partial \Phi_n}{\partial \eta}\right|_{\eta=1} \quad ,$$

where $\partial \Phi_n / \partial \eta |_{\eta=1}$ is obtained by differentiation of (2.42) and evaluated using $A_n^{(I)}$ in the determination of $c_{k,j}$, (2.40). The values of A_n and $\Re_n$, obtained from this technique are detailed in Table 2.4 for $n \leq 7$. Comparison with the values evaluated using the exact solution, which are presented in Table 2.3 for $\alpha = 3.83171$, shows agreement to at least five decimal places. As n increases the values for Φ_n and $\Re_n$ do become progressively less accurate due to the accumulation of truncation errors.

Table 2.4

The values for A_n and $\mathcal{R}_n$ evaluated from the series solution with $\alpha = 3.83171$.

n	A_n	$\mathcal{R}_n$	$\Phi_n\|_{\eta=1}$
1	1.29596	1.00000	-0.52196
2	5.76515	-5.82488	1.38969
3	4.66803,1	4.62982,1	-7.04183
4	4.83666,2	-4.16886,2	4.61443,1
5	5.74607,3	3.98671,3	-3.44509,2
6	7.42359,4	-3.97448,4	2.80624,3
7	1.01525,6	4.08824,5	-2.43499,4

This occurs because the nth order coefficients are evaluated from a combination of the previously determined lower order terms, which creates unavoidable error amplification for large n. Thus it was decided to obtain only the first seven terms.

EXAMINING THE SERIES FOR R AND ϕ

R and ϕ can be considered to be series in $R_1 e^{-\alpha\zeta}$, where R_1 is arbitrary. It can easily be seen that altering the size of R_1 is equivalent to a translation in ζ, hence it is sufficient to take R_1 to be either +1 or -1. Taking R_1 positive creates an alternating series for R. Conversely, for the case $R_1 = -1$, the initial constant, which defines the radius for large z, is the sole positive term. This describes a rapidly narrowing pipe, but, in the region $R << 1$, the series for R does not converge and consequently the flow characteristics can not be investigated here. However, for R_1 positive, the oscillatory behaviour of the terms in the series for R suggests a better form for an analytic solution. When considering solutions that are of the form presented in this section the choice of perturbation parameter is somewhat arbitrary. Only when the coefficients are actually determined can its suitability be assessed. The convergence of the series can vary widely and is dependent upon the choice made. There is evidence that reparametrizing the series can make a vast improvement and much interest, notably from Van Dyke [6], has been shown

in improving series of this type. Choosing an alternative perturbation parameter ξ such that

$$(2.44) \qquad \xi = \frac{Gx}{1 + Gx} \quad , \qquad \text{with} \quad x = R_1 e^{-\alpha\zeta} \quad ,$$

where G is a suitable arbitrary constant. The series for R and ϕ can be written

$$(2.45) \qquad R = \sum_{k=0}^{\infty} B_k \xi^k \quad , \qquad \phi = \sum_{k=0}^{\infty} \psi_k \xi^k \quad ,$$

where B_k is a constant and $\psi_k = \psi_k(\eta)$. Substituting these into (2.10) and (2.11) with boundary conditions (2.12) would yield formulae for the new series in a similar way to the solutions found for $\mathcal{R}$ and Φ. However, since every term of both the new and the original series must match, the new analytic coefficients B_k and ψ_k can easily be deduced. For ζ large, it is known that R = 1 and that the flow is Poiseuille. To determine the relationship between R_k and B_k, and ϕ_k and ψ_k, the series coefficients are matched for z large. For $|Gx| < 1$, (2.44) can be expanded to yield the relation

$$(2.46) \qquad \xi^k = (Gx)^k[1 - kGx + \tfrac{1}{2}k(k + 1)G^2x^2 - \ldots] \quad ,$$

which gives

$$B_1 = {}^1/_G(R_1)$$

(2.47) $$B_2 = {}^1/_{G^2}(R_2 + GR_1)$$

$$B_3 = {}^1/_{G^3}(R_3 + 2GR_2 + G^2R_1) \qquad \text{etc.} \quad ,$$

and similarly for ψ_k and ϕ_k.

THE CHOICE OF G

The effectiveness of the new series for R and ϕ will be determined by the choice of the parameter G. It is clear from (2.47) that for different values of G the individual terms in these series will be different. It can be shown that for any series there is an optimum perturbation parameter and consequently there would be a best choice of G if only one series were being considered. However, in this case there are at least two series (one being a double series which can be considered as many series, one for each η!). Hence, there is no one, distinct value for G that should be used, but it can be seen that some choices are better than others in enabling an understanding of the flow. This suggests that the series for the radius and the potential function need to be considered separately, the effects of different values for G investigated and then a compromise made. Similarly, if alternative eigenvalues are used, a new choice of G will need to be made to improve the new series.

CHARACTERISTICS OF THE FLOW

Using the new series for R and ϕ, substitution into (2.9) gives the radial and axial velocites in the pipe. Since

$$\phi = \lambda \sum_{n=0}^{\infty} \Phi_n x^n \qquad \text{and} \quad R = \sum_{n=0}^{\infty} \mathcal{R}_n x^n \quad ,$$

where $\mathcal{R}_0 = \mathcal{R}_1 = 1$ and $x = R_1 e^{-\alpha\zeta}$, then

$$u = \lambda\{(1 - \eta^2 \sum_{j=0}^{\infty} \sum_{k=0}^{\infty} \mathcal{R}_j \mathcal{R}_k x^{j+k}) - \alpha \sum_{n=0}^{\infty} n\Phi_n x^n + v\alpha\eta \sum_{n=0}^{\infty} n\, \mathcal{R}_n x^n\} \quad ,$$

(2.48) and

$$v = \lambda \frac{\sum_{n=0}^{\infty} \Phi_n' x^n}{\sum_{n=0}^{\infty} \mathcal{R}_n x^n} \quad ,$$

where ' denotes differentiation with respect to η.

To visualise the flow it is necessary to consider the special cases which arise by taking specific values for λ, R_1 and α in (2.48). λ appears in these velocities as a scale factor, and as such, graphs of u/λ and v/λ give the identical velocity profiles as u and v. λ negative reverses the direction of the flow. The sign of R_1 creates either an expanding (+1) or a contracting (-1) pipe. The possible values of α are defined by the boundary conditions.

Profiles are shown for $\alpha = 3.8317$. Similar graphs can be generated for other values of α, however, a different perturbation parameter, i.e. a different value for G, would be needed to optimise the particular series, and in addition it should be noted that the error accumulation is greater for larger values of α. Figure 2.15 illustrates the changes in axial velocity as the pipe expands. For large z the flow is parabolic, but as z decreases and the radius of the pipe slowly increases the velocity of the flow near the axis of the tube decreases until for $z \simeq 0.7$ back flow occurs. Figure 2.16 shows the radial velocity along the lines $\eta = 0.2, 0.4, 0.6, 0.8$. For z large the radial flow is zero, but as z decreases a flow towards the centre of the pipe develops.

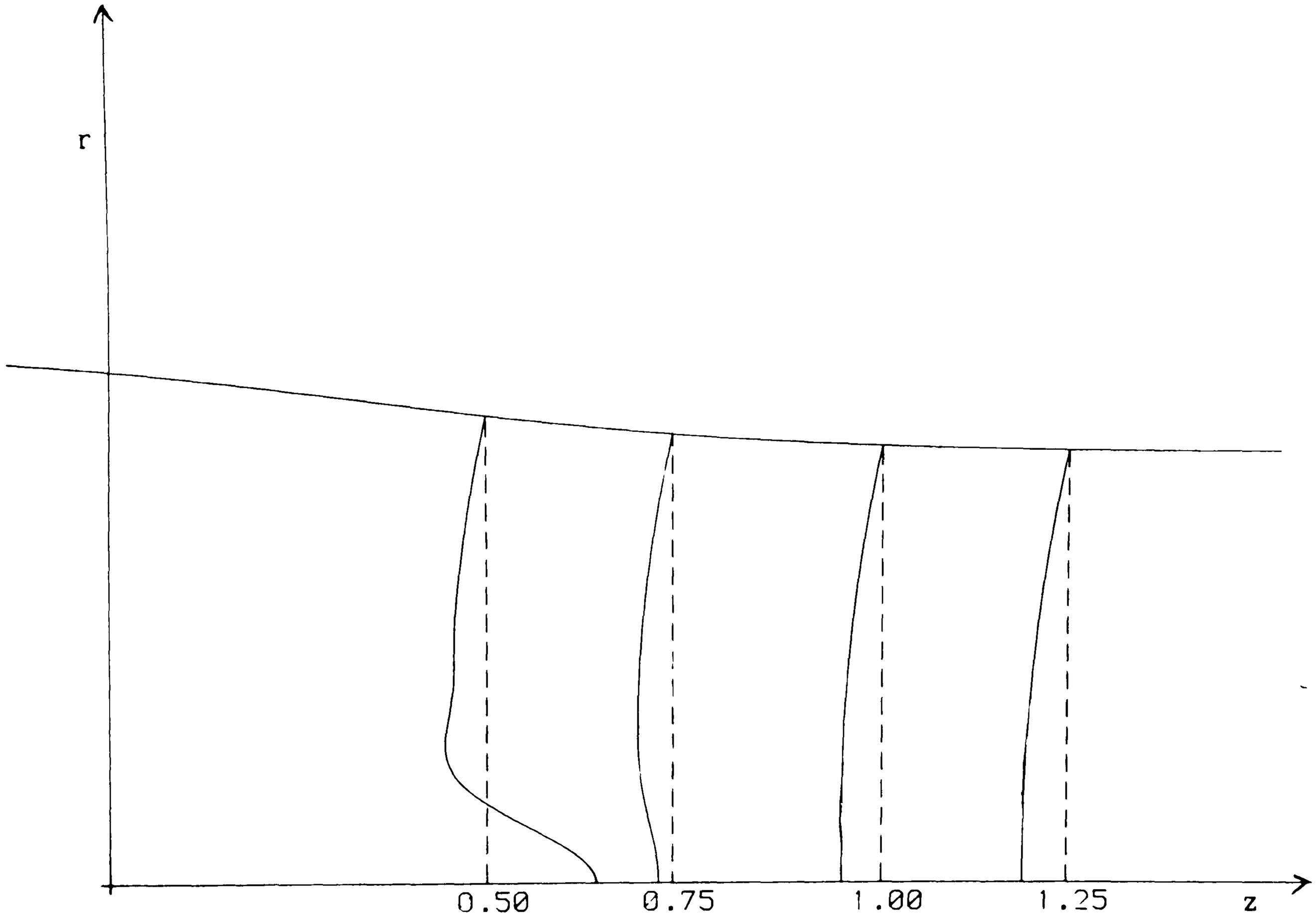

Figure 2.15

Axial velocity profiles for $\alpha = 3.8317$ and $G = 8.0$.

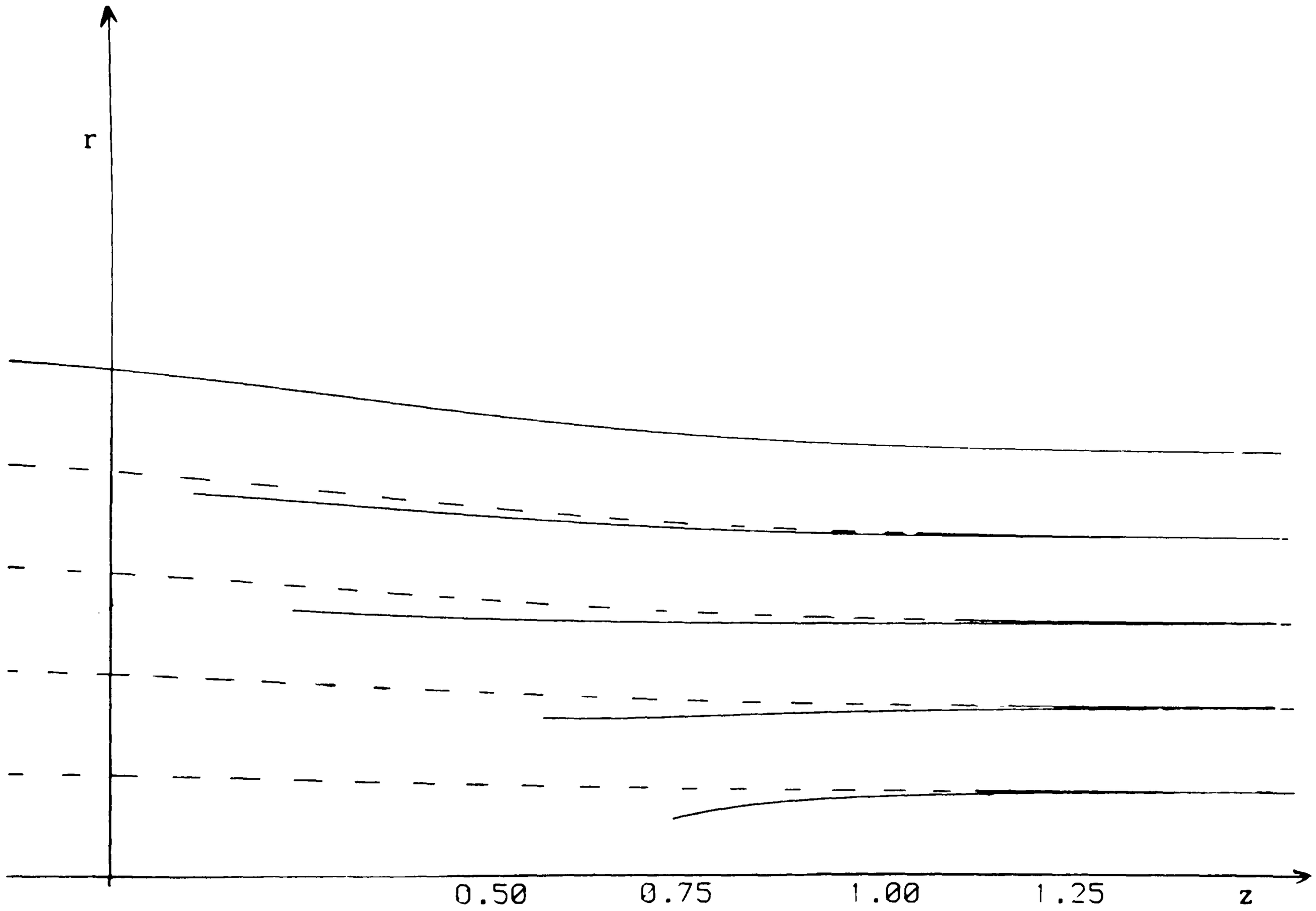

Figure 2.16

Radial velocity profiles for $\alpha = 3.8317$ and $G = 8.0$.

HIGHER ORDER SOLUTION USING MORE THAN ONE EIGENVALUE

Earlier in the section the two distinct cases, namely the first order solution summed over all eigenvalues and the higher order solution with one eigenvalue, have been considered. It now remains to draw the two approaches together into a general solution of the variable width problem. It will be shown that these solutions are complicated, but further analytic investigation is worthwhile.

The forms that have been assumed in 2.2 for R and ϕ (2.26) yield the system of differential equations equations (2.27). The solution of the first of these is

$$\Phi_1 = AJ_0(\alpha\eta) \ ,$$

which is not a unique result as there are an infinity of 'α's such that Φ_1 satisfies the boundary condition $J_1(\alpha) = 0$. This is illustrated by the first order solution for a large number of eigenvalues presented in 2.1. However, the extension to higher order terms using more than one eigenvalue will not be as straight forward as in the one eigenvalue case shown earlier. It is now possible to have 'cross' terms. They are formed by the products of the radius and potential functions that occur in the differential equation (2.27). Each term depends on two or more different eigenvalues and consequently a new notation is necessary to allow for the larger number of coefficients that are now needed. The potential is now written as

$$\phi = \lambda \sum_{i_1} \cdots \sum_{i_u} \Phi^{i_1 \cdots i_u}_{i_1+\cdots+i_u} e^{-(i_1\alpha_1+\cdots+i_s\alpha_s)\zeta} ,$$

where s is the number of eigenvalues being used,

$\alpha_1, \ldots, \alpha_s$ are the eigenvalues of the problem,

$i_1, \ldots, i_s$ are the coefficients of the $\alpha_1, \ldots, \alpha_s$ respectively in the exponent and

$i_1 + \ldots + i_s$ is the order of the term.

Similarly, the radius function is defined to be

$$R = \sum_{i_1} \cdots \sum_{i_u} R^{i_1 \cdots i_u}_{i_1+\cdots+i_u} e^{-(i_1\alpha_1+\cdots+i_s\alpha_s)\zeta} ,$$

To increase the understanding of the appearance and the form of the cross terms it is beneficial initially to investigate the simplest case, that of two eigenvalues.

USING TWO EIGENVALUES

Considering case for two eigenvalues. The potential function and the wall profile can be written as

$$\Phi = \lambda \sum_{i} \sum_{j} \Phi^{i\ j}_{i+j} e^{-(i\alpha_1+j\alpha_2)\zeta} ,$$

and

$$R = \sum_{i} \sum_{j} R^{i\ j}_{i+j} e^{-(i\alpha_1+j\alpha_2)\zeta} ,$$

where $R^{i\ j}_{i+j}$ is a constant and $\Phi^{i\ j}_{i+j} = \Phi^{i\ j}_{i+j}(\eta)$. Then the differential equation (2.11) becomes

$$(2.49)\quad \Phi^{n\ m}_{n+m}{}'' + (1/\eta)\Phi^{n\ m}_{n+m}{}' + (n\alpha_1 + m\alpha_2)^2\Phi^{n\ m}_{n+m}R^{0\ 0}_{0\ 0}{}^2$$

$$+\sum_{j=0}^{m-1}\sum_{q=0}^{m}{}'_{0\le j+q\le m}[(n\alpha_1 + j\alpha_2)^2\Phi^{n\ j}_{n+j} + q(m - j - q)\alpha_2{}^2\eta^2\Phi^{n\ j}_{n+j}{}'']$$

$$+ q\alpha_2[(2m - 4j - 3q)\alpha_2 - 2n\alpha_1]\eta\Phi^{n\ j}_{n+j}{}']R^{0\ q}_{q}\ R^{0\ m-j-q}_{m-j-q}$$

$$+\sum_{i=0}^{n-1}\sum_{p=0}^{n}{}'_{0\le i+p\le n}[(i\alpha_1 + m\alpha_2)^2\Phi^{i\ m}_{i+m} + p(n - i - p)\alpha_1{}^2\eta^2\Phi^{i\ m}_{i+m}{}'']$$

$$+ p\alpha_1[(2n - 4i - 3p)\alpha_1 - 2m\alpha_2]\eta\Phi^{i\ m}_{i+m}{}']R^{p\ 0}_{p\ 0}\ R^{n-i-p\ 0}_{n-i-p\ 0}$$

$$+\sum_{i=0}^{n-1}\sum_{j=0}^{m-1}\sum_{p=0}^{n}\sum_{q=0}^{m}{}'_{\substack{0\le i+p\le n\\ 0\le j+q\le m}}[(i\alpha_1 + j\alpha_2)^2\Phi^{i\ j}_{i+j} + (p\alpha_1 + q\alpha_2)[(n - p - i)\alpha_1$$

$$+(m - q - j)\alpha_2]\eta^2\Phi^{i\ j}_{i+j}{}'' + (p\alpha_1 + q\alpha_2)[(2n - 4i - 3p)\alpha_1$$

$$+(2m - 4j - 3q)\alpha_2]\eta\Phi^{i\ j}_{i+j}{}']R^{p\ q}_{p+q}\ R^{n-i-p\ m-j-q}_{n+m-i-j-p-q} = 0\ ,$$

for n or m > 2, with boundary conditions

$$(2.50)\quad \frac{\partial\Phi^{n\ m}_{n+m}}{\partial\eta} = 0 \quad \text{on } \eta = 0,\ 1,$$

and

$$(2.51)\quad -(n\alpha_1 + m\alpha_2)\Phi^{n\ m}_{n+m}\Big|_{\eta=1} = \lambda\sum_{p=0}^{n}\sum_{q=0}^{m}{}'R^{p\ q}_{p+q}\ R^{n-p\ m-q}_{n+m-p-q} \text{ on } \eta = 1\ .$$

Equation (2.49) is the system of differential equations for two eigenvalues presented for order n + m.

Now, the equations will be solved in a similar way to that for the one eigenvalue case, that is for successive values of (n + m).

Considering n + m = 0.

There is only one case, that is Φ_{00}. In this case equation (2.49) reduces to

$$\Phi_{00}'' + (1/\eta)\Phi_{00}' = 0 \ ,$$

which, in conjuction with the boundary conditions (2.50), requires that

$$\Phi_{00}' = 0 \qquad \text{on } \eta = 0,\ 1,$$

and gives Φ_{00} = constant, which since ϕ is a potential, can be taken to be zero. Substitution into (2.51) yields

$$R_{00}^{\ 2} = a^2 \ .$$

Without loss of generality a^2 can be taken to be 1 and so $R_{00} = 1$.

Considering $n + m = 1$

Here there are two cases to consider, that is $n = 1$, $m = 0$ and $n = 0$, $m = 1$. For $n = 1$, $m = 0$ equation (2.49) reduces to

$$\Phi_{1}^{0\,\prime\prime} + (1/\eta)\Phi_{1}^{0\,\prime} + \alpha_1^2 \Phi_{1}^{0} = 0 \ .$$

The solution of this is the Bessel function of the first kind as obtained earlier in the section, that is

$$\Phi_{1}^{0} = A_{1}^{0} J_0(\alpha_1 \eta) \ , \tag{2.52}$$

where A_{1}^{0} is an arbitrary constant to be determined from the boundary conditions. Similarly

$$\Phi_{1}^{0\,\prime} = A_{1}^{0\,\prime} J_0(\alpha_2 \eta) \ ,$$

where α_1 and α_2 are any two zeros of J_1. On application of condition (2.51) the arbitrary constants are determined to be

$$A_{1}^{0} = - \frac{2R_{1}^{0}}{\alpha_1 J_0(\alpha_1)} \ , \text{ and similarly } A_{1}^{0\,\prime} = - \frac{2R_{1}^{0\,\prime}}{\alpha_2 J_0(\alpha_2)} \ .$$

It can easily be seen that these are the results obtained when considering only one eigenvalue with Φ_{1}^{0} replacing Φ_1, and R_{1}^{0} replacing R_1 etc..

It is evident that the one eigenvalue solution will occur whenever either n or m is zero. As such it is only necessary to consider the cases when neither n nor m is zero.

Considering n + m = 2

From the one eigenvalue solution

$$\Phi^{20}_{2} = A^{20}_{2} J_0(2\alpha_1\eta) - A^{10}_{1} R^{10}_{1} \alpha_1\eta J_1(\alpha_1\eta) ,$$

with

$$A^{20}_{2} = \frac{R^{10\ 2}_{1}}{J_1(2\alpha_1)} , \text{ and } R^{20}_{2} = -R^{10\ 2}_{1}[\frac{\alpha_1 J_0(2\alpha_1)}{J_1(2\alpha_1)} + \tfrac{1}{2}] ,$$

and a similar expression is obtained for Φ^{02}_{2} by interchanging n and m, and substituting α_2 for α_1.

However, a new case, the first example of a cross term, is introduced, that is n = m = 1. For this the differential equation (2.49) reduces to

$$\Phi'^{\ ''}_{2} + (1/\eta)\Phi'^{\ '}_{2} + (\alpha_1 + \alpha_2)^2\Phi'^{\ }_{2}$$

$$(2.53) \qquad = -\{(2\alpha_1^{\,2}\Phi^{0\ }_{1}{}' - \alpha_2(\alpha_2 + 2\alpha_1)\eta\Phi^{0\ '}_{1}{}')R^{0}_{1}{}'$$

$$+ (2\alpha_2^{\,2}\Phi^{0}_{1}{}' - \alpha_1(\alpha_1 + 2\alpha_2)\eta\Phi^{0\ '}_{1}{}')R^{10}_{1}\} ,$$

where α_1 and α_2 are any two eigenvalues. The solution of (2.53) is

$$\Phi^{11}_{2} = A^{11}_{2} J_0[(\alpha_1 + \alpha_2)\eta] - A^{10}_{1} R^{01}_{1} \alpha_1 \eta J_1(\alpha_1 \eta) \tag{2.54}$$

$$- A^{01}_{1} R^{10}_{1} \alpha_2 \eta J_1(\alpha_2).$$

The arbitrary constants are determined by the boundary conditions (2.50) and (2.51) to be

$$A^{11}_{2} = \frac{2R^{10}_{1} R^{01}_{1}}{J_1(\alpha_1 + \alpha_2)} ,$$

and

$$R^{11}_{2} = - \frac{R^{10}_{1} R^{01}_{1} (\alpha_1 + \alpha_2) J_0(\alpha_1 + \alpha_2)}{J_0(\alpha_1 + \alpha_2)} - R^{10}_{1} R^{01}_{1} ,$$

There are distinct similarities between this cross term solution and the one for one eigenvalue found earlier in 2.2. Φ^{11}_{2} is of the same form as Φ^{20}_{2} and Φ^{02}_{2}, incorporating all their salient features and, in addition, maintaining the symmetry of the equations in α_1 and α_2.

Considering n + m = 3.

Continuing by considering only the cases where neither n nor m are zero creates two new equations to solve, that is those obtained by taking

$n = 2$, $m = 1$ and $n = 1$, $m = 2$. Substituting for the first pair into (2.49) and solving the differential equation obtained gives

$$\Phi_3^{21} = A_3^{21} J_0[(2\alpha + \alpha_2)\eta] - 2A_2^{20} R_1^{01} \alpha_1 \eta J_1(2\alpha_1\eta)$$

$$- A_2^{11} R_1^{10} (\alpha_1 + \alpha_2)\eta J_1[(\alpha_1 + \alpha_2)\eta]$$

$$- A_1^{10} R_2^{11} \alpha_1 \eta J_1(\alpha_1\eta)$$

$$- A_1^{10} R_1^{10} R_1^{01} [\alpha_1^2\eta^2 J_0(\alpha_1\eta) - \alpha_1(\alpha_1\eta)]$$

$$- \tfrac{1}{2}A_1^{01} R_1^{10} R_1^{10} [\alpha_2^2\eta^2 J_0(\alpha_2\eta) - \alpha_2(\alpha_2\eta)] ,$$

where A_3^{21} and R_3^{21} can be found from (2.50) and (2.51) to be

$$A_3^{21} = -\frac{1}{(2\alpha_1 + \alpha_2)J_1(2\alpha_1 + \alpha_2)} \{4\alpha_1^2 A_2^{20} R_1^{01} J_0(2\alpha_1)$$

$$+ (\alpha_1 + \alpha_2)^2 A_2^{11} R_1^{10} J_0(\alpha_1 + \alpha_2)$$

$$- \alpha_1^2 A_1^{10} R_2^{11} J_0(\alpha_1) + A_1^{10} R_1^{10} R_1^{01} \alpha_1^2 J_0(\alpha_1)$$

$$+ \tfrac{1}{2}A_1^{01} R_1^{10} R_1^{10} \alpha_2^2 J_0(\alpha_2)\} ,$$

and

$$R^{21}_{3} = -\tfrac{1}{2}(2\alpha_1 + \alpha_2)[A^{21}_{3} J_0(2\alpha_1 + \alpha_2) - 2A^{20}_{2} R^{01}_{1} \alpha_1 J_1(2\alpha_1)$$

$$- A^{11}_{2} R^{10}_{1} (\alpha_1 + \alpha_2) J_1(\alpha_1 + \alpha_2)$$

$$- A^{10}_{1} R^{10}_{1} R^{01}_{1} \alpha_1^2 J_0(\alpha_1) - \tfrac{1}{2} A^{01}_{1} R^{10}_{1} R^{10}_{1} \alpha_2^2 J_0(\alpha_2)].$$

Similarly, using the symmetry of the equations, Φ^{12}_{3} can be obtained by interchanging n and m, and substituting α_1 for α_2 and vice versa. It should be stressed that the solutions that have been obtained are for any values of α_1 and α_2 such that $J_1(\alpha_1) = J_1(\alpha_2) = 0$, and consequently the general second order solution can be found by summing over all possible pairs of eigenvalues.

Solutions for larger values of (n + m) can be found in a similar way.

Clearly, the two eigenvalue solution is only a special case of the three eigenvalue solution, which in its turn, is a special case of the one for many eigenvalues. As a result, the solutions obtained to the two eigenvalue problem are only a subset of those which would be found for the general problem. For example, all the terms of the third order general solution have been found except any involving the product of three different eigenvalues.

In principle, further solutions can be found for a large number of eigenvalues. However, the complexity of the differential equations encountered, even for small numbers of eigenvalues, questions the wisdom

of proceeding further explicitly. For example, the equation equivalent to (2.49) but with three eigenvalues has been derived and is more than three times as long as (2.49). Nevertheless, a good deal of information can be extracted about the results for three or more eigenvalues from the one and two eigenvalue solutions.

As indicated earlier, new cross terms are introduced when the order of the differential equations are equal to the number of eigenvalues used. From an inspection of the similarities between Φ_{2}' and Φ_2, it can be established how Φ_{2}' can be constructed from Φ_2 by maintaining the salient features of the solution and, in addition, introducing a symmetry in α_1 and α_2. It seemed likely, and a basic investigation confirmed that, the cross terms for higher order could be found in an analagous way.

CONCLUSION

This Section has concentrated on the investigation of an axi-symmetric flow through an impermeable, cylindrical pipe with changing radius, using the new solution of the Navier-Stokes equations (2.6). The form for the potential function and radius description was taken to be that of an exponential series in the axial parameter which, in theory, allowed an exact solution of the system of differential equations for the potential function and ultimately, via the boundary conditions, the radius function. The solution is complex and to increase the understanding it is tackled in stages. Section 2.1 presents the solution as a first order perturbation, but using a large number of eigenvalues. Conversely, Section 2.2 considers only one eigenvalue, but a large number of terms. The solutions for the higher order terms becomes progressively more complicated and only the first five are found analytically, using an algebraic computing package. These are later re-inforced and extended to seventh order using a polynomial series in the radial parameter. The series description is then improved by using a new perturbation parameter which better described and improved the understanding of the flow. Finally, the salient features of both these methods are brought together in the general solution. The differences that are met when combining both a large number of eigenvalues and higher order terms is illustrated using two eigenvalues, concentrating on the previously unencountered cross terms which are novel to these particular cases since they contain more than one eigenvalue.

REFERENCES

1. TERRILL, R.M., Laminar Flow in a Porous Tube, Trans. ASME, Vol. 105, 1983, pp.303.

2. TERRILL, R.M., Laminar Flows in circular pipes whose cross-sectional area varies slowly in the axial direction, Phys. of Fluids, Vol. 29, 1986, pp.2357.

3. WATSON, G.N., Theory of Bessel Functions, C.U.P., 1922.

4. HEARN, A.C. (ed.), REDUCE User's Manual Vs.3.2, The Rand Corp., 1985.

5. GARG, V.K. & ROULEAU, W.T., Stabilty of Poiseuille flow in a thin elastic tube, Phys. of Fluids, Vol. 17, 1974, pp.1103.

6. VAN DYKE, M.D., Analysis and improvement of perturbation series, Quart. J. Mech. Appl. Math., Vol.27, 1974, pp.423.

SECTION 3.

VARIABLE WIDTH WITH SUCTION

INTRODUCTION

Most of the research into flow through cylindrical tubes with mass transfer at the walls has concentrated on flow along pipes with constant injection or suction. The new exact solution of the Navier-Stokes equations valid for all Reynolds number, [1], was developed as a solution to steady, laminar, incompressible, axi-symmetric flow along a pipe of constant radius. The novel feature of this solution was that variation in the flow through the wall allowed either maintenance of the shape of the axial velocity profile for any flow or else to gradually change one specified axial velocity distribution at a given cross-section to another, similarly specified, further downstream. Further developments involving calculations of suction velocities depending on the structure of the boundary [2], and the incorporation of slip at the boundary [3], also concentrate solely on pipes of constant cross-sectional area.

In the previous sections the author has considered the case of flow along a circular pipe with impermeable walls and with slowly varying cross-sectional area. In this section, the previously uninvestigated case of exact, analytical solutions for flow along a porous pipe with variable mass transfer and varying cross-sectional area has been considered. This article presents a selection of velocity distributions and corresponding classes of wall profiles that satisfy the Navier-Stokes equations exactly which are obtained by assuming that the tangential velocity component on the wall to be zero. Streamlines of these flows with the corresponding families of boundaries are presented for a selection

of salient parameters of the problem. For each case an exact expression for the required radial throughflow, as a function of z, is obtained.

FORMULATION OF THE PROBLEM

Consider the steady, laminar, axi-symmetric motion of an incompressible fluid along a porous tube of radius R(z). A cylindrical polar co-ordinate system (r,θ,z) is chosen, where Oz lies along the centre of the tube, r is the distance measured radially and θ is the azimuthal angle. Let u and v be the velocity components in the direction of z and r increasing respectively. Then, for an axi-symmetric flow, the equation of continuity is

$$\frac{\partial}{\partial r}(rv) + r\frac{\partial u}{\partial z} = 0 \quad , \tag{3.1}$$

and the Navier-Stokes equations are

$$u\frac{\partial u}{\partial z} + v\frac{\partial u}{\partial r} = -\frac{1}{\rho}\frac{\partial p}{\partial z} + \nu\nabla^2 u \quad ,$$

(3.2)

$$u\frac{\partial v}{\partial z} + v\frac{\partial v}{\partial r} = -\frac{1}{\rho}\frac{\partial p}{\partial r} + \nu\left(\nabla^2 v - \frac{v}{r^2}\right) \quad ,$$

where

$$(3.3) \qquad \nabla^2 \equiv \frac{\partial^2}{\partial r^2} + \frac{1}{r}\frac{\partial}{\partial r} + \frac{\partial^2}{\partial z^2} ,$$

and where p is the pressure, ρ is the density and ν is the kinematic viscosity.

The symmetry condition for the axi-symmetric flow gives the boundary condition,

$$(3.4) \qquad v = 0 \qquad \text{on} \quad r = 0 .$$

In addition, it is assumed that the tangential velocity on the wall, r = R(z), is zero, that is

$$(3.5) \qquad u(z)\cos\omega + v(z)\sin\omega = 0 \qquad \text{on} \quad r = R(z) ,$$

where ω is the angle between the tangent and the pipe axis. Thus substituting for ω in (3.5) from $\tan\omega = R'(z)$ yields

$$(3.6) \qquad u + vR'(z) = 0 \qquad \text{on} \quad r = R(z) ,$$

where ' denotes differentiation with respect to z.

It has been shown by [1] that the equations (3.1) and (3.2) are satisfied by

$$(3.7) \qquad u = \lambda(a^2 - r^2) + \frac{\partial \phi}{\partial z} , \qquad v = \frac{\partial \phi}{\partial r} ,$$

where λ and a are arbitrary constants, provided $\phi(r,z)$ satisfies Laplace's equation

$$(3.8) \qquad \nabla^2 \phi = 0 .$$

On substituting for u and v from (3.7) into the equations (3.4) and (3.6) the boundary conditions become

$$(3.9) \qquad \frac{\partial \phi}{\partial r} = 0 \qquad \text{on} \quad r = 0 ,$$

and

$$(3.10) \qquad \lambda(a^2 - R^2) + \frac{\partial \phi}{\partial z} + R' \frac{\partial \phi}{\partial r} = 0 \qquad \text{on} \quad r = R(z) .$$

THE ANALYTIC SOLUTION

A solution of (3.8) is sought subject to conditions (3.9) and (3.10). Since the axi-symmetric Laplace equation is homogeneous, it is reasonable to assume that ϕ is a homogeneous function of r and z. Consequently, the form for ϕ is taken to be

$$(3.11) \qquad \phi = \sum_{\rho=0}^{n}{}' f_\rho r^\rho z^{n-\rho} ,$$

where f_ρ are constants to be determined and n is the order of the solution. On substituting for ϕ from (3.11), (3.8) becomes

$$\frac{z^{n-1}}{r} f_1 + \sum_{\rho=0}^{n-2} [(\rho + 2)^2 f_{\rho+2} + (n - \rho)(n - \rho - 1) f_\rho] r^\rho z^{n-\rho-2} = 0, \tag{3.12}$$

which, on equating coefficients, yields

$$\begin{aligned} f_1 &= 0 \\ f_{\rho+2} &= -\frac{1}{(\rho + 2)^2} (n - \rho)(n - \rho - 1) f_\rho \qquad \text{for all } \rho , \end{aligned} \tag{3.13}$$

where f_0 is some suitably chosen arbitrary constant.

Since n and ρ are both integers and $n \geq \rho$, it can readily be seen that (3.13) generates a finite series for each n. It follows that each value of n will create different solutions of the differential equation. Applying the boundary conditions to these solutions, the symmetry condition is automatically satisfied, while (3.10) becomes a differential equation which must be solved for the unknown boundary profile.

CASE 1. $n = 2$

Substituting $n = 2$ into (3.13) gives

$$\phi = \alpha(2z^2 - r^2) \ ,$$

where α is a constant, the value of which is obtained by choosing $f_0 = 2\alpha$ in (3.13). Substituting for ϕ into (3.10) yields

$$2\alpha RR' + \lambda R^2 = \lambda a^2 + 4\alpha z \ ,$$

which, by defining $\lambda^* = \lambda/\alpha$, can be written as

$$(3.14) \qquad 2RR' + \lambda^* R^2 = \lambda^* a^2 + 4z \ ,$$

where λ^* and a are arbitrary constants. Equation (14) can be integrated exactly to give the class of boundaries

$$(3.15) \qquad R^2 = Ae^{-\lambda^* z} + \frac{4}{\lambda^{*2}}(\lambda^* z - 1) + a^2 \ ,$$

where A is an arbitrary constant of integration. The radial and axial velocities are obtained by substituting for ϕ into (3.7) and are

$$(3.16) \qquad u = \alpha[\lambda^*(a^2 - r^2) + 4z] \ , \qquad v = -2\alpha r \ .$$

It can immediately be seen that for a given cross-section, the magnitude of the radial velocity v, increases linearly with distance from the pipe axis. The cross-pipe axial velocity profile is parabolic. For any given cross-section z^*, the axial velocity can be considered to be

$$u = -\lambda r^2 + C \ ,$$

where the constant C depends on the distance downstream. For $C/\lambda \leq 0$ and $C/\lambda \geq R^2$ the flow is uni-directional but the flow for $C/\lambda \leq 0$ is in the opposite direction to that for $C/\lambda \geq R^2$. For the intermediate values $0 < C/\lambda < R^2$ a region of flow reversal occurs. The actual values of these velocities, and the wall shape itself are dependent on the choice of the arbitrary constants A, λ^* and a. The changes in these velocities are best illustrated by the streamlines of the flow. Let ψ be the streamfunction defined by

$$(3.17) \qquad u = \frac{1}{r}\frac{\partial \psi}{\partial r} \ , \qquad v = -\frac{1}{r}\frac{\partial \psi}{\partial z} \ ,$$

then substituting u and v from (3.16) into (3.17) and carrying out suitable integration and differentiation gives

$$(3.18) \qquad \psi = \alpha[2r^2 z + \tfrac{1}{4}\lambda^* r^2(2a^2 - r^2)] \ .$$

To investigate the streamfunction and wall profiles in more detail, it is necessary to consider the effect of the different range of values of the arbitrary constants of the problem; λ^*, a and A. An inspection of (3.15) and (3.18) shows that it is sufficient to consider $\lambda^* > 0$ and $a \geq 0$, since $\lambda^* = -c$ generates the same flow pattern and boundary profiles as $\lambda^* = c$, but with the direction reversed. It is worth noting that the streamfunction ψ is independent of the choice of A and so by varying the value of A a family of wall profiles can be generated, that will enclose one particular flow with the required zero tangential velocity on the boundary. Further, the parameter α does not influence the problem. The wall description (3.15) is independent of α, and even though the values of the streamfunction on the streamlines are different for the different choices of α, the pattern itself remains unchanged. Taking λ^* large reduces the equations to those for Poiseuille Flow, that is

$$R \sim a \quad \text{and} \quad u \sim \lambda(a^2 - r^2) , \quad v \sim 0 .$$

The interesting cases exist for λ^* small. It should be noted that, since $\lambda^* = \lambda/\alpha$, taking λ^*small does not necessarily imply that λ itself is small. Since α is an arbitrary parameter of the problem, its value can be chosen in such a way to ensure that λ^* is small regardless of the size of λ. Clearly, this means that the interesting cases are <u>not</u> necessarily a perturbation of a slow flow solution. Figures 3.1-3.4 illustrate the streamfunction and corresponding families of boundaries for $\lambda^* = 1, 2, 4$ with $a = 2$, and $\lambda^* = 2$, $a = 0$.

The requirement that there is zero tangential velocity at the wall implies that the boundaries and the streamlines are orthogonal, and as such that

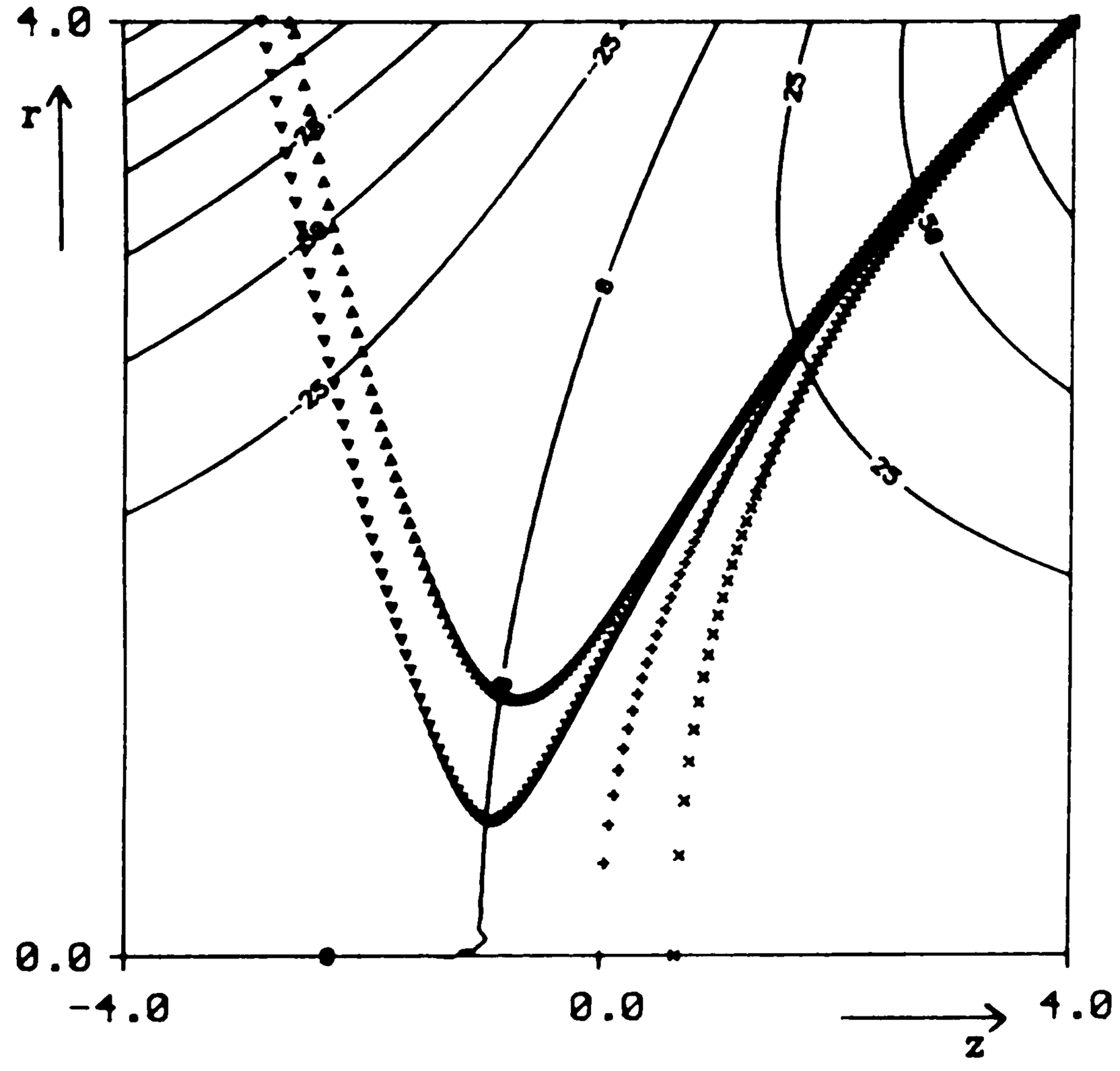

Figure 3.1.

Streamlines and boundary profiles for $\lambda^* = 1$, a = 2 and A = 2.0, 1.6, 0.0, -5.0.

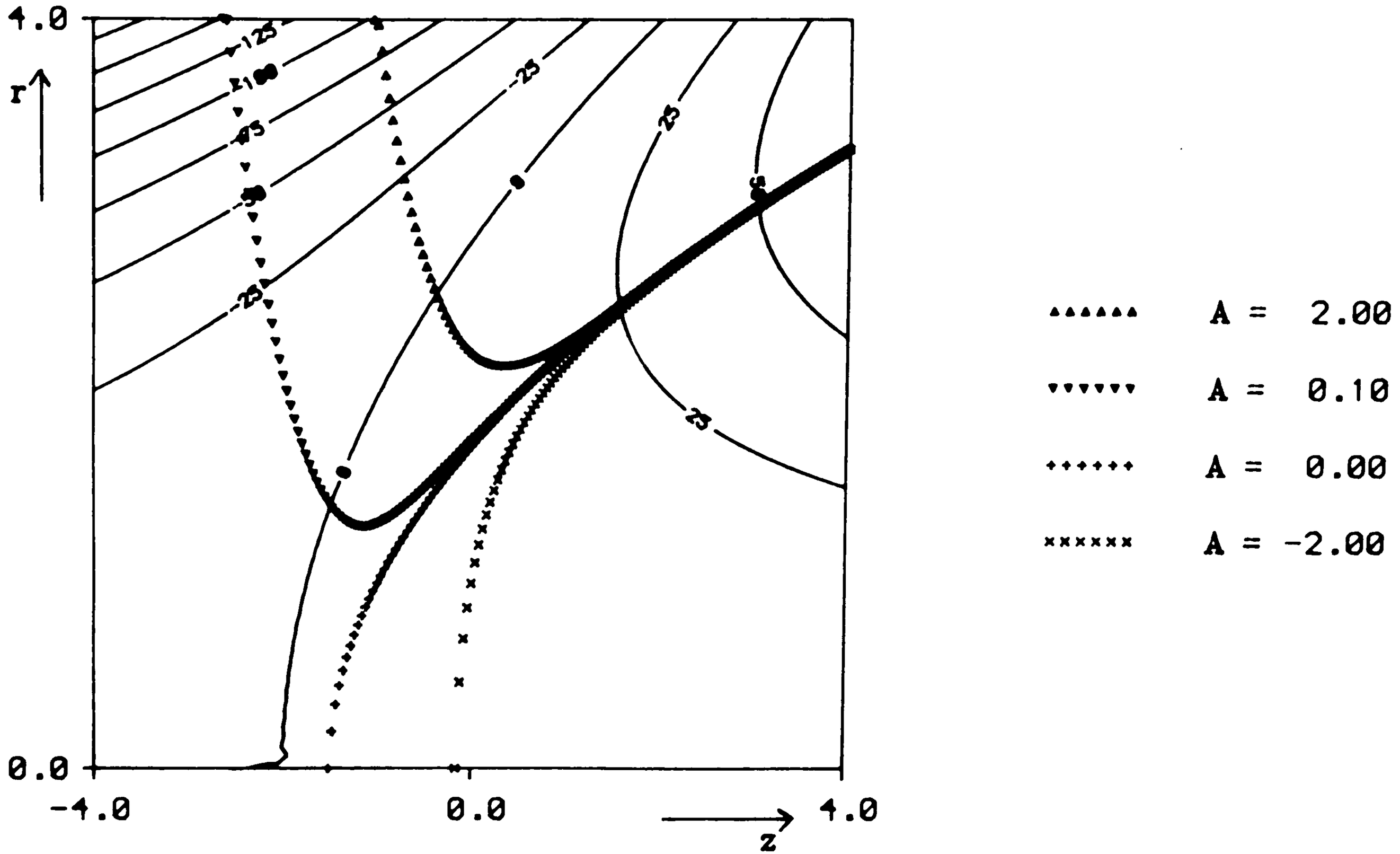

Figure 3.2.

Streamlines and boundary profiles for $\lambda^* = 2$, $a = 2$ and $A = 2.0, 0.1, 0.0, -2.0$.

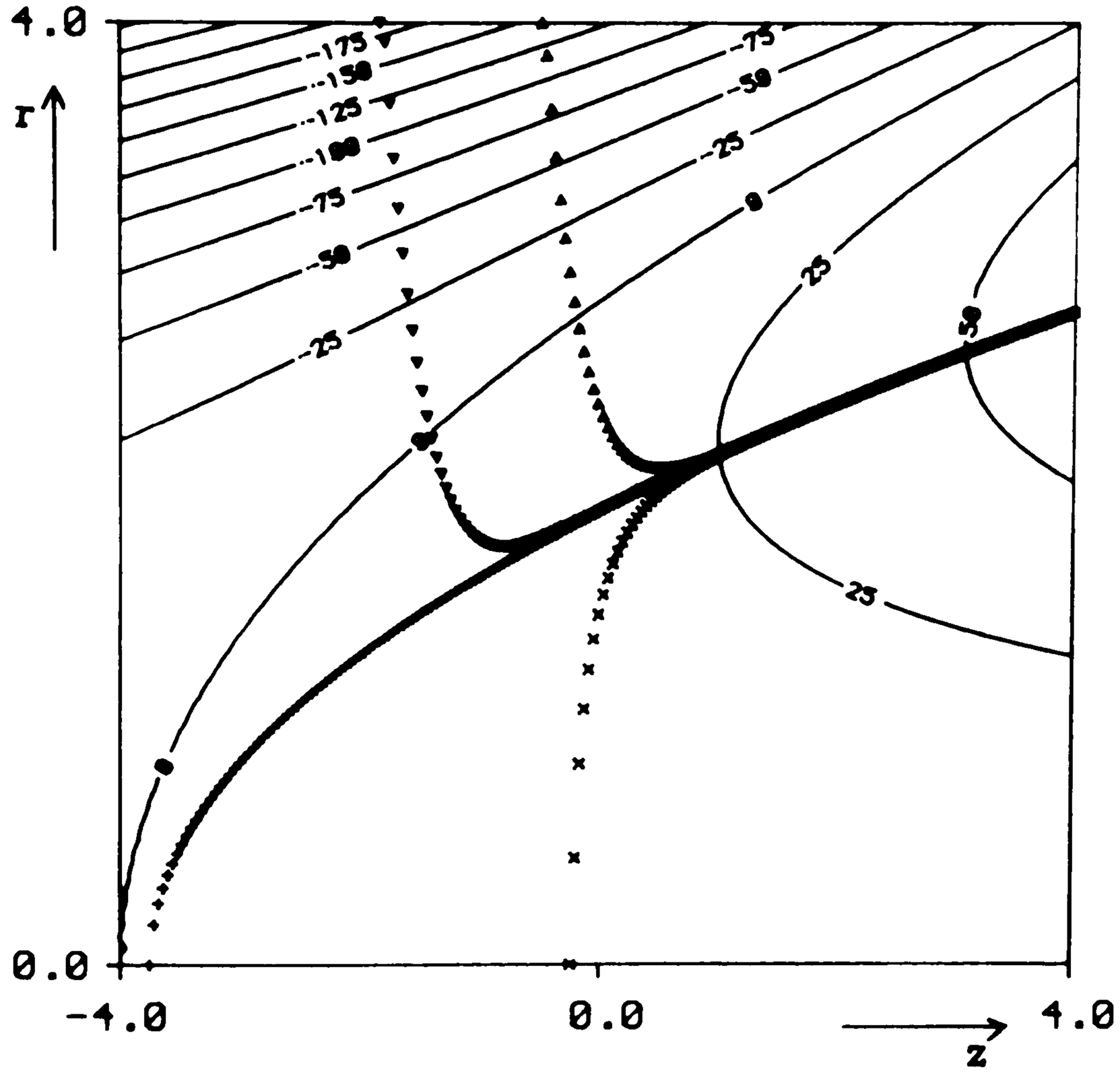

▲▲▲▲▲▲ A = 2.00

▼▼▼▼▼▼ A = 0.01

◆◆◆◆◆◆ A = 0.00

✖✖✖✖✖✖ A = -1.50

Figure 3.3.

Streamlines and boundary profiles for $\lambda^* = 4$, a = 2 and A = 2.0, 0.01, 0.0, -1.5.

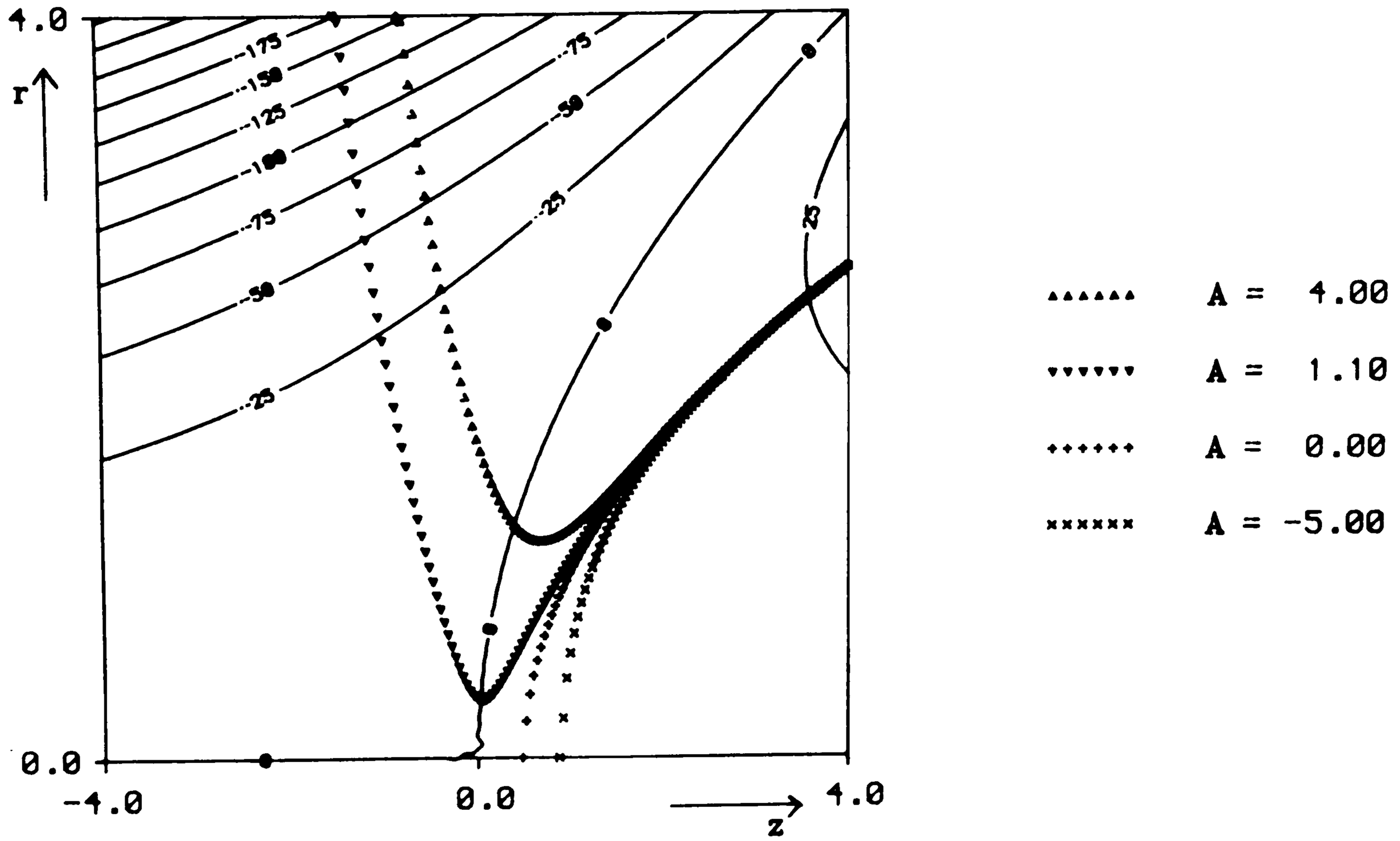

Figure 3.4.

Streamlines and boundary profiles for $\lambda^* = 2$, a = 0 and A = 4.0, 1.1, 0.0, -5.0.

boundaries could be constructed geometrically. The values of A in the figures are chosen to best illustrate the range of shapes which can be obtained as a solution. It should be noted that it is necessary for R to be real. Consequently, values of R are obtained only for the range of z such that $R^2 \geq 0$. As a result it is possible for the pipe to have two distinct parts. These boundaries can exist independently of each other, but in these cases the streamfunction is valid only in the relevant range of z. If $A \leq 0$, the pipe has only one branch and is closed, alternatively if

$$A \geq \frac{4}{\lambda^*} e^{-\frac{1}{4}\lambda^{*2}a^2},$$

then, for all z, $R^2 \geq 0$ and the pipe narrows and then quickly expands again. The special case when A is equal to the above value gives a pipe which narrows to a cusp. Otherwise, the profile has two distinct parts. For z large and positive the boundary is independent of A and

$$R^2 \sim \frac{4z}{\lambda^*},$$

while for z large and negative the pipe rapidly contracts, if $A \leq 0$, or eventually expands if $A > 0$. Hence, the family of boundaries tend to these shape far up and downstream. Consequently, it is sufficient to present the figures for the range $-4 \leq z \leq 4$.

The quantity of fluid flowing in/out through the wall can be determined by considering the normal velocity at the boundary. Let the velocity normal to the boundary be S(z); then resolving the velocities gives

$$(3.19) \qquad S(z) = v(z)\cos\omega - u(z)\sin\omega \qquad \text{on} \qquad r = R(z) \ .$$

Since ω is the angle of inclination of the tangent to the wall, this can be re-written as

$$(3.20) \qquad S(z) = (1 + R'(z)^2)^{-\frac{1}{2}}\{v(z) - u(z)R'(z)\} \qquad \text{on} \qquad r = R(z) \ .$$

Multiplying both the numerator and denominator by R and substituting from (3.16) and (3.14) it can be shown that

$$(3.21) \qquad S(z) = -2\alpha\{R^2 + (RR')^2\}^{\frac{1}{2}} \ ,$$

where the positive square root is taken to ensure that the direction of the flow is in agreement with that predicted by the velocity equations (3.16). R^2 and RR' can be obtained from (3.15), thus

$$S(z) = -2\alpha\{\tfrac{1}{4}\lambda^{*2}A^2e^{-2\lambda^* z} - Ae^{-\lambda^* z} + \frac{1}{\lambda^*}(\lambda^* a^2 + 4z)\}^{\frac{1}{2}} \ .$$

From (3.21) it can immediately be seen that for $\alpha > 0$, S(z) is negative for all z and so there are no regions of suction. Conversely, for $\alpha < 0$

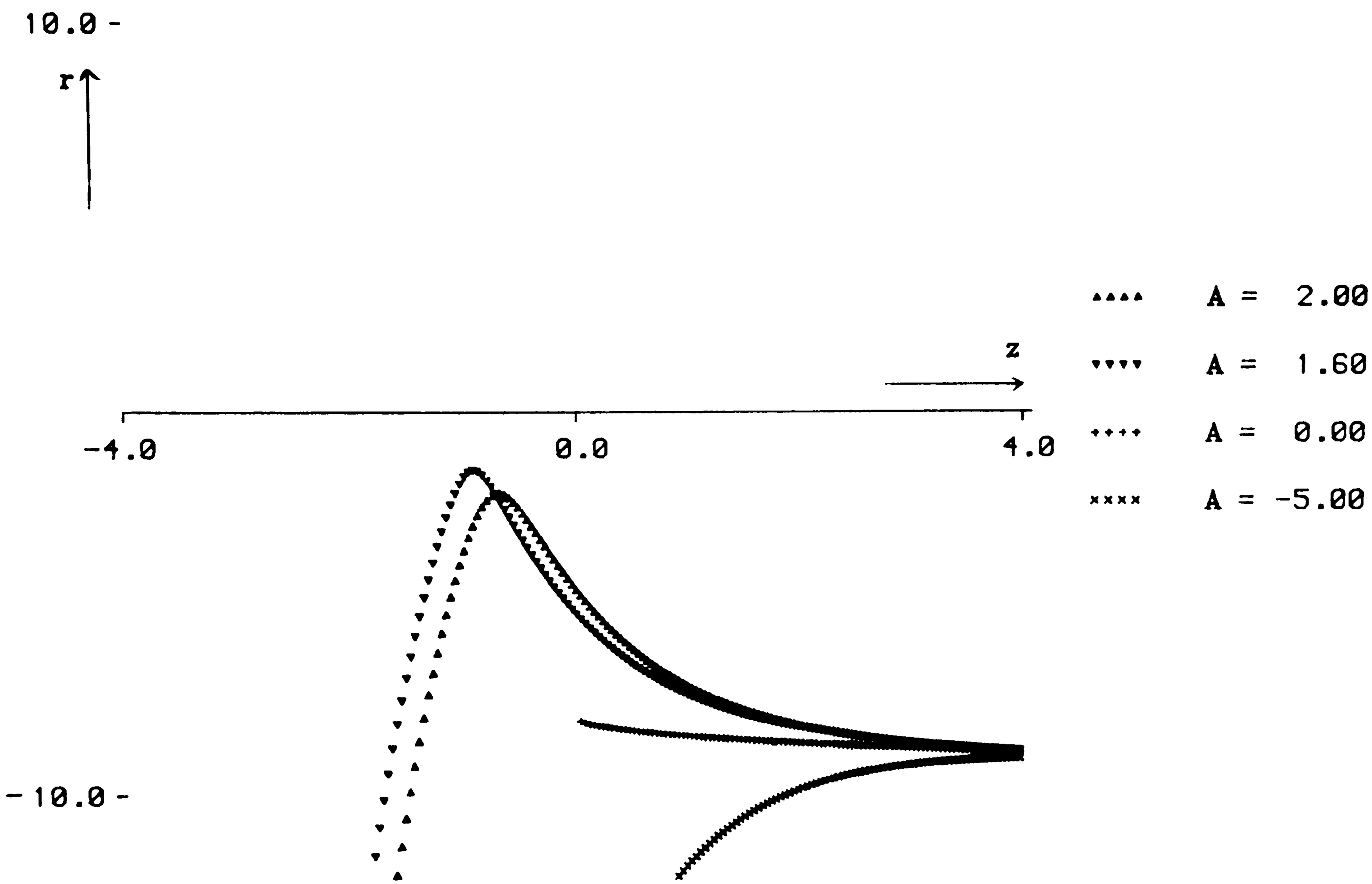

Figure 3.5.

Injection profiles for $\lambda^* = 1$, a = 2 and A = 2.0, 1.6, 0.0, -5.0.

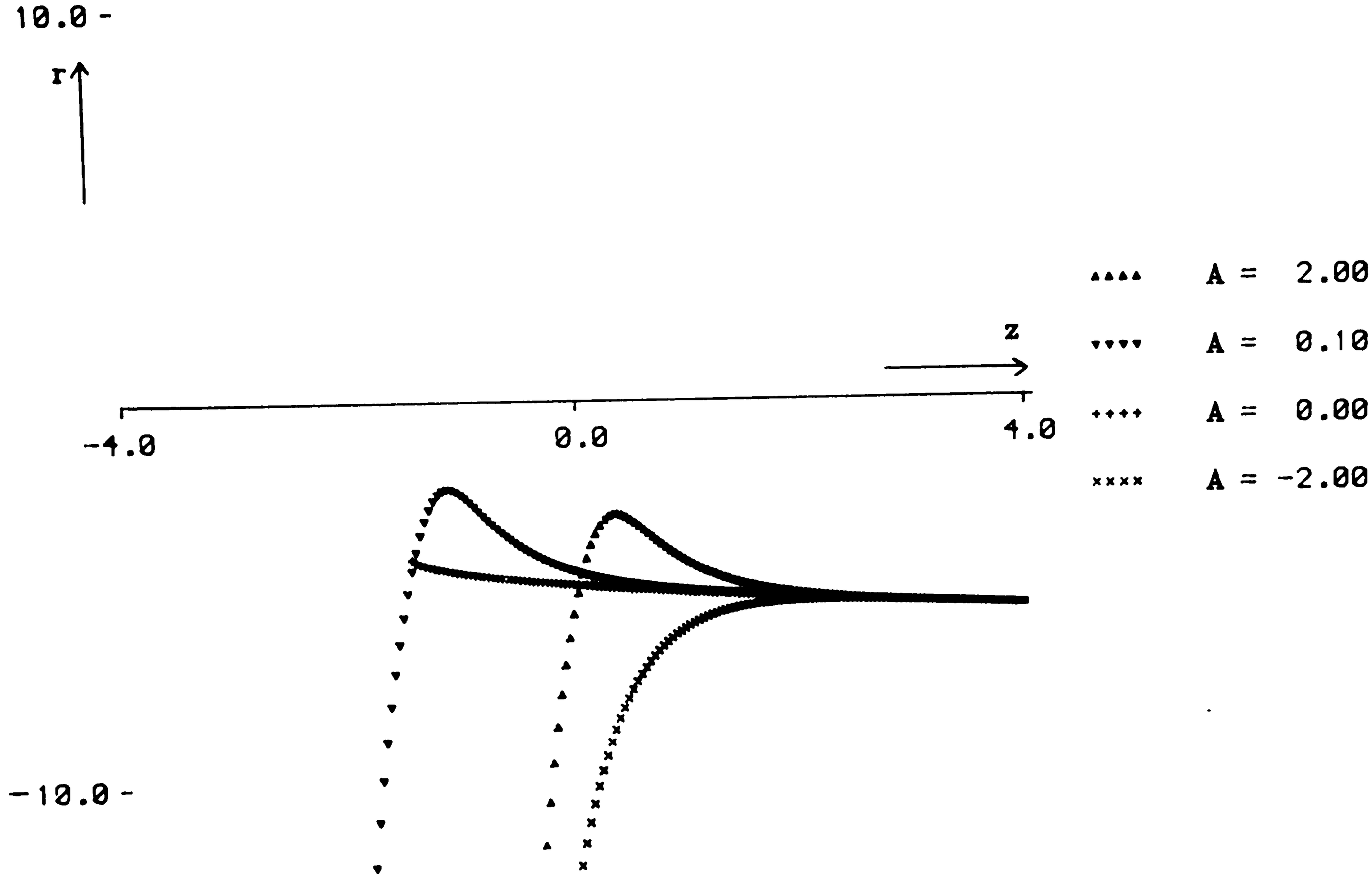

Figure 3.6.

Injection profiles for $\lambda^{*} = 2$, a = 2 and A = 2.0, 0.1, 0.0, -2.0.

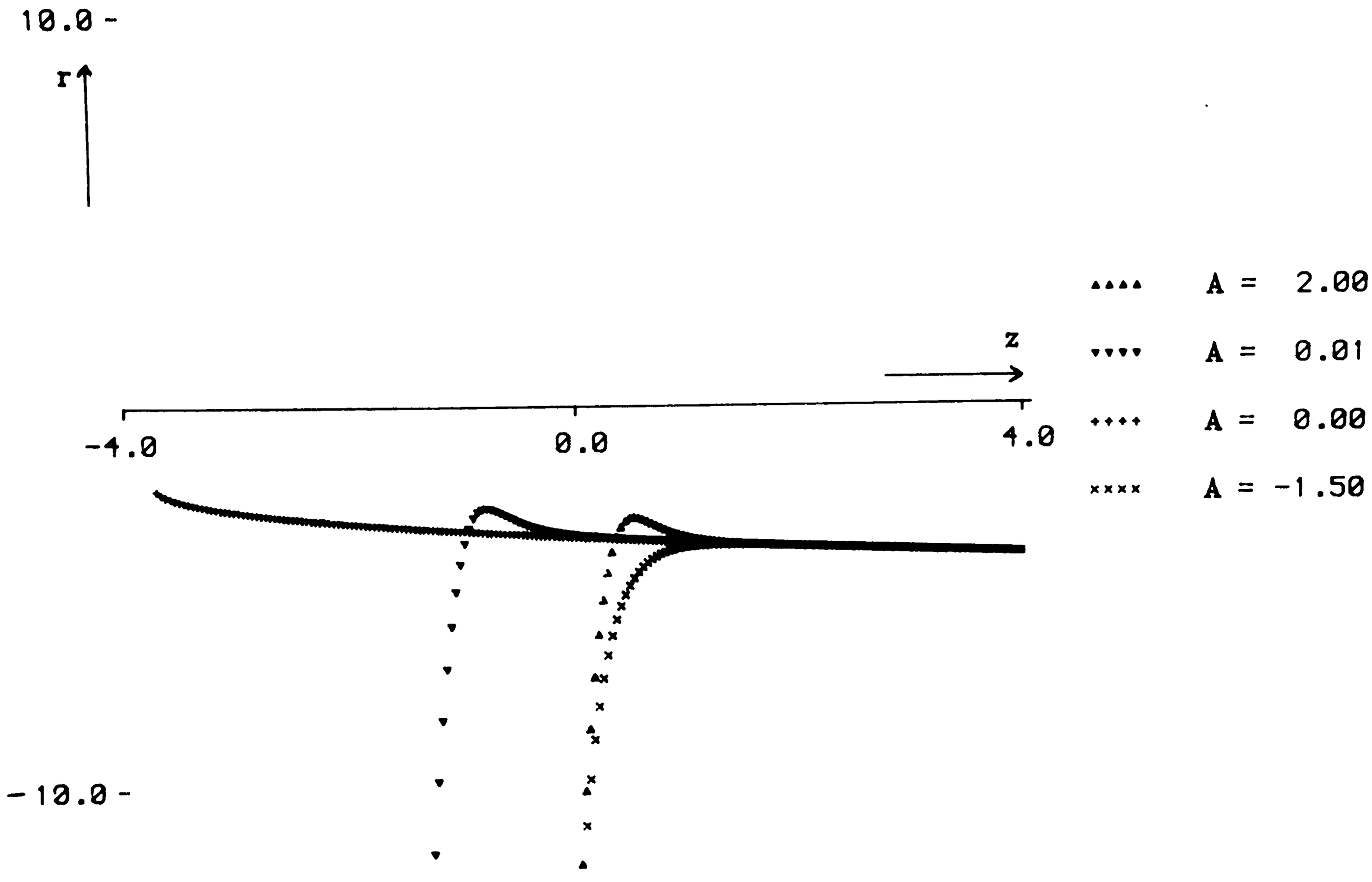

Figure 3.7.

Injection profiles for $\lambda^{*} = 4$, a = 2 and A = 2.0, 0.01, 0.0, -1.5.

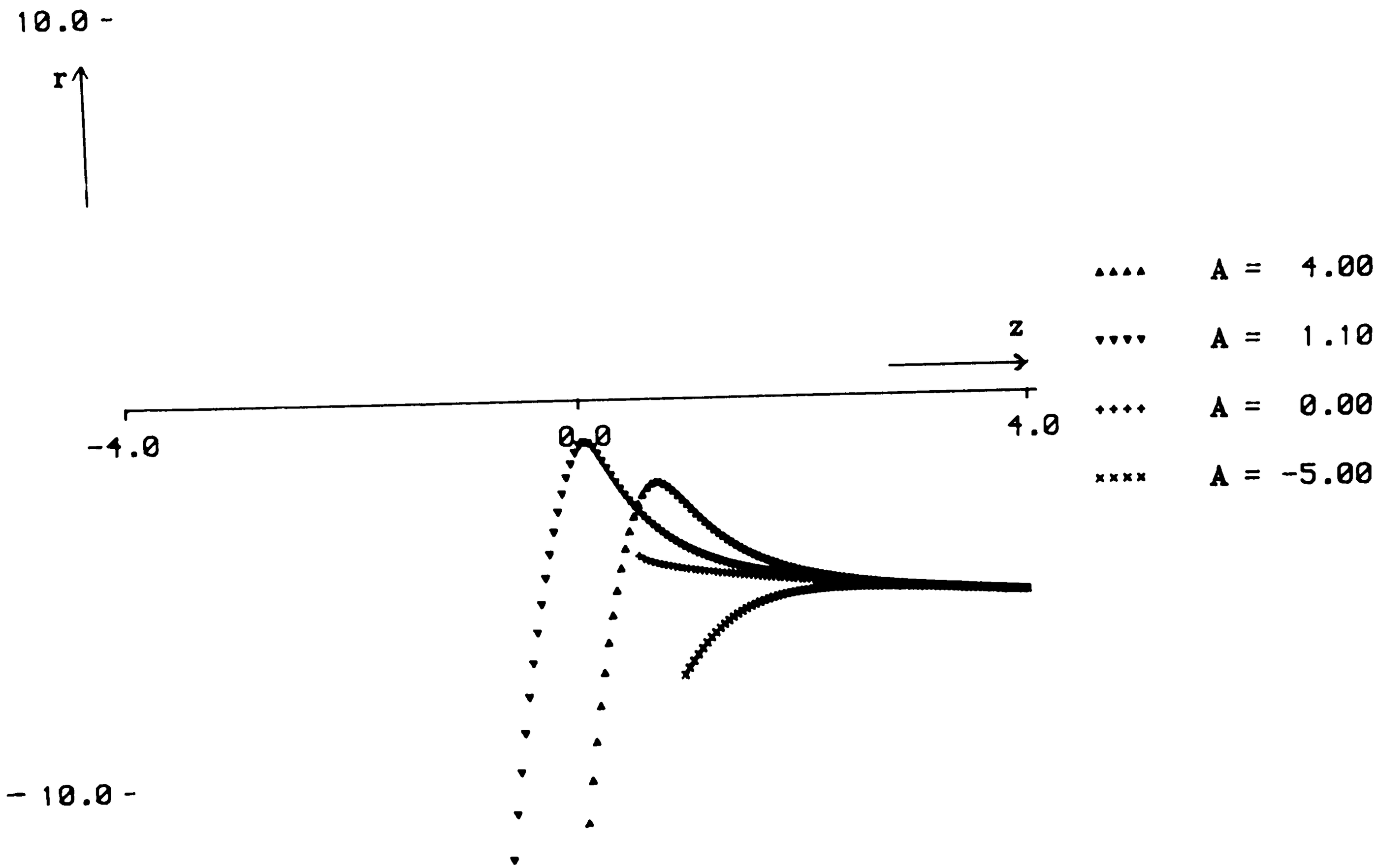

Figure 3.8.

Injection profiles for $\lambda^* = 2$, a = 0 and A = 4.0, 1.1, 0.0, -5.0.

there are no regions of injection. Differentiating (3.21) shows that if $R^2 > 0$ for all z then the minimum injection occurs at the minimum radius. This is demonstrated effectively by the graphs of wall shapes and suction. Figures 3.5-3.8 depict the injection profiles corresponding to the cases presented in Figs. 3.1-3.4. For z large and positive, the through flow is independent of A and

$$S \sim -2\{ \frac{4z}{\lambda^*} \}^{\frac{1}{2}} ,$$

while for z large and negative the through flow rapidly increases if $\alpha < 0$, or decreases if $\alpha > 0$. Hence, it is sufficient to present the through flow for $-4 \leq z \leq 4$. It should be noted that in the cases when the tubes are closed, the injection is evaluated only in the regions where $R \geq 0$.

CASE 2. n = 3

Substituting n = 3 into (3.13) and (3.11) gives

$$\phi = \beta[2z^3 - 3r^2z] ,$$

where β, like α in Case 1, is an arbitrary constant obtained by choosing $f_0 = 2\beta$ in equation (3.13). Substituting ϕ into (3.10) gives

(22) $$(\lambda^* + 3)R^2 + 6RR'z = \lambda^* a^2 + 6z^2 \ ,$$

where $\lambda^* = \lambda/\beta$ and a are arbitrary constants. Equation (3.22) can be integrated exactly to yield

(3.23) $$R^2 = Az^{-(\lambda^*+3)/3} + \frac{6}{(\lambda^* + 9)} z^2 + \frac{\lambda^* a^2}{(\lambda^* + 3)} \ ,$$

where A is an arbitrary constant of integration, and $\lambda^* \neq -3$ and -9. These two cases need to be considered separately. When $\lambda^* = -3$ integration of (3.22) yields

(3.24) $$R^2 = A + z^2 - a^2 \ln|z| \ ,$$

while for $\lambda^* = -9$, the integration gives

(3.25) $$R^2 = Az^2 + 2z^2 \ln|z| + \frac{3a^2}{2} \ .$$

Differentiating ϕ and substituting the differentials into (3.7) gives the velocities

(3.26) $$u = \beta[\lambda(a^2 - r^2) + 6z^2 - 3r^2] \ , \qquad v = -6\beta rz \ .$$

At a given cross-section the size of the radial velocity increases linearly towards the boundary and the axial velocity profile is again

parabolic. The streamfunction for this flow is obtained by substituting (3.26) into (3.16) and is

$$\psi = \beta\{3r^2z^2 + \tfrac{1}{4}r^2[2\lambda^* a^2 - (\lambda^* + 3)r^2]\} \quad , \tag{3.27}$$

which is symmetric about both $r = 0$ and $z = 0$. As in Case 1 it is sufficient to consider $a \geq 0$. However, to ensure that R^2 is always real it is necessary to take a real root of $z^{-[(\lambda^*+3)/3]}$. Clearly, for $\lambda^* < -3$, R^2 is finite for all z, otherwise R^2 is undefined at $z = 0$. Again, values of R are obtained only for the range of z such that R is real, that is, $R^2 \geq 0$. Choosing different values of A generates a class of wall profiles that satisfy the zero tangential velocity condition on the boundary.

Figures 3.9-3.14 show contours of the streamfunction ψ, with a selection of the boundaries that satisfy the velocity conditions. There are two general streamline distributions corresponding to whether $\lambda^* \geq -3$ or $\lambda^* < -3$.

For $\lambda^* \geq -3$ the streamfunction has two asymptotes, $r = \pm \sqrt{\ }^2/_{(\lambda^* + 3)}[6z^2 + \lambda a^2]$. There is no flow across these lines and consequently the fluid is confined to the three distinct sections bounded by them (Fig.3.12-3.14). It should be observed that for these values of λ^* and $A \neq 0$, the boundary is infinite at $z = 0$.

For $\lambda^* < -3$ the streamline patterns include some closed contours which enclose regions of 'trapped' fluid (Fig.3.9-3.11).

The symmetry of the streamfunction about $z = 0$ was mentioned earlier. However, the wall is symmetric about $z = 0$ only when $(^{\lambda^*}/_3 + 1)$

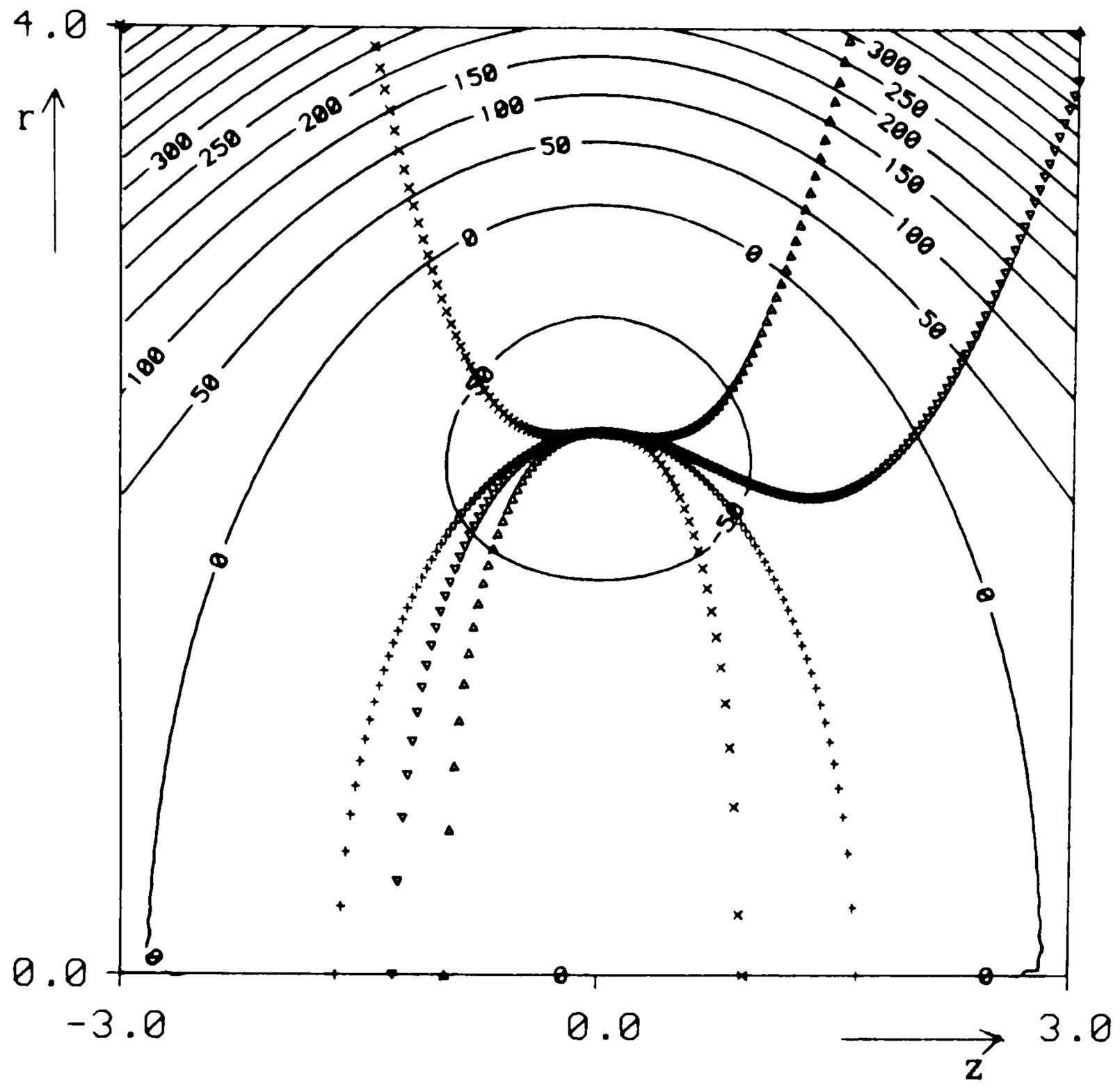

▲▲▲▲▲▲ A = 4.0

▽▽▽▽▽▽ A = 1.0

++++++ A = 0.0

×××××× A = -5.0

Figure 3.9.

Streamlines and boundary profiles for λ^{*} = -12, a = 2 and A = 4.0, 1.0, 0.0, -5.0

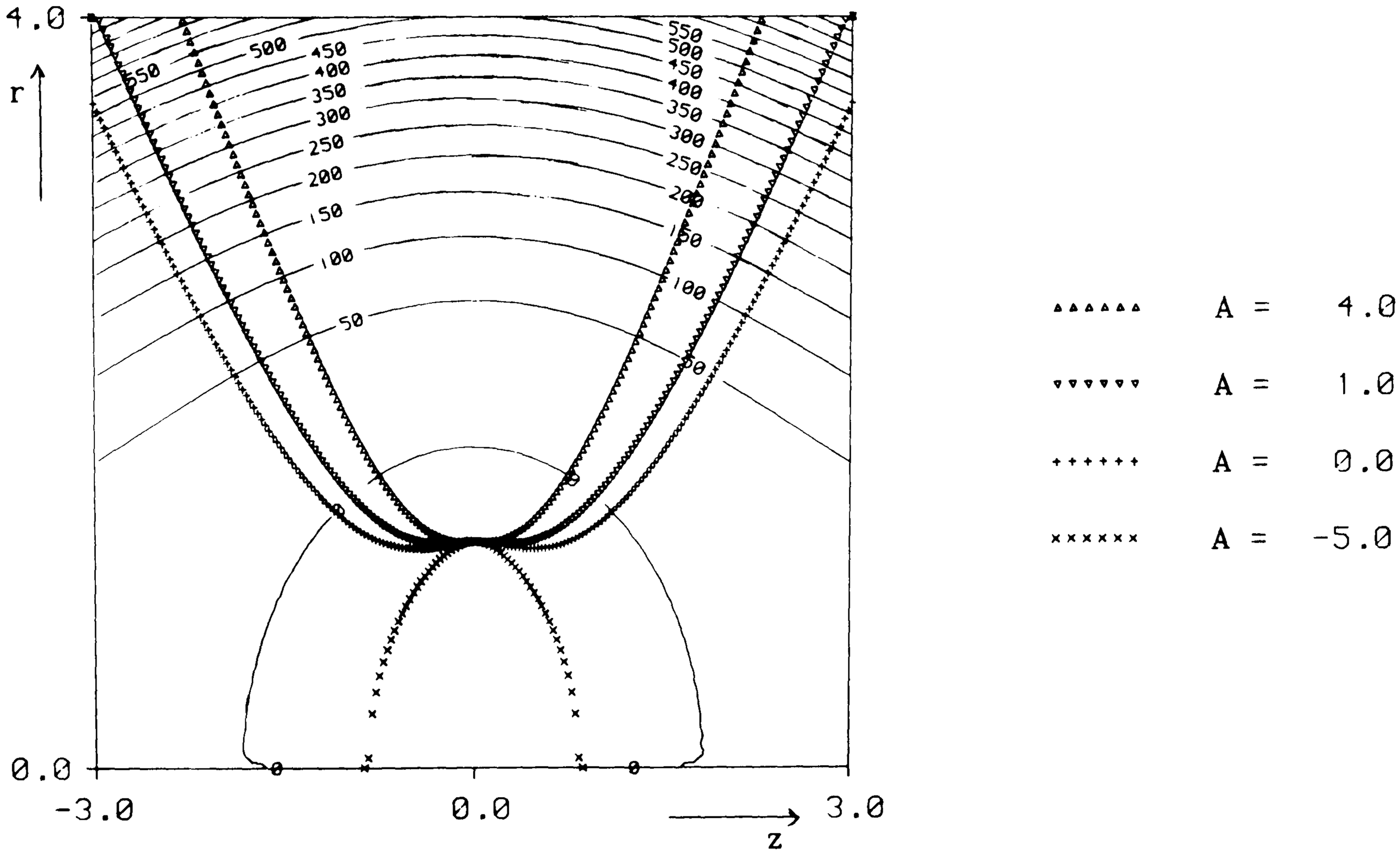

Figure 3.10.

Streamlines and boundary profile for $\lambda^* = -9$, a = 2 and A = 4.0, 1.0, 0.0, -5.0

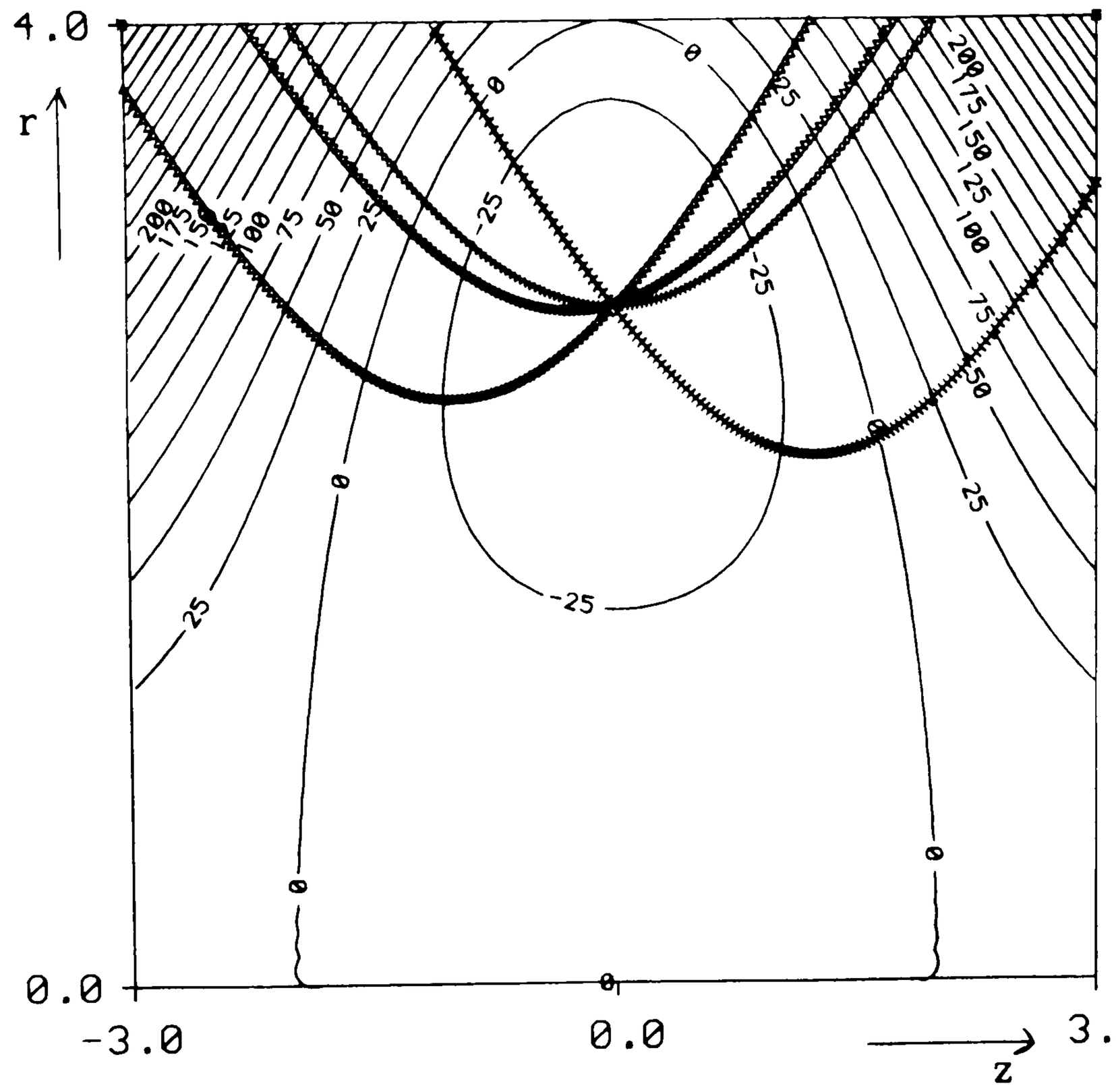

▲▲▲▲▲▲ A = 4.0

▼▼▼▼▼▼ A = 1.0

++++++ A = 0.0

×××××× A = -5.0

Figure 3.11.

Streamlines and boundary profiles for λ^* = -6, a = 2 and A = 4.0, 1.0, 0.0, -5.0

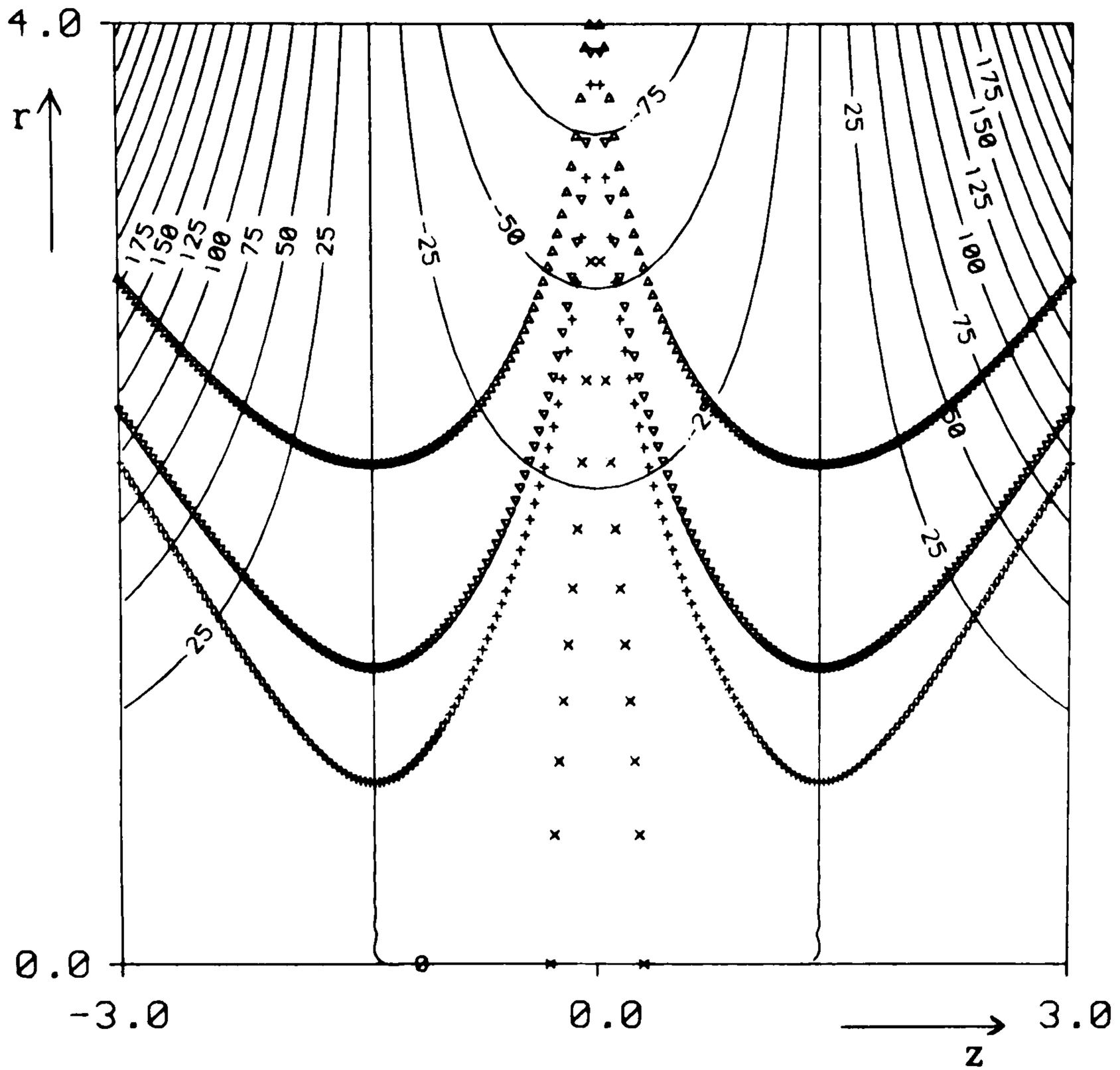

Figure 3.12.

Streamlines and boundary profiles for $\lambda^* = -3$, a = 2 and A = 4.0, 1.0, 0.0, -5.0

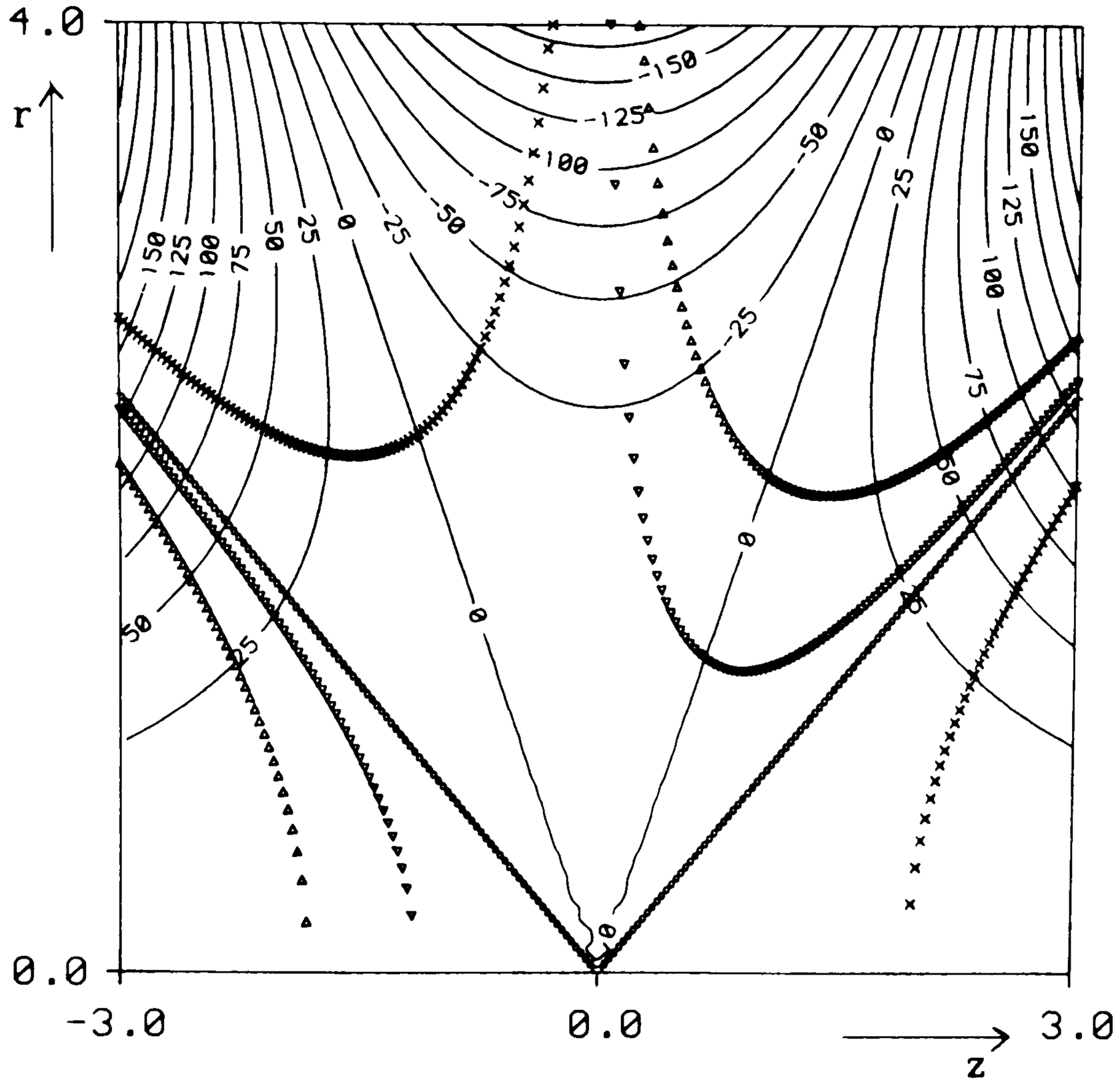

▲▲▲▲▲▲ A = 4.0

▼▼▼▼▼▼ A = 1.0

++++++ A = 0.0

×××××× A = -5.0

Figure 3.13.

Streamlines and boundary profiles for $\lambda^* = 0$, a = 2 and A = 4.0, 1.0, 0.0, -5.0

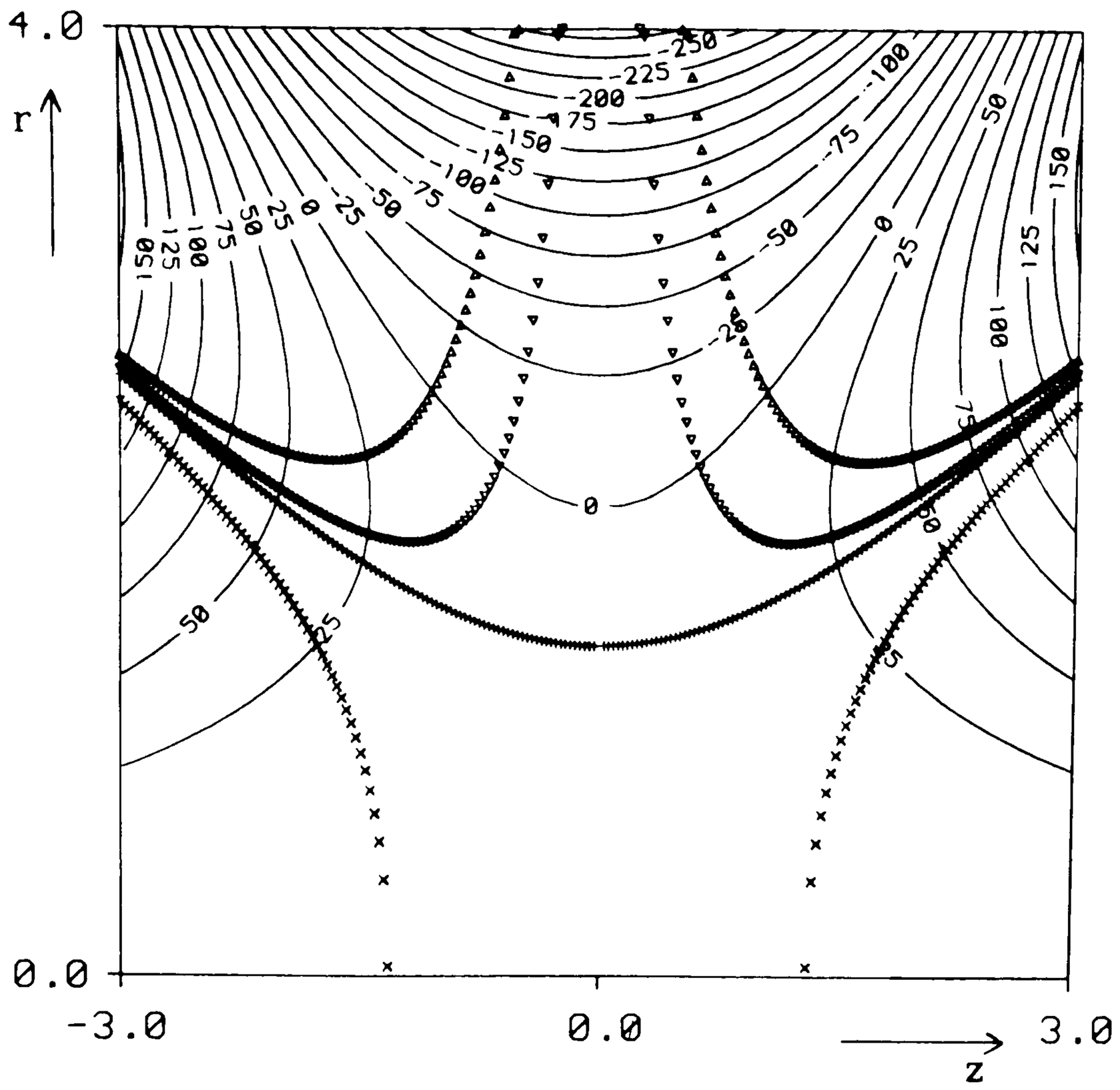

▲▲▲▲▲▲ A = 4.0

▼▼▼▼▼▼ A = 1.0

++++++ A = 0.0

×××××× A = -5.0

Figure 3.14.

Streamlines and boundary profiles for λ^* = 3, a = 2 and A = 4.0, 1.0, 0.0, -5.0

is even, that is $\lambda^* = -9, -3, 3, 9, ..$etc.(Fig.3.13-3.14), or for all λ^* when the arbitrary constant of integration A is chosen to be zero.

To investigate the through flow the velocities (3.26) are substituted into (3.20) to yield

$$S(z) = -6\beta z\{R^2 + (RR')^2\}^{\frac{1}{2}} , \tag{3.28}$$

taking the positive square root to ensure that the flow direction is in agreement with that predicted by the velocity equation (3.26), and where R^2 and RR' can be found from equation (3.24) if $\lambda^* = -3$, equation (3.25) if $\lambda^* = -9$ and equation (3.23) otherwise. This clearly shows that there are two distinct regions of through flow. That is, for $\alpha > 0$ regions of injection for $z > 0$ and suction for $z < 0$, and vice versa for $\alpha < 0$. Figures 3.15-3.20 illustrate the through flow needed to produce the streamlines presented in Figures 3.9-3.15. The in/out flow is plotted for values of z such that R(z) is real and greater than zero.

CASE 3. n = 4

Substituting n = 4 in the recurrence relation (3.13) gives the potential ϕ to be

$$\phi = \gamma(8z^4 - 24r^2z^2 + 3r^4) ,$$

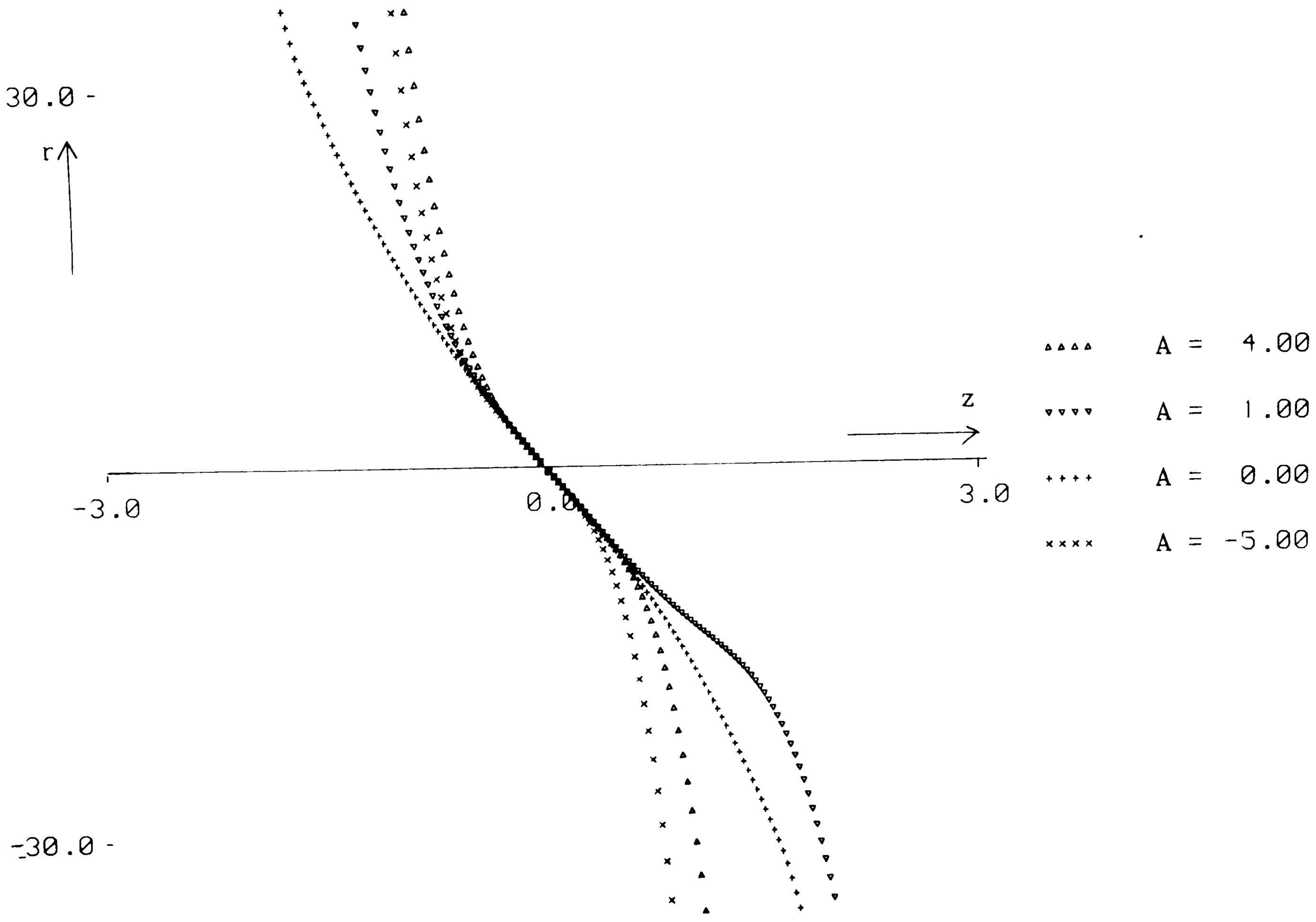

Figure 3.15.

Injection profiles for λ^* = -12, a = 2 and A = 4.0, 1.0, 0.0, -5.0

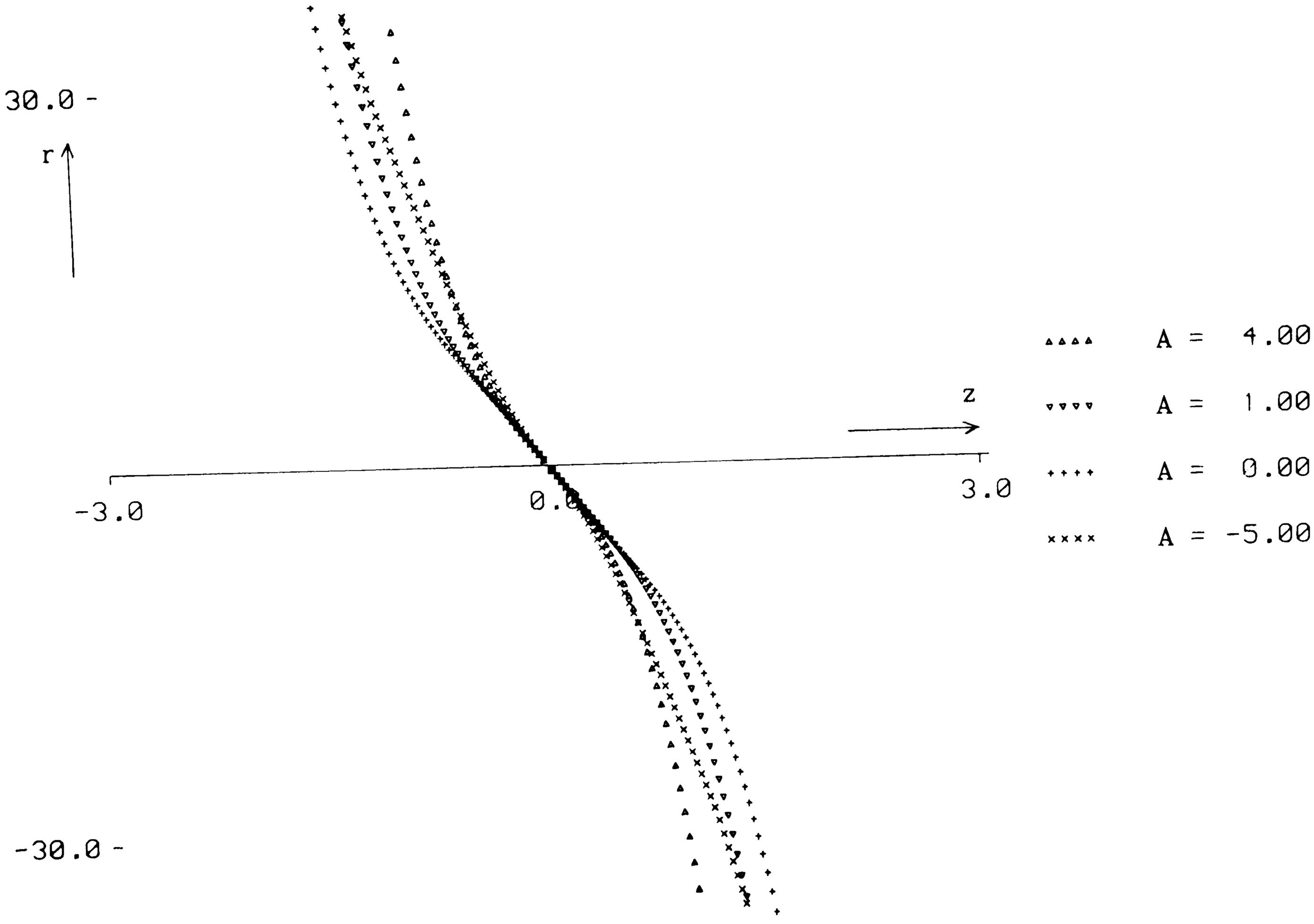

Figure 3.16.

Injection profile for $\lambda^* = -9$, a = 2 and A = 4.0, 1.0, 0.0, -5.0

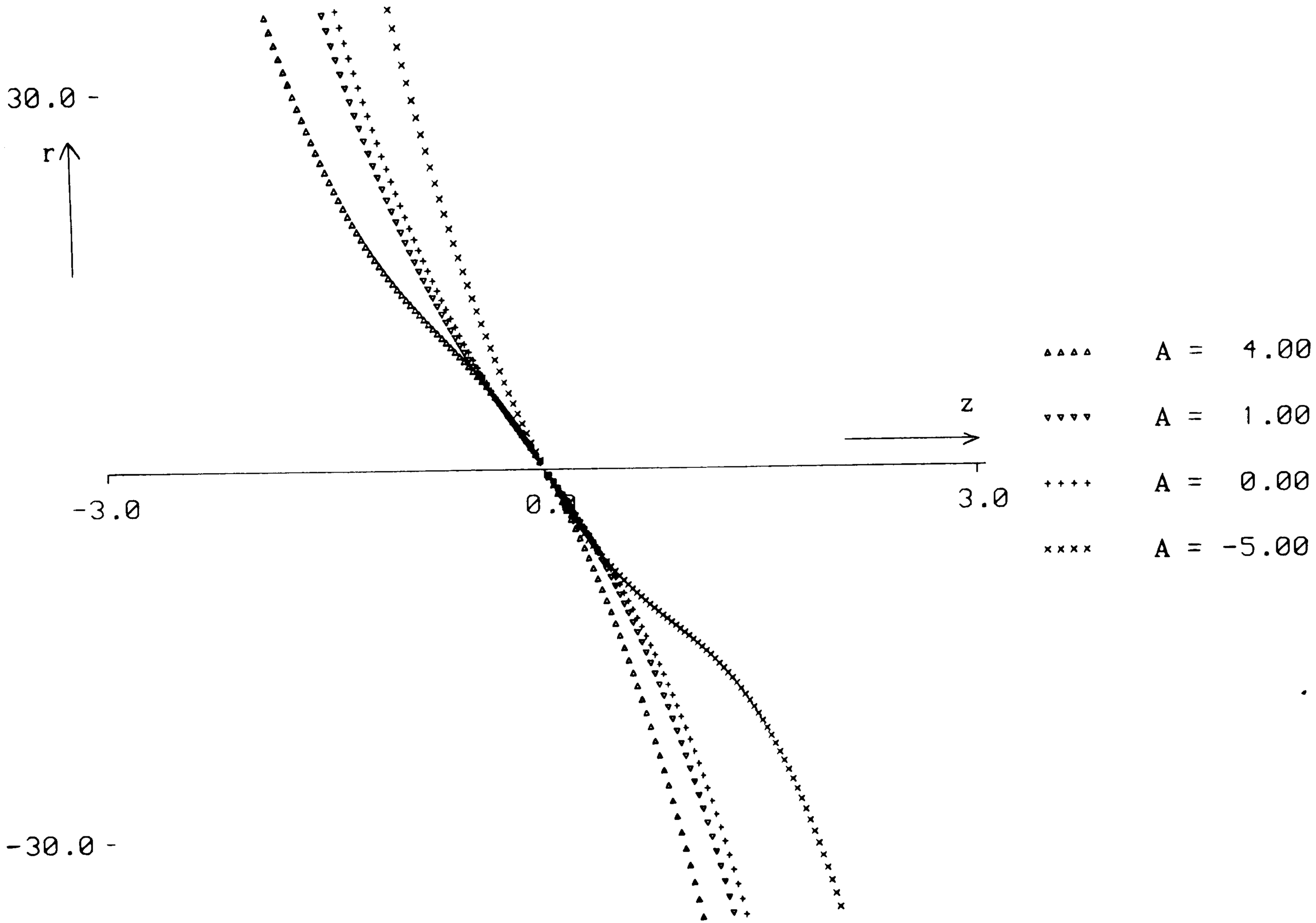

Figure 3.17.

Injection profiles for λ^{*} = -6, a = 2 and A = 4.0, 1.0, 0.0, -5.0

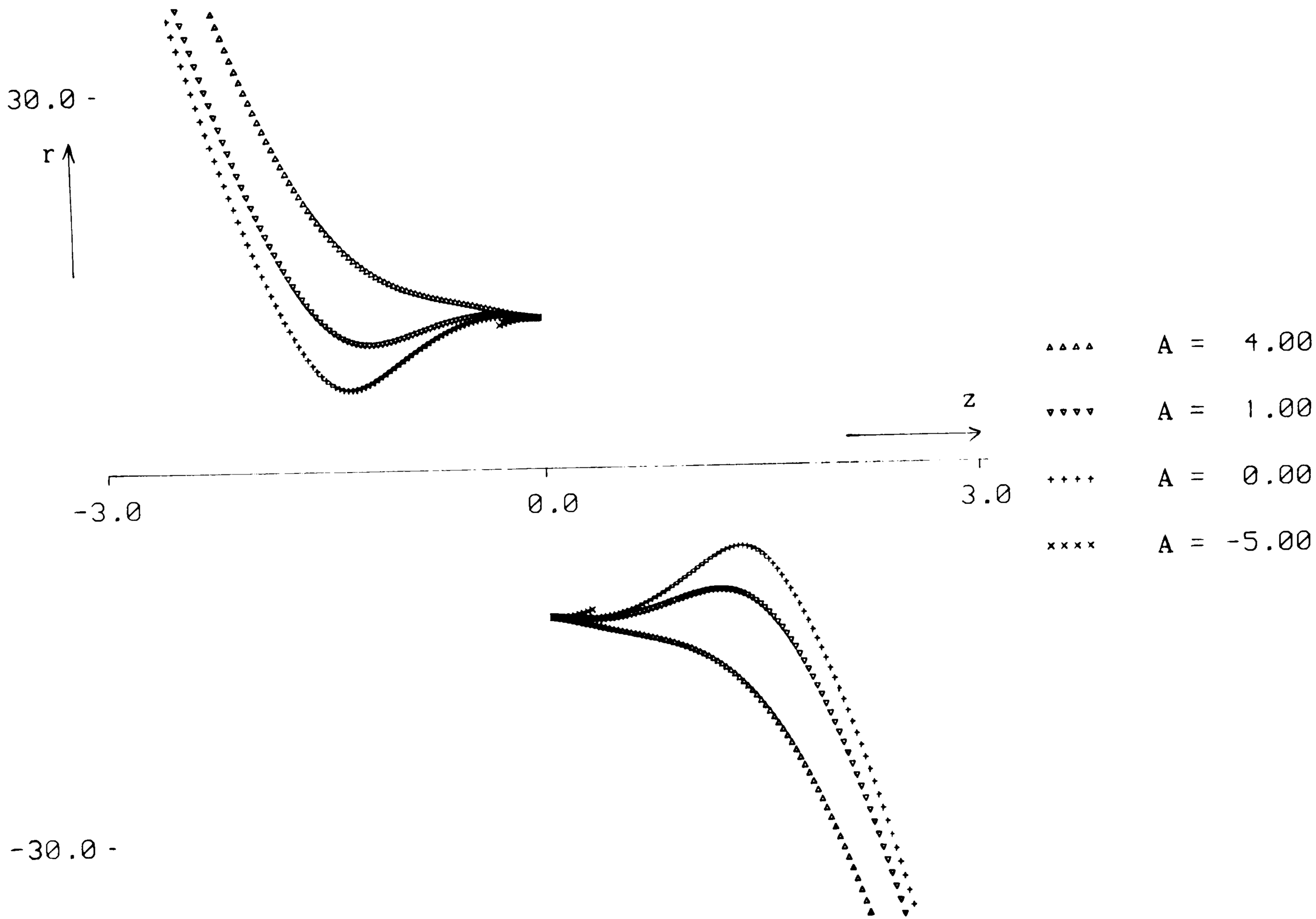

Figure 3.18.

Injection profiles for $\lambda^* = -3$, a = 2 and A = 4.0, 1.0, 0.0, -5.0

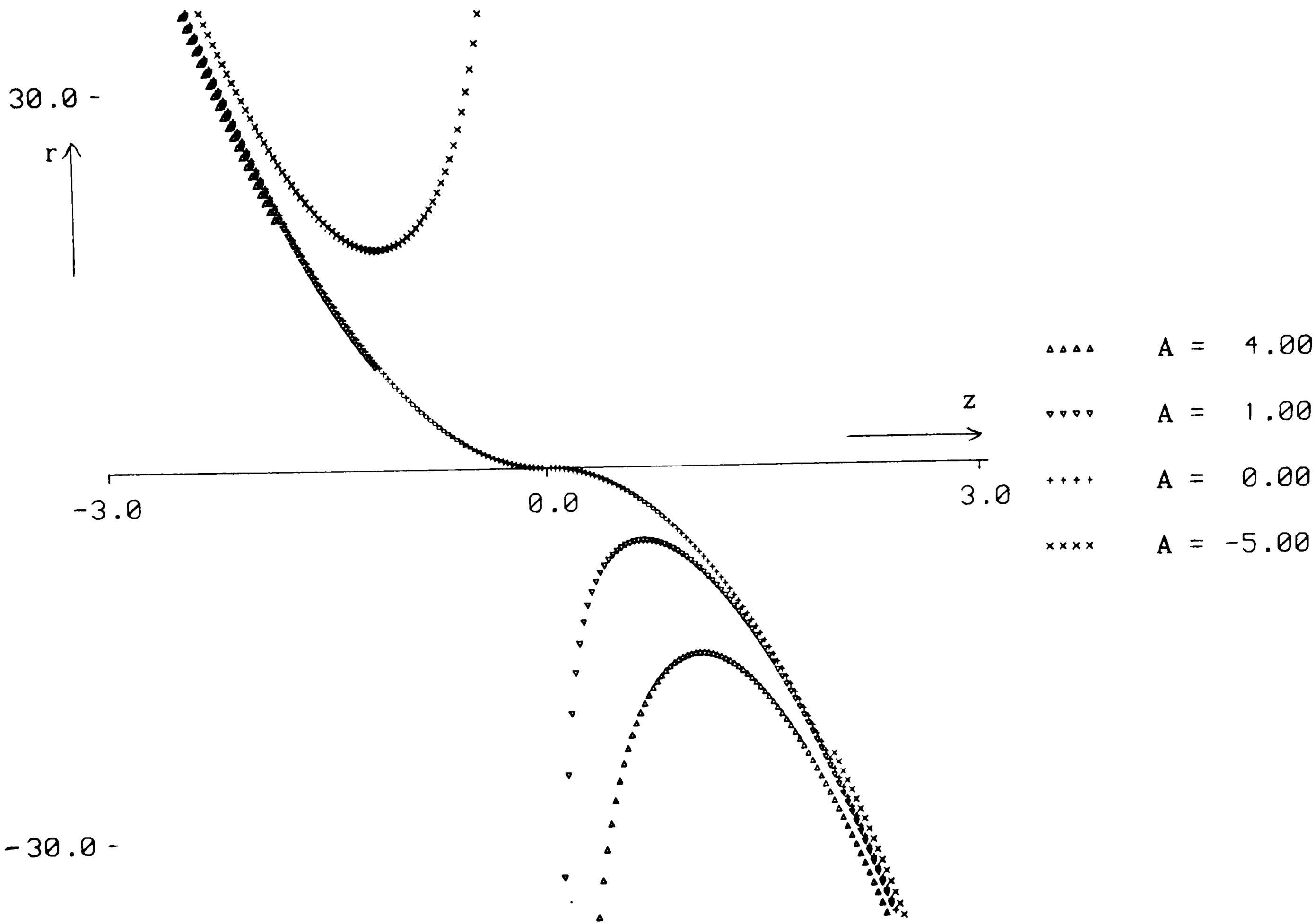

Figure 3.19.

Injection profiles for $\lambda^{*} = 0$, a = 2 and A = 4.0, 1.0, 0.0, -5.0

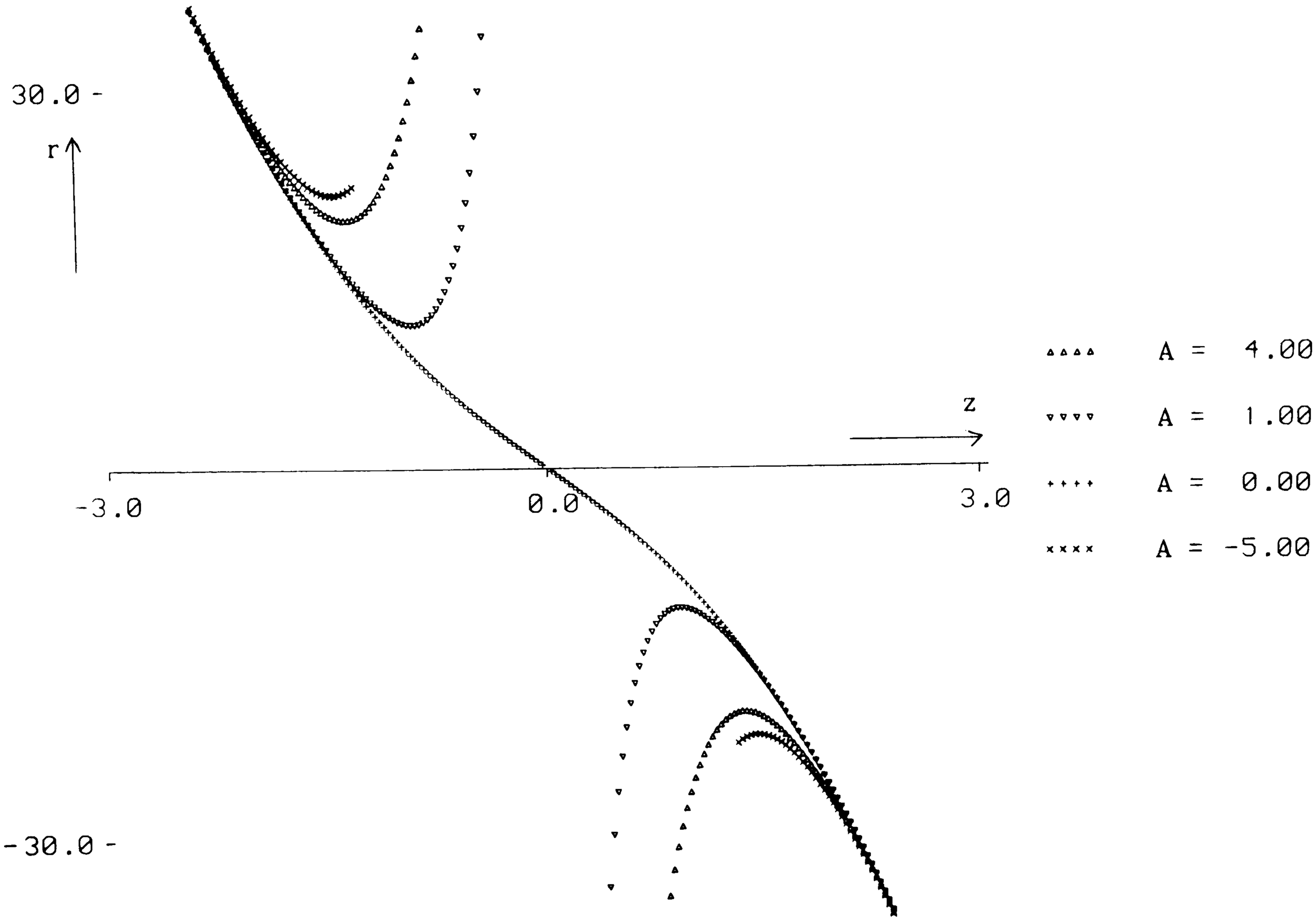

Figure 3.20.

Injection profiles for $\lambda^* = 3$, a = 2 and A = 4.0, 1.0, 0.0, -5.0

where γ is an arbitrary constant obtained by taking $f_0 = 8\gamma$ in (3.13). Substituting for ϕ into (3.10) the differential equation for the boundary is found to be

$$(3.29) \qquad 12R^3R' - 48RR'z^2 - 48R^2z - \lambda^* R^2 = -32z^3 - \lambda^* a^2 \ ,$$

where $\lambda^* = \lambda/\gamma$, and a are arbitrary constants. This equation (3.29) can be written more concisely by using the transformation

$$R^2 = V + 4z^2 \ ,$$

which when substituted into (3.29) yields

$$6VV' - \lambda^* V = 160z^3 + 4\lambda^* z^2 - \lambda^* a^2 \ .$$

The author has not been able to obtain a general solution to this equation, although it is clearly possible to solve it numerically. However, a particular solution can be found by considering R^2 to be a polynomial in z, such that

$$(3.30) \qquad R^2 = V - 4z^2 = Bz^2 + \frac{\lambda^* Bz}{18(B - 4)} + \frac{\lambda^{*2} B(B - 6)}{4320(B - 4)} \ ,$$

where

(3.31) $$3B^2 - 24B + 8 = 0 .$$

From the potential function ϕ, the velocities and streamfunction for this case can be obtained, that is

(3.32) $$u = \gamma[\lambda^*(a^2 - r^2) + 16z(2z^2 - 3r^2)] ,$$
$$v = 12\gamma r(r^2 - 4z^2) ,$$

and

$$\psi = \gamma\{\tfrac{1}{2}\lambda^* r^2[a^2 - \tfrac{1}{2}r^2] + 4r^2z[4z^2 - 3r^2]\} ,$$

where λ^* and a are arbitrary constants. In this case there are only two boundaries rather than the family of profiles obtained in Cases 1 and 2. These are given by (3.30) using $B = 4 \pm {}^2/_3\sqrt{30}$, which are the solutions of the quadratic (3.31). The injection/suction needed to maintain this flow can be obtained by the substitution of the velocities (3.32) into (3.19).

For $n > 4$, potential functions can be found in the same way from equations (3.11) and (3.13). These generate non-linear, first order differential equations for the radius function, but with progressively higher degree. As for $n = 4$, particular cases can be found for these larger values of n, but no general solution. It can be shown that R^2 is a solution of all the differential equations for the boundary, regardless of the value of n, if R^2 is taken to be a quadratic in z.

COMBINING SOLUTIONS

An important classification for differential equations is whether or not they are linear. The theories and techniques for solving linear equations are extensive. However, for nonlinear equations the situation is less satisfactory. General methods for solving such equations are to a large extent lacking, and the theory associated with them is also more complicated than that for linear equations. As a result, nonlinear differential equations are not usually considered advantageous.

The Axi-symmetric Laplace equation is itself a linear differential equation and as such any linear combination of solutions is also a solution. That is, if

$$\nabla^2\Phi = 0 \qquad \text{and} \qquad \nabla^2\Psi = 0 \ ,$$

then

$$\nabla^2[\alpha\Phi + \beta\Psi] = 0 \ .$$

Consequently, in this case it is possible to combine two or more previous solutions, for example Φ_2 and Φ_3, to produce a further solution to the Laplace equation. This new 'combination' solution can now be substituted into (3.10) to generate a differential equation for the boundary profile. However, this equation is nonlinear. As a result, the boundary obtained by solving this differential equation is not a linear combination of the boundaries corresponding to the combination of potential functions. The nonlinearity would not normally be considered advantageous, however, in

this case it allows a totally new solution of the problem to be generated from those already known.

For example, writing

$$\Phi = \alpha\Phi_2 + \beta\Phi_3 = \alpha(2z^2 - r^2) + \beta(2z^3 - 3r^2z) ,$$

where α and β are arbitrary constants. Suitable differentiation of ϕ and its substitution into (3.10) yields

$$(3.33) \qquad (\lambda + 3\beta)R^2 + (\alpha + 3\beta z)2RR' = 6\beta z^2 + 4\alpha z + \lambda a^2 ,$$

which can be integrated to give

$$R^2 = A(\alpha + 3\beta z)^{-(1+\lambda/3\beta)} + \frac{2}{3\beta(\lambda + 9\beta)}(\alpha + 3\beta z)^2 - \frac{2\alpha^2}{3\beta(\lambda + 3\beta)}$$

$$+ \frac{\lambda a^2}{\lambda + 3\beta} ,$$

for $\lambda \neq -3\beta$ and -9β, and $\beta \neq 0$. Considering the special case when $\beta = 0$, equation (3.33) reduces to the differential equation for the wall profile encountered in Case 1. The other two special cases integrate to give

$$R^2 = z^2 + \frac{2\alpha z}{3\beta} - \left(\frac{2\alpha^2 + 9\beta^2 a^2}{3\beta^2}\right)\ln(\alpha + 3\beta z) + A ,$$

for $\lambda^* = -3\beta$ while

$$R^2 = A(\alpha + 3\beta z)^2 + \frac{2(\alpha + 3\beta z)^2}{9\beta^2} \ln(\alpha + 3\beta z) + \frac{2\alpha^2}{18\beta^2} + \frac{3a^2}{2} ,$$

for $\lambda^* = -9\beta$. It can immediately be seen that taking $\alpha = 0$ gives the results presented in Case 3. Different choices of α and β give a variety of different solutions to the problem, none of which are a direct combination of any two or more of the others. This technique is not confined to combinations of two solutions. Any number of analytic solutions, general or particular, as well as numerical ones can be used to obtain a new flow and boundary configuration.

CONCLUSION

This article has presented a wide range of solutions for flow along pipes with impermeable walls and varying cross-sectional area. The method that was employed considered the potential functions to be homogenous polynomials in r and z. Two cases were shown in detail. These were special in that a general solution of the nonlinear differential equation for the boundary function could be obtained using the quadratic and cubic potential functions. Graphs of the streamfunctions and the corresponding family of the boundaries were used to illustrate both cases. In addition, the necessary injection/suction profiles were presented. For those of

higher order, that is quartic and above, a quadratic particular solution for R was found, however it was noted that a numerical method would be needed to obtain a general solution.

Finally, the combining of previous solutions was discussed. Inspection of the governing pair of differential equations for the potential function, ϕ, and the wall profile, R, yields that the former is linear and the latter nonlinear. It is particularly interesting to see that the linear combination of potential functions generate a completely new boundary which is not a linear combination of the those already obtained.

REFERENCES

1. TERRILL, R.M., Laminar Flow in a Porous Tube, Trans. ASME, Vol. 105, 1983, pp.303.

2. TERRILL, R.M., Fluid Flow in a region bounded by a porous cylindrical pipe, Phys. of Fluids, Vol. 29, 1986, pp.625.

3. TERRILL, R.M., A note on Laminar Flow through a porous pipe with slip, IMA. J. Appl. Maths., Vol. 33, 1984, pp.169.

4. TERRILL, R.M., Laminar Flows in circular pipes whose cross-sectional area varies slowly in the axial direction, Phys. of Fluids, Vol. 29, 1986, pp.2357.

CONCLUSION

The aim of this research has been to find applications of the New Solution

$$u = \lambda(a^2 - r^2) + \phi_z \ , \qquad v = \phi_r \ ,$$

with

$$\nabla^2\phi = 0 \ ,$$

to a range of axi-symmetric fluid problems.

The Peristaltic problem presented in Section 1 showed a use of the solution in an already well worked field, producing an analytic solution for all Reynolds number, and with fewer restrictions than in previous research. The extension to using a second order nonlinear waveform as a boundary allowed a greater understanding of the effects of the periodic terms on the characteristics of the flow.

A further application employed the New Solution to give an insight into the flow through a pipe with a slowly varying cross-sectional area. The use of a perturbation series put a limitation on the range of validity of the solution obtained. The solution to this problem could be further developed using a completely numerical method, however, at this time there is no known technique that could be used to generate a solution with the appropriate geometry and boundary conditions.

The addition of mass transfer at the boundary opened a new direction for the research. In this case the new solution was used to investigate analytically an interesting and unexplored problem. A number of exact solutions have been found, but some of the differential equations obtained

were nonlinear and needed a wholly numerical approach. In this instance the New Solution has given a preliminary view of a completely new area of potential research.

The cases presented in this thesis are only a small number of the possible applications of this exciting New Solution to axi-symmetric flow. It would be possible to use the New Solution as the basis of a perturbation solution of the Navier-Stokes equations. The higher order terms of the perturbation solution would be obtained from a linearized Navier-Stokes equation and so, unlike the New Solution, would be Reynolds Number dependent. It is thought that it could be used in other fields, most specifically in the investigation of accelerating flows and heat transfer problems. The development of this solution is still in its infancy and it will be exciting to uncover problems that could be tackled using it in the future.